DEVELOPMENT, VALIDATION AND UTILISATION OF EXPERIMENTAL ASSAYS FOR DETECTION AND QUANTIFICATION OF ENDOGENOUS CARDIOTONIC STEROIDS

By

Dannie Fobian

A thesis submitted to

The University of Birmingham

for the degree of

DOCTOR OF PHILOSOPHY

Institute of Cardiovascular Sciences

College of Medical and Dental Sciences

The University of Birmingham

June 2020

UNIVERSITY OF
BIRMINGHAM

University of Birmingham Research Archive

e-theses repository

This unpublished thesis/dissertation is copyright of the author and/or third parties. The intellectual property rights of the author or third parties in respect of this work are as defined by The Copyright Designs and Patents Act 1988 or as modified by any successor legislation.

Any use made of information contained in this thesis/dissertation must be in accordance with that legislation and must be properly acknowledged. Further distribution or reproduction in any format is prohibited without the permission of the copyright holder.

ABSTRACT

Digoxin is commonly used for the treatment of patients with atrial fibrillation (AF) with/without heart failure (HF). However, in clinical practice the response to digoxin therapy is variable. The primary cellular target of digoxin, the Na+/K+ ATPase pump, is shared with a group of hormones called cardiotonic steroids (CTS). CTS are elevated in patients with cardiovascular disease. Differing levels of endogenous CTS in individual patients may explain the varied response to digoxin and susceptibility to adverse drug reactions. Thus validated methodologies to measurements of levels and effects of CTS are necessary.

In this thesis two methodologies were developed 1) a cell-based assay for assessment of effects of CTS and 2) an ouabain competitive ELISA with aim to use for patients from the RATE control Therapy Evaluation in permanent Atrial Fibrillation (RATE-AF) trial.

HEK293t cell-based assay developed were able to measure consistently changes in sodium sensitive fluorescents using SBFI sodium fluorescent dye. Changes were observed between different CTS were observed in IC50 values and maximal effects on sodium sensitive fluorescents and when calibrated to sodium levels. Extraction methodology was able to be optimised to extract potential cardiotonic steroids out of spiked human plasma. Competitive ELISA methodology developed and validated for detecting of ouabain levels from spiked and extracted samples. Some cross-reactivity with the primary antibody was observed from digoxin.

Significant lowered intracellular Na^+ levels was observed in HEK293t cells when applied with serum from patients with type 2 diabetes, heart failure, myocardial infarction and with a number of unexpected hospitalisations due to AF or HF. Lastly, increased levels of endogenous ouabain were detected in more severe HF (NYHA IV vs NYHA II) and in unexpected hospitalisations caused by AF or HF. Furthermore, endogenous ouabain concentrations correlated with AF (mEHRA) and HF (NYHA class) disease severity. The results presented in this thesis suggests endogenous CTS to have an important role in HF and potentially also AF. Thus, further work with CTS and the potential of these assays to be used to measure biomarkers could help better patient stratification.

ACKNOWLEDGEMENTS

I would like to thank my supervisor Dr Davor Pavlovic for his outstanding support and patience throughout this journey. His enthusiasm for my work and absolutely fantastic discussions has been key to get through these studies. I also want to thank my other supervisors Professor Dipak Kotecha and Professor Paulus Kirchhof for their helpful advice and guidance.

I am very thankful to all of the members of the Heart Failure and Arrhythmias cluster. You have all been awesome and always been very helpful and I feel lucky to have been working with you all and learn from all of you as well. I particularly want to thank Clara Apicella and Dr Andrew Holmes for day in day out support and always having time to talk when needed. Your support and encouragement have kept me going and been absolutely crucial to completing this journey.

Finally, I want to thank my family for their constant encouragement and believe in me to succeed and my wife Sophie who without her endless support, patience and willingness to move to England none of this would have been possible.

TABLE OF CONTENTS

ABSTRACT i

ACKNOWLEDGEMENTS iii

TABLE OF CONTENTS iv

LIST OF FIGURES x

LIST OF TABLES xiv

LIST OF ABBREVIATIONS xv

CHAPTER 1. INTRODUCTION 1

1.1 Physiology of the heart 1

1.1.1 Gross anatomy and function of the heart 1

1.1.2 Cardiomyocytes and cardiac excitation-contraction coupling 3

1.1.3 Resting membrane potential 6

1.1.4 The cardiac action potential 8

1.1.5 The cardiac conduction system 10

1.1.6 Autonomic control of the heart 11

1.2 Cardiac arrhythmias 14

1.2.1 Atrial fibrillation 14

1.2.2 Pathophysiology of AF 15

1.2.3 Permanent AF, Treatments and RATE-AF 18

1.3 The Na+/K+-ATPase: structure and function 22

1.3.1 Na+/K+-ATPase 22

1.3.2 NKA Regulation 25

1.4 Cardiotonic Steroids 26

1.4.1 The Biosynthesis of CTS and Effects on Tissues 27

1.4.2 Effects of CTS on signaling 28

1.4.3 Detection of CTS 30

1.4.4 Interaction between CTS – Ouabain and Digoxin Antagonism 31

1.5 This Thesis 32

CHAPTER 2. MATERIALS AND METHODS 33

2.1. Fluorescent assay for measuring intracellular Na^+ 33

2.1.1. Culture of the HEK293t cells 33

2.2.1. Measurement of intracellular Na^+ in HEK293t cells 35

2.3. Detection and quantification of ouabain by ELISA 37

2.3.1. Primary antibody and Ouabain-BSA Coat 37

2.3.2. ELISA methodology 37

2.4. Samples from the BBC-AF Registry and the RATE-AF Trial 39

2.5. Solid-phase Extraction methodology 40

2.5.1. C18 Bond Elute SPE Method 40

2.5.2. Thermo sola SPE Method 41

2.6. Data analysis and statistics 42

CHAPTER 3. METHOD DEVELOPMENT FOR DETERMINING THE EFFECTS OF CTS IN HEK293 CELLS 43

3.1. Introduction and aims 43

3.2. Additional methodology and data handling 45

3.2.1 Extraction and analysis of raw data 45

3.2.2 Analysis of dose-response curves 45

3.3 Results 46

3.3.1 Development of an assay for intracellular Na^+ determination 46

3.3.2 Dose-Dependent Effects of Cardiotonic Steroids Using Asante Natrium Green 2 Dye 50

3.3.3 Potential Biphasic Effects of Cardiotonic Steroids Using Asante Natrium Green 2 52

3.3.4 Investigating Antagonism of Cardiotonic Steroids Using the Asante Natrium Green 2 54

3.3.5 Effects of BBC-AF patient samples on intracellular Na^+ 55

3.3.6 Optimisation of the SBFI dye for Measurement of intracellular Na^+ 59

3.3.7 Increasing sensitivity of the intracellular Na^+ cell-based assay using the SBFI 60

3.3.8 Dose-dependent Effects of Cardiotonic Steroids Using the SBFI Dye 61

3.3.9 Potential Biphasic effects and interactions of Cardiotonic Steroids with SBFI 64

3.3.10 Investigating Antagonism of Cardiotonic Steroids Using the SBFI 67

3.3.11 Extraction of cardiotonic steroids and potential matrix effects with SBFI 68

3.3.12 Calibration of Na^+ signals with SBFI dye 72

3.4 Discussion 75

3.4.1 Development of intracellular sodium assay 75

3.4.2 Dose-response effects of cardiotonic steroids 77

3.4.3 Bimodality of cardiotonic steroids 78

3.4.4 Extraction necessity and effects of patient samples on intracellular Na^+ 79

3.4.5 Calibration to intracellular Na^+ levels 80

3.5 Conclusions 81

CHAPTER 4. DEVELOPMENT OF A COMPETITIVE ELISA FOR THE MEASUREMENT OF OUABAIN CONCENTRATION 82

4.1. Introduction and aims 82

4.2. Analysis of ELISA data 83

4.2.1 Extraction and analysis of raw data 83

4.2.2 Analysis of Standard curves 84

4.2.3 Sample analysis 85

4.3. Results 85

4.3.1 Development of ELISA 85

4.3.2 Validation of cross-reactivity of primary antibody 96

4.3.3 Detection of Cardiotonic steroids from spiked serum/plasma samples 109

4.4. Discussion 112

4.4.1 Development of ELISA 112

4.4.2 Structural effects on cross-reactivity of the ouabain primary antibody 113

4.5. Conclusion 119

CHAPTER 5. UTILISATION OF VALIDATED ASSAYS FOR RATE-AF PATIENT PLASMA SAMPLES 120

5.1. Introduction and aims 120

5.2. Analysis of RATE-AF trial data 121

5.3. Results 126

5.3.1 Population characteristics of RATE-AF patients 126

5.3.2 Correlations of basic research parameters with calibrations 128

5.3.3 Correlations of basic research parameters with numerical RATE-AF variables 130

5.3.4 Analysis of categorical variables 133

5.3.5 The two treatment arms at baseline 147

5.4. Discussion 149

5.4.1 Correlations with NT-proBNP 149

5.4.2 Endogenous ouabain and intracellular sodium in disease states 149

5.4.3 Baseline differences and future work 152

CHAPTER 6 FINAL CONSIDERATIONS AND FUTURE STUDIES 154

6.1. Outcomes 154

6.2. Study limitations 156

6.2.1 HEK293t cell limitations 156

6.2.2 ELISA limitations 157

6.3. Future work 158

6.3.1 HEK293t experiments 158

6.3.2 Animal studies 159

6.3.4 IPS-CMs 160

6.3.5 ELISA experiments 160

6.3.6 RATE-AF patient Cohort 161

REFERENCES 162

LIST OF FIGURES

Figure 1.1 Gross anatomy and blood flow patterns of the heart……..3

Figure 1.2 Schematic of Ca^{2+} movements and time course of action potential……...6

Figure 2.3 Schematic of the signal transduction pathways activated by sympathetic (Noradrenaline) or parasympathetic (Acetylcholine) in pacemaker/myocardial cell……12

Figure 1.4 A Post-Albers kinetic scheme – Transport of Na+ and K+ over the membrane via several enzymatic steps……..22

Figure 1.5 The structure of Na+/K+-ATPase. The NKA is comprised of an α subunit and a β subunit……24

Figure 1.6 The steroid structure of bufadienolides and cardienolides…….26

Figure 1.7 Proposed model of synthesis of CTS and acute and chronic effects on different tissues……...28

Figure 1.8 Schematic overview of the two pathways for the interaction between CTS and NKA i.e. the ionic and the signaling pathway……..30

Figure 2.1 The general methodology of the developed intracellular sodium assay utilising HEK293t cells……..36

Figure 3.1 Optimisation of intracellular sodium assay in HEK293t cells……48

Figure 3.2 Dose response curves generated with various CTS……50

Figure 3.3 Investigations of biphasic responses with various CTS……..52

Figure 3.4 Investigations of antagonism responses with ouabain and digoxin……53

Figure 3.5 Investigations of effects of BBC-AF samples……..56

Figure 3.6 Comparison of BBC-AF patients treated with digoxin or beta-blockers……57

Figure 3.7 Optimisation of SBFI dye and direct comparison with ANG2 in HEK293t cells……. 58

Figure 3.8 Investigation of effects of monensin……60

Figure 3.9 Dose response curves generated with various CTS……62

Figure 3.10 Investigations of biphasic responses with various CTS. Cardenolides (digoxin, ouabain) and a bufadienolide (marinobufagin) was investigated at range of 0.1-10 nM……...64

Figure 3.11 Investigations of interactions of ouabain and digoxin……..65

Figure 3.12 Dose response curves generated with ouabain, digoxin and marinobufagenin and respective extractions……68

Figure 3.13 Calibration of tyrode 1 nM fresh ouabain, digoxin and equimolar of each……..72

Figure 4.1 Effects of varying the primary antibody dilution factor and coating concentration……86

Figure 4.2 Effects of varying the primary antibody dilution factor and coating concentration……87

Figure 4.3 Incubation time of primary antibody……...89

Figure 4.4 Choice of BSA type as blocking agent……91

Figure 4.5 Choice of plate type……93

Figure 4.6 Cross-reactivity assessment of digoxin……...96

Figure 4.7 Cross-reactivity assessment of marinobufagenin……99

Figure 4.8 Cross-reactivity assessment of testosterone……...102

Figure 4.9 Cross-reactivity assessment of dexamethasone……104

Figure 4.10 Steroid structure of the steroids included in the cross-reactivity investigations……106

Figure 4.11 Detection of cardiotonic steroids in extracts from spiked samples……108

Figure 5.1 Flow chart of the RAte control Therapy Evaluation in permanent Atrial Fibrillation (RATE-AF) trial……..118

Figure 5.2 Correlation data from basic research parameters measure from 160 patients from the RATE AF trial……..126

Figure 5.3 Correlation matrix of HEK293t raw data, HEK293t Monensin raw and ELISA calibrateddata with the included variables from the 160 patients from the RATE-AF trial……..128

Figure 5.4 Correlation of HEK293t without or with monensin and calibrated ELISA response vs the NT-proBNP levels from 160 patients……129

Figure 5.5 Gender specific differences investigated……...131

Figure 5.6 Effect of type 2 diabetes……133

Figure 5.7 Classification of NYHA investigated……135

Figure 5.8 Classification of mEHRA……..137

Figure 5.9 History of myocardial infarctions……..139

Figure 5.10 History of strokes investigated……141

Figure 5.11 History of unplanned hospitalisations investigated……143

Figure 5.12 Comparison of baseline from RATE-AF treatment arms……..145

LIST OF TABLES

Table 2.1 Composition of the solutions utilised in the HEK293t cell-based intracellular sodium experiments…….35

Table 2.2 Composition of the solutions utilised in the ELISA……37

Table 3.1 Half maximal inhibitory concentration (IC50), maximal effect (Imax) and rank of the NKA inhibition by various cardiotonic steroids……50

Table 3.2 Half maximal inhibitory concentration (IC50), maximal effect (Imax) and rank of the NKA inhibition by various cardiotonic steroids with SBFI……..61

Table 3.3 Half maximal inhibitory concentration (IC50) of the NKA inhibition by CTS and extractions…….69

Table 4.1 Table of calculated cross-reactivity from both raw and calibrated values of Digoxin, Marinobufagenin, Testosterone and Dexamethasone……..105

Table 4.2 The studies found to investigate the cross-reactivity of cardiotonic steroids are compared in the table above……...115

Table 5.1 List of variables of interest measured/recorded in RATE-AF patient cohort.....120

Table 5.2 Population characteristics of the RATE-AF patient cohort…….123

LIST OF ABBREVIATIONS

Aa	Amino acids
AADs	Antiarrhythmic drugs
AF	Atrial Fibrillation
ADP	Adenosine diphosphate
ANG-2	Asante Natrium Green 2
AP	Action Potential
APD	Action Potential Duration
ATP	Adenosine triphosphate
AV node	Atrioventricular node
cAMP	Cyclic adenosine monophosphate
CHF	Congestive Heart Failure
CMs	Cardiomyocytes
CTS	Cardiotonic Steroids
CV	Conduction Velocity
DAD	Delayed Afterdepolarisations
DIG	Digitalis Investigation Group
DMEM	Dulbecco's Modified Eagle´s Medium
EAD	Early Afterdepolarisations
ECG	Electrocardiogram
EO	Endogenous Ouabain
HBRC	Human Biomaterials Resource Centre

HEK293t	Human Embryonic Kidney 293t
HF	Heart Failure
hiPSC-CMs	Human Induced Pluripotent Stem Cell-derived Cardiomyocytes
I_{CaL}	L-type Ca^{2+} Current
I_f	Funny Current
I_{K1}	Inward Rectifier K^+ Current
I_{max}	Maximal inhibition
I_{ti}	Transient Inward Current
K^+	Potassium ion
mEHRA	Modified European Heart Rhythm Association score of atrial fibrillation
NCX	Na^+/Ca^{2+} Exchanger
NHE	Na^+/H^+ exchanger
NKA	Na^+/K^+-ATPase
OAC	Oral anticoagulant
QoL	Quality of Life
pEF	Preserved ejection fraction
PKA	Protein kinase A
PKC	Protein kinase C
PLB	Phospholamban
PLM	Phospholemman
RATE-AF	Rate Control Therapy Evaluation in Permanent Atrial Fibrillation

RCT	Randomised clinical trial
rEF	Reduced ejection fraction
RP	Refractory Period
Rpm	Rounds per minute
RYRs	Ryanodine receptors
SA node	Sinoatrial node
SBFI	Sodium-binding benzofuran isophthalate
SD	Standard deviation
SEM	Standard error of the mean
SERCA	Sarcoplasmic reticulum Ca^{2+} ATPase
SR	Sarcoplasmic Reticulum
TM	Transmembrane
WL	Wavelength
WTμ	Wildtype

CHAPTER 1. INTRODUCTION

1.1 Physiology of the heart

1.1.1 Gross anatomy and function of the heart

In mammals the heart is a muscle located in the thoracic cavity. The main task of the heart is to work as a pump in the circulatory system allowing the transport of blood around the body via the blood vessels due to the created pressure gradients. This allows for transport of both oxygen, nutrients and waste to be delivered between capillary beds by a process called convection transport. The specific transport from the blood to individual tissues and cells are carried out by diffusion (1).

The inside of the heart in lined by the endocardium which comprised of a thin layer of endothelial muscle cells covering connective tissue, allowing easier flow of the blood within the chambers but are also involved in regulation of performance during contractions (2). The outer layer of the heart, the epicardium, contains mesothelial cells over a layer of connective tissue and are important for the generation of the pericardial fluid (2). The heart is encased in a thin protective fluid filled sac, the pericardium, which stabilises the heart position ensuing the cardiac geometry during the pressure volume changes of the different chambers in the heart as its fused to the diaphragm and also isolates the heart from the surroundings (3).

The heart is comprised of 4 chambers, each with unique origin, anatomy and functions during the cardiac cycle. The two largest chambers of the heart, the left (LV) and right

(RV) ventricles, are positioned caudally to the left (LA) and right (RA) atria which both are smaller chambers. The wall of the LV is much thicker than the RV as much higher pressure is needed to successfully deliver the blood through the systemic circulation compared to the pulmonary circulation. The RA receives the deoxygenated blood from the systemic circulation via superior and inferior vena cava but also receives blood from the coronary circulation. The RA also contains the sinoatrial (SA) node (For cardiac conduction see 1.3) that generates an electrical signal initiating contraction and leading the blood to flow from the RA into the RV via the tricuspid valve. Following contraction, the blood is pumped into the pulmonary circulation for oxygenation in the lungs prior to returning the LA via the pulmonary veins. LA contraction pumps the oxygenated blood into the LV via the mitral valve. Finally, the blood when ejected from the LV flows through the aortic valve into the aorta enabling the delivery of oxygen, nutrients and more to the different tissues. This circular pattern of the blood flow is maintained by the pressure gradients created by the ventricles and the valves both in chambers but also in most veins ensures one-way transport of the blood (1, 2).

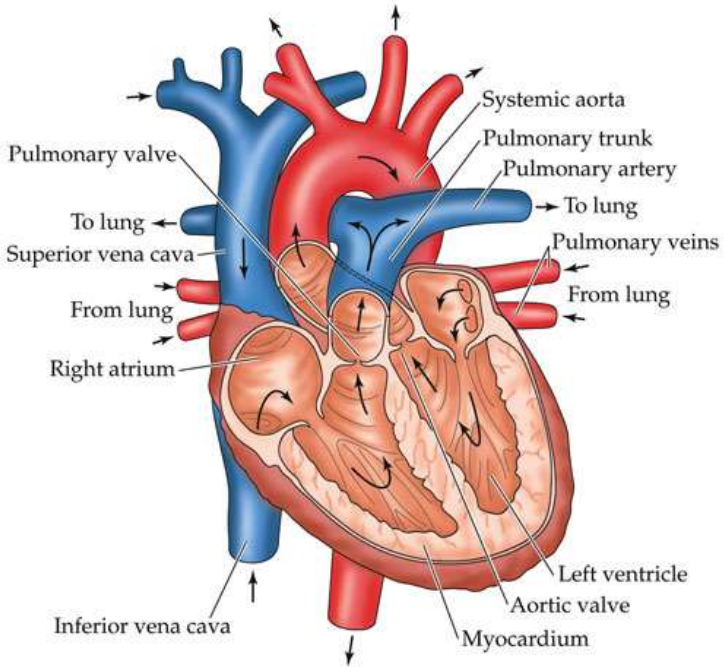


Figure 3.1 Gross anatomy and blood flow patterns of the heart. The arrows indicate the blood flow pattern through the different chambers of the heart. The blue and red colors indicate deoxygenated and oxygenated blood flow, respectively. Image extracted from (4).

1.1.2 Cardiomyocytes and cardiac excitation-contraction coupling

The heart is comprised mainly of cardiomyocytes (CMs) when measured by volume but also contain cardiac fibroblasts, smooth muscle cells, conduction cells, endothelial cells and resident immune cells. Cardiac fibroblast is the most abundant cell type in the myocardium with estimates of >50% of the total amount of cells(5, 6). The cardiac fibroblasts are essential to regulate the extracellular matrix that support the integrity of the CMs by providing a platform for connections through e.g. integrins (2, 6). Cardiomyocytes are the contractile cells and by volume make up more than 70% of the heart (6).

CMs have a single nucleus, abundant mitochondria and are connected via intercalated discs (7). CMs also have striations that are especially well transversely aligned in ventricular CMs. The intercalated discs are comprised of a narrow space between cells, that are kept together by desmosomal proteins to ensure integrity and by gap junctions, which are low resistance channels between cells allowing rapid movement of ions. This rapid movement of ions is absolutely key for propagation of the action potential to spread very fast, allowing a synchronous beating of the atria or ventricle (2, 7).

Each CM contains bundles with contractile properties called myofibrils. Each of the myofibrils contain numerous sarcomeres which is the basic contractile unit of a cardiomyocyte. The contraction of sarcomeres is caused by the thinner actin filaments sliding in between the bigger myosin filaments in a process that creates cross-bridges between the two filaments (8, 9). The binding sites on the actin subunits at rest are covered by tropomyosin molecules, which have a troponin complex attached alongside it which contains a Ca^{2+} sensitive complex, troponin C. Troponin C will upon a rise in free Ca^{2+} in the sarcoplasm allow the myosin-binding site to be available for cross-bridging due to molecular changes after binding, enabling contraction and structural changes in the myosin head positioned advancing the filament forward. The structural movements of the myosin head are energised by hydrolysing adenosine triphosphate (ATP) into adenosine diphosphate (ADP). The released energy activates the myosin head allowing the structural change leading to the contraction. The bigger the rise in Ca^{2+}, the higher number of myosin-binding sites accessible, and the bigger the contraction, as the contractile power

is proportional to the extent of crossbridge formation. This means that changes in Ca^{2+} caused by sympathetic nerve stimulation or drugs for example like digoxin (see explanation below) can cause changes in the contractility of the heart. The increase in Ca^{2+} is mainly due to release of Ca^{2+} from the sarcoplasmic reticulum (SR), which is triggered by the increase in Ca^{2+} via opening of the voltage-gated Ca^{2+} channels. Opening of the voltage-gated Ca^{2+} channels is initiated by the depolarisation of the membrane as a result of the opening of the sodium channels, responsible for the upstroke of the action potential (AP). The shortening of the sarcomeres will be sustained, as long as Ca^{2+} levels remains high, hindering ventricular relaxation until Ca^{2+} levels are lowered. When the Ca^{2+} voltage-gated channels close, the majority of the excess Ca^{2+} is sequestered back in the sarcoplasmic reticulum by the ATP-driven Ca^{2+} pump, sarco-endoplasmic reticulum calcium-ATPase (SERCA). Some Ca^{2+} is also extruded from the CM by the sodium-calcium exchanger (NCX). When Ca^{2+} levels fall and thus Ca^{2+} is no longer bound to troponin C, changing the conformational structure of the protein limiting the cross bridging. This allows the sarcomere length to be restored, with subsequent muscle relaxation (2, 10). See Figure 1.2 for summary.

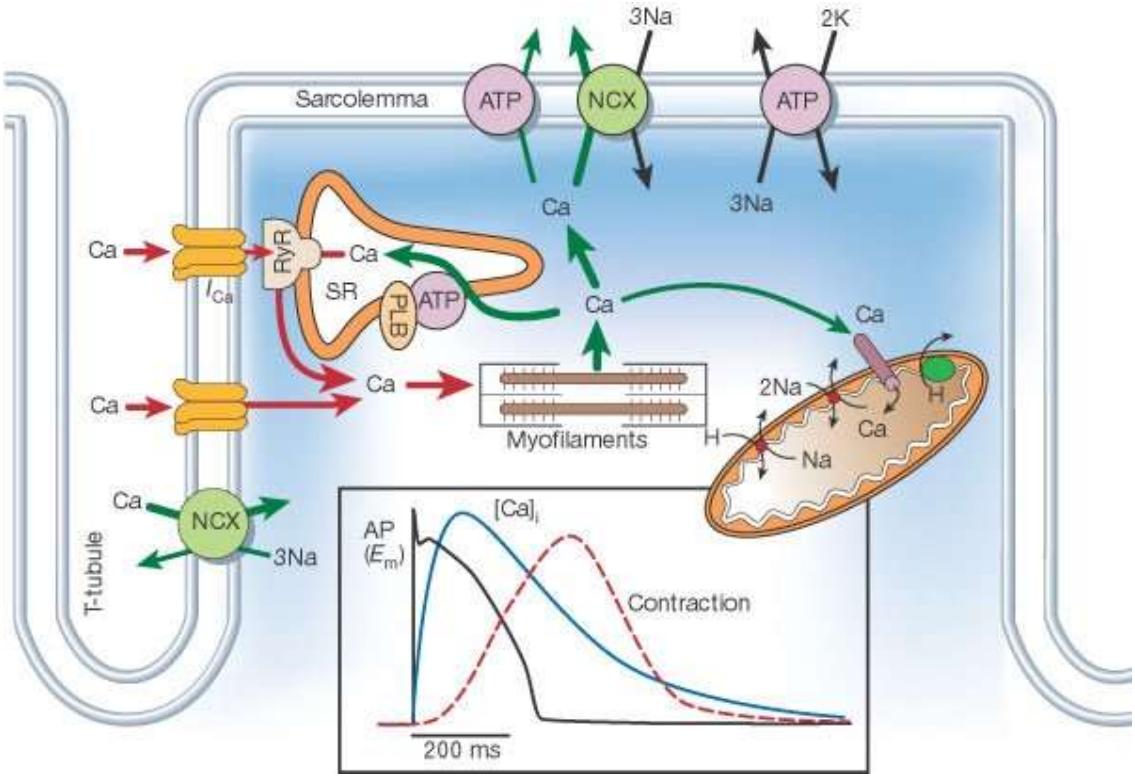


Figure 1.2 Schematic of Ca^{2+} movements and time course of action potential. The inlet shows the time course of an action potential with the delayed Ca^{2+} transient followed by contraction. Image extracted from (10).

1.1.3 Resting membrane potential

The resting membrane potential is an electrical potential difference across the membrane in a quiescent cell. This electrical potential difference is essential for transport of nutrients, ions (and water) and also involved in the AP generation (11).

The ionic gradients across the membrane and membrane permeability are 2 factors important for the establishment of the resting membrane potential. The ion gradients most important in cardiomyocytes are the gradients of Na^+, K^+, Cl^- and Ca^{2+}. Inside

cardiomyocytes K^+ is high while outside is low, meanwhile Na^+ are low concentrations inside and high outside. This distribution is maintained by the work of the sodium-potassium ATPase (NKA) which actively pumps K^+ ions into the cell in exchange for Na^+ ions(12). Thus, favouring inward diffusion of Na^+ ions and outward directed diffusion of K^+ ions. The cardiomyocytes also contain much lower levels than extracellular concentration of Cl^- and Ca^{2+} ions, strongly favouring inward directed diffusion(1). The diffusion of any of these ions rely on each ion's permeability. Cardiomyocytes have different permeability for different ions, but are mainly permeable to K^+ due to the presence of leaky K^+ channels. Thus, the resting membrane potential in cardiomyocytes is relatively close to the Nernst potential for K^+(E_K). The Nernst potential is the voltage difference across the membrane that equals the driving force of the ion gradient resulting in no diffusion gradient for the specific ion(1, 11). This can be expressed by the Nernst equation for K^+ as follows:

$$E_K = -\frac{R * T}{z * F} ln \frac{[K^+]_o}{[K^+]_i} = -96\ mV$$

E_K = Nernst potential for K^+; R = Ideal gas constant (8.314 $J*K^{-1}*mol^{-1}$); T = Temperature in Kelvin; z=1 valence of K^+; F= Faraday's constant (96.485 $C*mol^{-1}$); $[K^+]_o$ is the extracellular K^+ concentration = 4 mM; $[K^+]_i$ is the intracellular K^+ concentration =135 mM.

Ventricular cardiomyocytes have resting membrane potentials around -80 to -90 mV, which is very close to the E_K. The deviation from the E_K is due to permeability of other ions. Thus, the resting membrane potential is usually better described by the Goldman equation as follows:

$$Resting\ membrane\ potential = \frac{R * T}{F} ln(\frac{P_K[K^+]_o + P_{Na}[Na^+]_o + P_{Cl}[Cl^-]_i}{P_K[K^+]_i + P_{Na}[Na^+]_i + P_{Cl}[Cl^-]_o})$$

R = Ideal gas constant (8.314 $J*K^{-1}*mol^{-1}$); T = Temperature in Kelvin; F= Faraday's constant (96.485 $C*mol^{-1}$); $[K^+]_o$ is the extracellular K^+ concentration; $[K^+]_i$ is the intracellular K^+ concentration; $[Na^+]_o$ is the extracellular Na^+ concentration; $[Na^+]_i$ is the intracellular Na^+ concentration; $[Cl^-]_o$ is the extracellular Cl^- concentration; $[Cl^-]_i$ is the intracellular Cl^- concentration; P_K is the permeability of K^+; P_{Na} is the permeability of Na^+; P_{Cl} is the permeability of Cl^-;

The leaky K^+ channels are not expressed equally in all cardiomyocytes which explains the difference in resting membrane potential between atrial and ventricular cells. With the atrial cardiomyocytes having a more depolarized resting membrane potential of -65 to80 mV(2, 13).

1.1.4 The cardiac action potential

Action potentials are generated in the SA nodal cells and from there spreads to the rest of the heart via cell-cell conduction. CMs have a stable resting membrane potential around -80 - -90 mV. Cells in SA and atrioventricular (AV) nodes have an unstable membrane potential, slowly depolarising until threshold around -60 mV is reached, initiating AP generation and propagating to adjacent CMs (2).

The nodal CMs have 3 phases of their AP. Nodal cells have a more positive resting membrane potential than the atrial and ventricular CMs. Phase 4 is characterised by slow

drift towards more positive membrane potential (around -55 mV) due to the entering of Ca^{2+} via T- and L-type Ca^{2+}channels and also the pacemaker current, which are nonspecific cation channels (Na^+ and K^+). Phase 0, the upstroke, in nodal cells is mainly due to further opening of L-type Ca^{2+}channels allowing inward current of Ca^{2+}. The upstroke in nodal cells have significantly smaller amplitude and slower upstroke than atrial and ventricular CMs. Furthermore, nodal cells have no plateau but instead the potential slowly returns to negative potentials (Phase 3) due to the opening of voltage sensitive K^+ channels, allowing K^+ ions to flow out(2).

In atrial and ventricular CMs, the upstroke (Phase 0) is much faster due to the activation of voltage sensitive Na^+ channels leading to a rapid increase in intracellular Na^+, causing a sharp depolarisation of the CM. Depolarised membrane potential leads to opening of the voltage sensitive K^+ channels (Ito1/2) and to a slight repolarisation of the membrane potential (Phase 1). Activity of the L-type Ca^{2+}channels and NCX as well as that of the IKr and IKs maintains a stable membrane potential known as the plateau phase (Phase 2). Gradually, L-type Ca^{2+}channels and NCX close and K^+ channels repolarise the membrane potential, returning to the resting membrane potential. After the activation of the voltage sensitive Na^+ channels, the CMs are completely unexcitable, known as the absolute refractory period, which is due to the lack of available voltage sensitive Na^+ channels able to be activated. During phase 3 after getting the membrane potential negative (~ -55mV), CMs are excitable to some extent, whereby a larger electrical stimulus will still be able to trigger an AP as enough of voltage sensitive Na^+ channels could be available. This is known as the relative refractory period (1, 2).

1.1.5 The cardiac conduction system

The cardiac AP is initiated by the SA node cells which at rest fires ~ 1 AP/sec to the adjacent CMs in the atria and leading to a synchronous beating of the atria. The AP propagates towards the AV node in the lower posterior region of the atrial septum. Conduction of the AP in the AV node is delayed prior to continuing through a bundle of fast conducting cells, named the bundle of His. The delay in the AV node allows the atria to contract before the ventricles, ensuring the blood fills the ventricles before their contraction. The ventricular conduction system is essential to ensure simultaneous contraction of the ventricular wall. Thus, bundle of His allows fast conduction through fibrous part of the annulus fibrosus prior to branching out (into left and right bundle branch) after it reaches the main muscular parts of the septum. The left bundle branch is comprised of two sets of fibres, one anterior and one posterior of the left side of the heart leading to the conduction to the LV. The right bundle branch extends over the right side of the interventricular septum supplying the right ventricle. Each branch conducts the AP signal into even bigger cells with faster conduction called the purkinje fibers ensuring the electrical signals reaches the subendocardial CMs. At the end of each of the purkinje fibers, the APs are conducted from cell to cell in an outward epicardial direction to spread throughout the whole ventricular wall. The AV node and purkinje fibers also have pacemaker activity like the SA node, although generating APs at a much slower rate, so in most cases the signal generated by the SA will determine the rate of the contraction of the ventricles hence setting the heart rate(2).

1.1.6 Autonomic control of the heart

The heart rate and contractility are also regulated by autonomic control i.e. the sympathetic and parasympathetic fibers. The parasympathetic nerve innervation of the heart is mainly in the SA node and the AV node, but also present in the conduction system and sparsely in atrial tissues(14). Parasympathetic nerve stimulation leads to the release of acetylcholine, which acts mainly on M2 muscarinic (M2) receptors. The released acetylcholine leads to decreased generation of cyclic adenosine monophosphate (cAMP). The decrease in cAMP leads to a decrease of I_f current, decrease in the current generated by the Ca^{2+} L-type channels and increase in IKAch channel opening. Finally, the activity of K_{ATP} channels are increased by the βγi subunit from the inhibitory GTP-binding protein (G_i) leading to a further hyperpolarisation of the membrane potential (See figure 1.3). In combination, these effects lead to a slower slope of AP generation, ultimately slowing the heart rate (15, 16). The parasympathetic innervations of the ventricles are less abundant although some studies in bigger mammals demonstrate stimulation can cause lowered contractility due to the lowered intracellular Ca^{2+} from the reduced activity of the L-type Ca^{2+} channels (17-20).

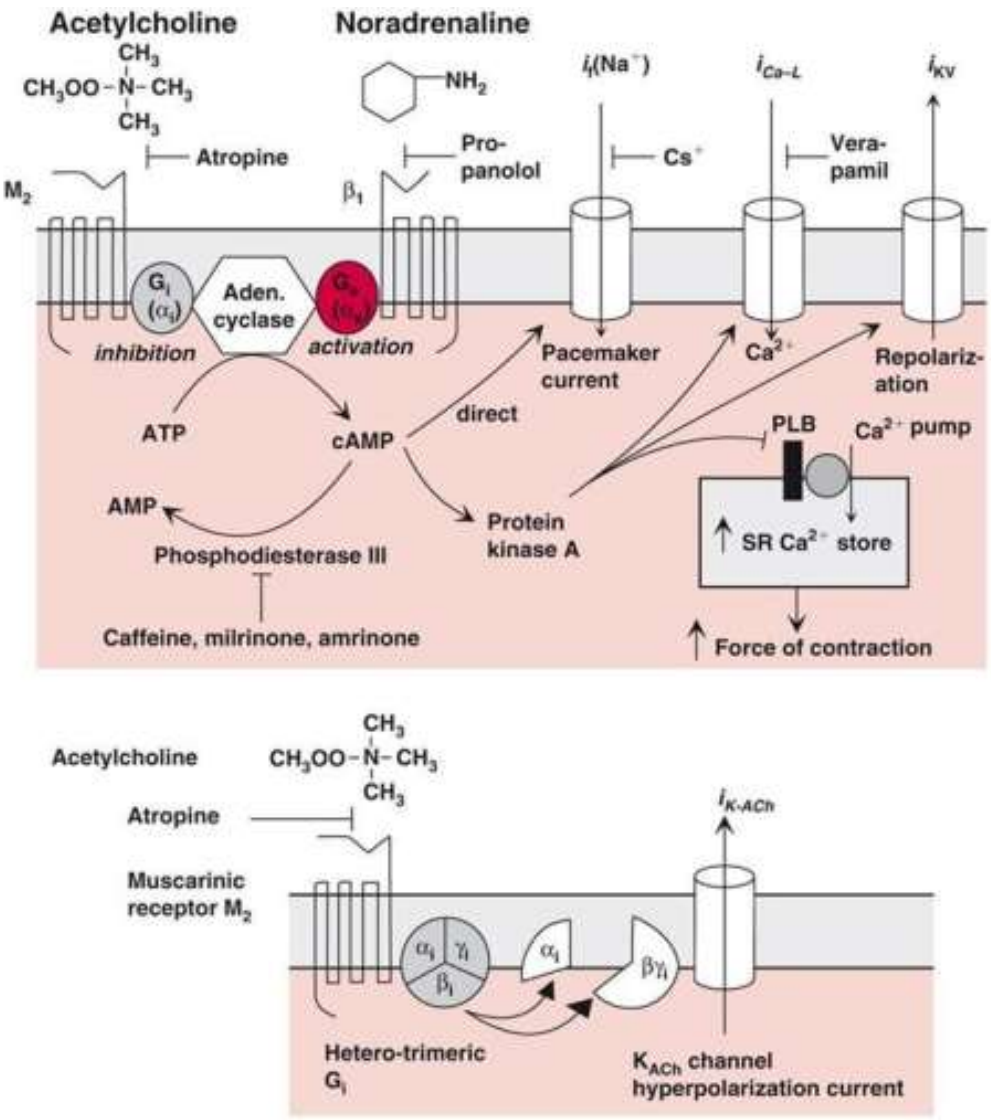


Figure 4.3 Schematic of the signal transduction pathways activated by sympathetic (Noradrenaline) or parasympathetic (Acetylcholine) in pacemaker/myocardial cell. Aden. Cyclase, adenylyl cyclase; AMP, adenosine monophosphate; ATP, adenosine triphosphate; β1, β1-adrenoceptors; Gi, inhibitory GTP-binding protein; Gs, stimulation GTP-binding protein; iCa-L, L-type Ca2+ channel current; if, funny current; iKV, Delayed rectifier voltage-activated current; L-type Ca2+ channel current; M2, muscarinic M2-receptor; PLB, phospholamban; SR, sarcoplasmic reticulum. Image extracted from(2).

The sympathetic nerve innervation is more widespread across the heart, including in the atria, the cardiac conduction system and the ventricles. The effects are exerted by stimulation of β_1-adrenergic receptors by noradrenaline and adrenaline. The innervation of the heart with sympathetic nerves are most dense in the atria and the base of the ventricles with a transmural gradient of nerves follow the duration of APs epicardial to endocardial layers which is essential for the normal activation and repolarisation of the left ventricle(21-23). β_1-adrenergic receptor stimulation increases the generation of cAMP from ATP via the stimulation GTP-binding protein (See figure 1.3). The cAMP directly increases the I_f current in nodal cells leading to increased AP generation rate, ultimately increasing heart rate. Via protein kinase A (PKA) the increased cAMP levels also lead to increased activity of Ca^{2+} L-type channels that leads to even further steeper slope of the pacemaker potential, increasing the heart rate (10, 24, 25). In non-nodal cells the changes in the Ca^{2+} L-type channels, the higher activity of the ryanodine receptors (RYR) and SERCA (due to lowered inhibition via phosphorylation of phospholamban (PLB)) and increased activity of the delayed rectifier channels K^+ channels (i_{KV}) result in increased Ca^{2+} levels available for the contractile apparatus resulting in increased contractile force generated and faster relaxation allowing a faster beating rate (essential for exercise for example)(26-28). The increased heart rate, increased contractility, faster relaxation and faster conduction through the AV node are in some patients commonly blocked with beta-blockers.

1.2 Cardiac arrhythmias

It is essential for proper functionality of the heart as a pump and hence the circulation of blood throughout the body that the cardiomyocytes are able to generate a coordinated and directed contraction. This is known as sinus rhythm where the heart of adult humans beat 60-100 beats/minute at rest depending on physical fitness and age. Several factors affecting the electrophysical properties of the heart can cause disturbances thatare proarrhythmic including acute ischemia, heart failure, cardiac fibrosis and cardiac hypertrophy. Changes can also be due to genetic changes in ion channels leading to specific channelopathies like e.g. long QT syndrome, a genetic abnormality in KCNQ1 leading to prolonged plateau phase increasing risk of Ca^{2+} overload and afterdepolarisations(29, 30).

All these possible changes in electrical or physical properties of the heart can lead to arrythmias either in the atria or ventricles. Atrial fibrillation (AF) is characterised by disorganised excitation and propagation through the affected atria so the atria is incapable of coordinated contraction leading to stagnation of blood in the atria and increasing the risk of stroke, but equally to often leading to irregular ventricular beating rate(29).

1.2.1 Atrial fibrillation

Atrial fibrillation (AF) is the most common heart rhythm disorder estimated in the Global Burden of Disease Study 2010 to be affecting approximately 20.9 and 12.6 million men and women worldwide, respectively (31). The number of people affected by AF is increasing year by year and is estimated to keep increasing, with numbers reaching 14-17 million people in Europe by 2030 and with 120,000–215,000 new diagnoses of AF per

year (32). AF is classified as paroxysmal AF or persistent AF, with each observed in a quarter of patients, while permanent AF is observed in around half the patients (32, 33). AF patients are associated with higher risk of developing other conditions including stroke (20-30 % of strokes are due to AF), heart failure, coronary artery disease, valvular heart disease, and cardiomyopathy(34, 35). As AF prevalence is predicted to keep increasing even more patients will experience significantly decreased quality of life (QoL) and it will also have a huge impact on public health (34, 35).

1.2.2 Pathophysiology of AF

The pathophysiology of AF is complex and there are many factors influencing the onset and maintenance of AF. There are two basic mechanisms sustaining the pathophysiology of AF: ectopic beats likely due to focal triggering via afterdepolarisations, and prematurely re-excited cardiomyocytes supporting re-entry circuits (36-38). Local ectopic firing or single localised re-entry circuit around the entry of the pulmonary veins are usually involved in incidents of AF (39, 40). The remodelling of the electric properties of the tissue due to altered expression and/or remodelled function of the cardiac ion channels leads to the development of functional re-entry substrates and contributes to persistent AF(39, 40).

1.2.2.1 Ectopic Firing

The ectopic activation in atrial tissue is caused by delayed afterdepolarisations (DADs), early afterdepolarisations (EADs) and in some case by enhanced automaticity of the tissue (36, 40). In normal atrial cells, the negative resting membrane potential is

maintained by a high permeability of K^+ through K^+ channels, especially the inward rectifier K^+ current (I_{K1}) and NKA(39, 40). Atrial cells are known to contain some I_f as well, which in sinoatrial node cells drives the initiation of APs (36, 40, 41). Under normal circumstances in atrial cells, the I_f has limited influence in the initiation of APs as it is overwhelmed by the high permeability through I_{K1}(38, 40). There is evidence that development of ectopic firing due to enhanced automaticity occurs due to changes in the relationship between the I_f and I_{K1} increasing the influence of I_f on the initiation of APs (36, 40, 42, 43).

EADs are early afterdepolarisations of the membrane potential during the repolarisation phase of the AP (39). The main driver of EADs is the prolongation of the AP duration (APD), due to prolonged activation of the L-type Ca^{2+} current (I_{CaL}), late sodium channels or NCX, leading to the inward movement of depolarising Ca^{2+} or Na^+ ions (36, 40, 44, 45) This can then lead to depolarisation of the membrane potential and triggering of another, premature, action potential.

DADs are depolarisations of the membrane potential during diastole(39). The induction of DADs is usually due to an abnormal release of calcium from the SR to the cytoplasm during diastole due to Ca^{2+} overload(39). NCX drives three Na^+ ions in for one Ca^{2+} ion extruded per cycle, which creates a net depolarising current namely the transient inward current (I_{NCX}). Activation of the NCX during the relative or absolute refractory period can trigger the firing of another AP(37, 39). Calcium overload and subsequent

triggering of AP is common in congestive heart failure and due to digoxin overdose(35, 38, 40, 43).

1.2.2.2 Re-entry Circuits

As previously described, re-entry circuits can either be *s*ingle localised re-entry circuits or multiple functional re-entry circuits varying in time and space. They are favored by a reduced effective refractory period, a slowed conduction velocity, and also by barriers hindering conduction (e.g. infarcted tissue, fibrosis, fatty deposits), which thereby enables the stabilisation of re-entry circuits(37, 43). These re-entry circuits if stabilised can maintain the progress of AF and impact on the progression from paroxysmal AF towards a more persistent or even permanent phenotype of AF (35, 37, 38, 40).

There are currently two competing theories trying to explain the concept of re-entry circuits*,* the leading circle theory and the spiral wave theory. Both theories rely on the optimal balance between refractoriness of the cells, excitability determinants, and the structural composition of the atrial tissue(41, 42). The leading circle theory describes the re-entry circuits to happen spontaneously within the travelled circuit length, named the wavelength (WL)(41). WL depends on the refractory period (RP) and the speed of conduction named the conduction velocity (CV)(42). The relation is given by the equation: WL=RP*CV. The WL thereby determines the ability of the creation of re-entry circuits. The bigger the WL, the lower the risk of re-entry circuits with the opposite being the case with a low WL(42). That means a potential lowering of either the RP in the individual cardiomyocytes or the CV would promote AF via creating re-entry circuits(41,

43). The spiral wave theory is focused on the stabilisation of spiral-wave rotors, which is caused by a reduced RP leading to the same promotion of AF due to the re-entry circuits (40, 42, 43). Both models are able to describe the occurrence of APD shortening in some AF cases, for example where patients have gain of function mutations of K^+ channels or when drugs have been used as therapies(43, 46).

The spiral wave model better explains the usefulness of Na^+ channel blockers as therapy in AF compared to the leading circle theory. On the other hand, the CV slowing due to either loss-of-function Na^+ channel and connexin mutations is easier explained by the leading circle theory(39, 43). Still, neither theory is able to completely explain all cases of the development of the re-entry circuits (38, 40, 46, 47).

1.2.3 Permanent AF, Treatments and RATE-AF

Upon diagnosis of permanent AF, rhythm control anti-arrhythmic drugs are no longer pursued, instead strategies for rate control are considered as frontline therapy (48). Many of these patients along with rate control therapy, also get treated with oral anticoagulation (OAC) therapy to reduce the high risk of stroke (49). Three groups of agents are used for rate control in AF including beta-blockers, calcium channel blockers (CCBs) and digoxin (50, 51). The use, background and limitation of the current treatment are briefly mentioned here.

CCBs like verapamil (See figure 1.3) used for AF patients exert mainly two effects on the heart. CCBs block the L-type Ca^{2+} channels which are channels involved in the generation of APs in nodal cells. Thus, with less Ca^{2+} flowing into the cells, the rate of AP generation slows down resulting in a lowered heart rate(2). In some patients with AF, the calcium channel blockers were shown to provide better rate control compared to beta-blockers(52). Secondly, CCBs lead to reduced contractile force due to its effects on L-type Ca^{2+} channels and thus reduced Ca^{2+} release from the SR and lowered Ca^{2+} availability for the cross bridging of filaments. This limits the use of CCBs in AF patients with concomitant heart failure with reduced ejection fraction (HFrEF) as they exert a negative inotropic effect reducing the ejection fraction even further(53, 54). Considering that around half the patients with AF have HFrEF, the use of the CCBs is limited for these patients (55).

Beta-blockers work by blocking the β1-adrenoceptors and thereby reducing sympathetic activity (see figure 1.3). Main effect is lowering of the amount of cyclic adeno mono phosphate (cAMP) generation inside the cell and thus 1) reducing the funny current (i_f) leading to decreased heart rate 2) decreased Ca^{2+} channel opening (L-type) 3) decreased conduction speed through AV node, increasing the delay between atrial and ventricular contraction(2).

Thus, beta-blockers are commonly used for hypertension and for angina patients, but also used as treatment of AF and heart failure (HF) (56). In HF studies with patients having reduced ejection fraction, beta-blockers have previously been shown to reduce all-cause

mortality in sinus-rhythm patients compared to placebo while this beneficial effect seems lost in patients with AF (56, 57). In patients with preserved ejection fraction (pEF), around half of patients, beta-blockers show a reduction of overall mortality in observational studies, while in the clinical trials so far no reduction was observed (55). Furthermore, beta blockers seem to be very well tolerated among all sinus rhythm and AF patients regardless of gender or age(58). Together this provides the basis for the wide use of beta-blockers.

Digoxin and digitoxin are cardiovascular therapies frequently used to treat patients with atrial fibrillation and/or heart failure, with variable clinical outcome(59-61). These medications are derived from the foxglove plant, and share structure, function and primary binding site on NKA with a range of other cardiotonic steroids (CTS). The use of foxglove extracts for treatment of dropsy and HF was initially described by the English botanist and doctor William Withering back in 1785(62). Ever since, the use of digoxin has been discussed as it is still not clear whether digoxin is beneficial and if so for which patient groups.

At therapeutic doses digoxin mainly exert effects through the inhibition of NKA leading to accumulation of Na^+ intracellularly which in return leads to increased Ca^{2+} levels via the NCX. Thereby left ventricular systolic contractile function is improved. The toxic range of doses are only slightly higher than therapeutic range, which could potentially lead to excessive accumulation of Ca^{2+} leading to Ca^{2+} store overload, which increases the risk of triggering DADs and arrhythmias(39, 63). Digoxin and ouabain have both been

shown to reduce heart rate(64), and this is likely to be the primary mechanism for beneficial effects observed in patients with atrial fibrillation and heart failure. In more recent times prescriptions of digoxin have decreased, as the evidence of its beneficial use was limited until 1997, when the Digitalis Investigation Group (DIG) trial was published(59). The DIG trial compared digoxin with placebo in treatment of HF. Patients with AF were excluded from the trial. The trial showed limited effects of digoxin on the overall mortality but reduced the hospitalisation and symptoms HFrEF patients(65). Furthermore, the benefits of digoxin were shown to be limited when observational studies detected a higher mortality in AF patients when treated with digoxin(66, 67). Importantly, the use of digoxin as treatment in AF patients has not yet been addressed in a randomised clinical trial (RCT) compared to for example the use of beta-blockers(60, 61). Furthermore, reports of toxic effects and challenges with correct digoxin dosing leaves many questions unanswered, in terms of its use in clinical settings for patients with HF and AF (59, 60, 65). The use of digoxin in clinical settings is not yet based on a RCT and still leaves questions in terms of benefits and safety for individual patients and especially for AF patients with concomitant HF(57, 60, 61).

On this basis, the Rate Control Therapy Evaluation in Atrial Fibrillation (RATE-AF) trial(68) was initiated in 2016 with the focus of comparing the use of beta-blockers and digoxin for treatment of permanent AF. The RATE-AF trial main outcome is QoL reported by patients. Secondly, both cardiac function, exercise capacity, and biomarkers of cellular and clinical effects will be investigated. This PhD project is a basic science project and was launched in links with part of the RATE-AF trial focusing on the

development of assays for detection and quantification of potential biomarkers from plasma samples received from the patients in the trial.

1.3 The Na+/K+-ATPase: structure and function

1.3.1 Na+/K+-ATPase

The Na+/K+-ATPase (NKA) was initially discovered by Skou et al, which showed NKA to be converting free energy of adenosine triphosphate (ATP) into electrochemical gradients (69). It was later established that NKA transports three Na^+ ions out and two K^+ ions in against their concentration gradients thereby establishing a Na^+ gradient over the membrane (70, 71). NKA ensures this transport in several smaller steps (Figure 1.4).

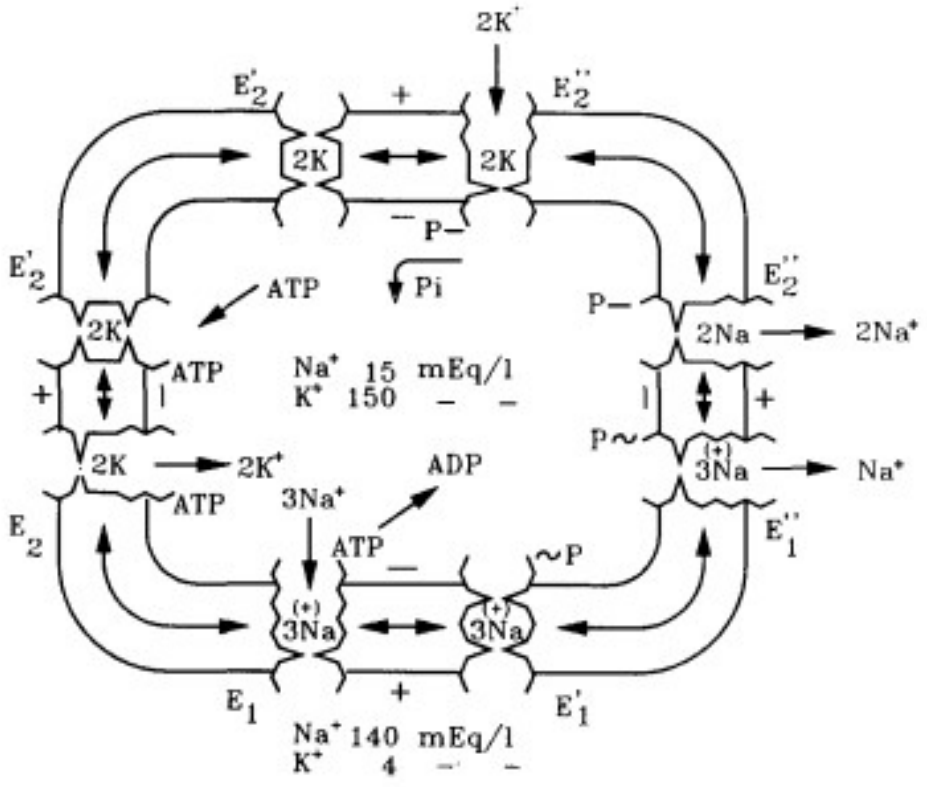


Figure 1.4 A Post-Albers kinetic scheme – Transport of Na+ and K+ over the membrane via several enzymatic steps. Adapted from Skou 1998(71).

First, 3 intracellular Na^+ ions bind to the high affinity cation ion site inducing a phosphorylation of NKA leading to adenosine diphosphate (ADP) leaving and closing in the 3 Na^+ ions. Secondly, another conformational change occurs opening up for 3 Na^+ ions to leave to the extracellular milieu. Two K^+ ions then bind to the exposed extracellular binding site leading to dephosphorylation of NKA leading to P_i leaving and the occlusion of the 2 K^+ ions. Finally, ATP binding induces conformational change leading to the release of the 2 K^+ to the intracellular space (71, 72). The NKA is located in the plasma membrane and consists of two subunits α and β subunit in a 1:1 ratio (Figure 1.5)(73). The α-subunit is composed of 10 transmembrane (TM) domains. The α-subunit has binding sites for several molecules including cardiotonic steroids (CTSs) (shown in red in Figure 1.5) on the extra-cellular side. On the intracellular side, there is a binding site for ATP (shown in blue in Figure 1.5), the phosphorylation domain (shown in yellow in Figure 1.5) and the actuator domain (shown in green in Fig. 1.5), which is responsible for the dephosphorylation step. The β-subunit is the regulatory unit and is composed of a single TM domain and is responsible for the trafficking and integration into the plasma membrane. The extracellular part of the β-subunit has interactions with the TM7-TM8 parts of the α-subunit. Several small regulating proteins containing the FXYD motif e.g. phospholemman (PLM) are expressed in cardiac tissue (Figure 1.5) and collocate with NKA in the plasma membrane(70, 71, 74).

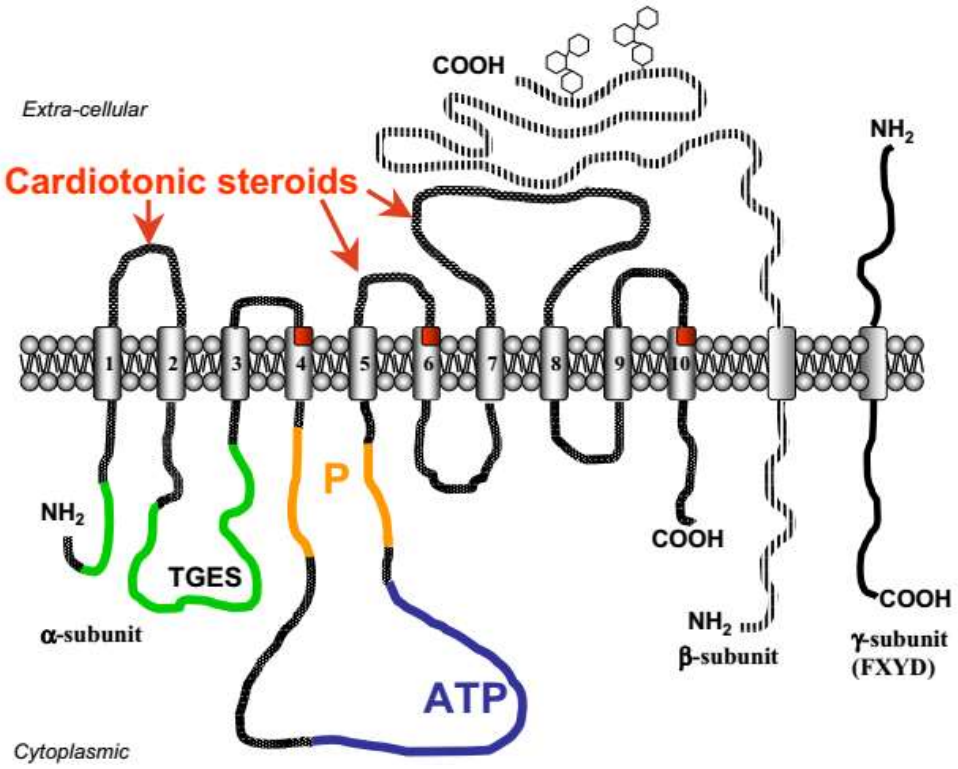


Figure 1.5 The structure of Na+/K+-ATPase. The NKA is comprised of an α subunit and a β subunit. FXYD motif containing small protein is associated very closely with the NKA in the membrane. Adapted from Bagrov et al., 2009(73).

The α-subunit of NKA has four isoforms while the β-subunit has three (72, 75). The majority of NKAs are in the α1/β1 isoform, which is expressed in most tissues and are the dominant isoforms in the heart (75, 76). The α2 is limited to being expressed in adult heart, both smooth and skeletal muscle, the brain and adipocytes (72, 75). The α3 and α4 isoforms are more tissue specific and localise mainly in excitable tissues and in the testes, respectively (70). β2 and β3 are both widely expressed in various tissues including brain, cartilage, and erythrocytes (77).

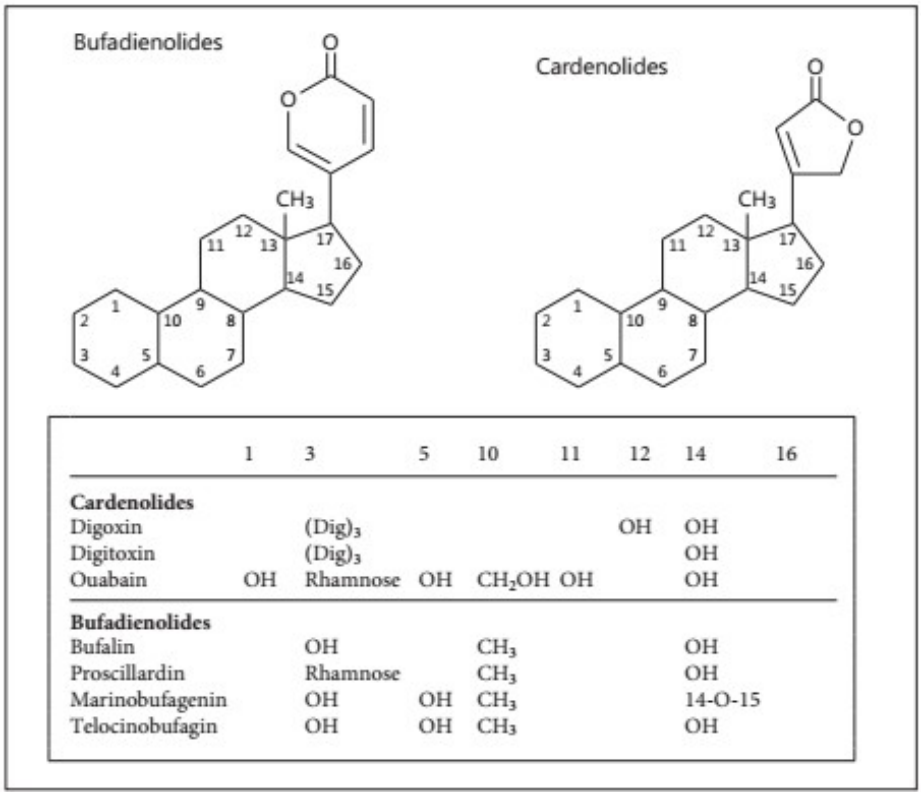
1.3.2 NKA Regulation

NKA regulates the intracellular Na^+ and K^+ concentrations generating an electrochemical gradient for other transporters to use(71). NKA-mediated regulation of intracellular Na^+ directly affects a number of transporters including the NCX and the sodium-hydrogen exchanger (NHE)(72). Both are driven by the Na^+ gradient and inhibition of NKA or an increased uptake of Na^+ via NCX in pathophysiological situations e.g. myocardial ischemia can lead to increased Na^+ intracellularly and subsequent inhibition of NCX and NHE which can lead to increased Ca^{2+} intracellularly and increased pH, respectively(72). Thus, a tight regulation of NKA activity is essential to maintain ion homeostasis and can be regulated in several ways by e.g. membrane-associated components such as PLM and many different circulating factors (e.g. CTSs) as well as a variety of hormones (72, 78).

In cardiac tissue PLM, a 72 aa long protein, is a major regulator of the activity of NKA, which can be explained by their very close association in the plasma membrane and contains sites for phosphorylation in its C-terminal terminus, which enables it to regulate NKA(79). Unphosphorylated PLM inhibits NKA activity, and phosphorylation of PLM relieves this inhibition(80). PLM is phosphorylated by two protein kinases namely PKA and protein kinase C (PKC). PKA can phosphorylate PLM at Ser-68 while PKC phosphorylates at either Ser-63, Ser-68 or Thr-69(80). The activity of PKA can be regulated by β-adrenergic stimulation of the cell via increases in intracellular cAMP(80, 81). While the activity of PKC is directly linked to intracellular Ca^{2+} and regulated by e.g. increased α-adrenergic stimulation leading to induction of the phospholipase C (PLC) pathway that ultimately leads to an increase in PKC activity (79-81).

1.4 Cardiotonic Steroids

The CTS can structurally be divided into two distinct groups: the cardenolides and bufadienolides. The main difference is that cardenolides like digoxin and ouabain have at their carbon 17 a 5-membered unsaturated lactone ring attached, while the bufadienolides have a double unsaturated 6-membered lactone ring attached (Fig.1.6)(76). Furthermore, cardenolides share a hydroxyl group at carbon 14 while in some bufadienolides a 14-15 epoxide is observed. Both the cardenolides and the bufadienolides are sometimes glycosylated at carbon 3(76). Interestingly, as CTS are structurally very similar, the ability of CTS to bind to and inhibit the NKA is very conserved(77).



	1	3	5	10	11	12	14	16
Cardenolides								
Digoxin		$(Dig)_3$				OH	OH	
Digitoxin		$(Dig)_3$					OH	
Ouabain	OH	Rhamnose	OH	CH_2OH	OH		OH	
Bufadienolides								
Bufalin		OH		CH_3			OH	
Proscillardin		Rhamnose		CH_3			OH	
Marinobufagenin		OH	OH	CH_3			14-O-15	
Telocinobufagin		OH	OH	CH_3			OH	

Figure 1.6 The steroid structure of bufadienolides and cardienolides. The bufadienolides have a double unsaturated 6-membered lactone ring attached while the cardenolides have a 5-membered unsaturated lactone ring attached. Furthermore, the main substitutions from the general structure is shown as well. Adapted from Pavlovic, 2014(76).

1.4.1 The Biosynthesis of CTS and Effects on Tissues

Increasing amounts of evidence suggest endogenous CTS are synthesised in the adrenal cortex in the adrenal gland from cholesterol and that this process is regulated by adrenocorticotropic hormone (ACTH) and angiotensin with initiation by ouabain synthesis in the hypothalamus in response to high salt intake (Figure 1.7) (70, 73, 82, 83). The acute effects of CTS are mediated by direct inhibition of NKA, resulting in increased cardiac output in the heart, excretion of more Na^+ by the kidneys and vasoconstriction of the smooth muscle cells in the vasculature(73, 76). Chronic exposure to CTS may lead to detrimental changes on various tissues, including cardiac hypertrophy, fibrosis, hypertension and arrhythmogenesis via a number of postulated mechanisms (Figure 1.7) (73, 76, 84). The complete biosynthesis pathways of these steroids still remain poorly understood. Even though several clinical studies have implicated endogenous CTS in disease, the exact involvement is still not fully elucidated and needs further experiments as many experiments in animals were carried out 1) at much higher concentrations compared to levels detected in circulation or those given to patients, and 2) were carried out more recently in animals like mice and rats which are known to have a much reduced sensitivity to CTS than humans (85, 86).

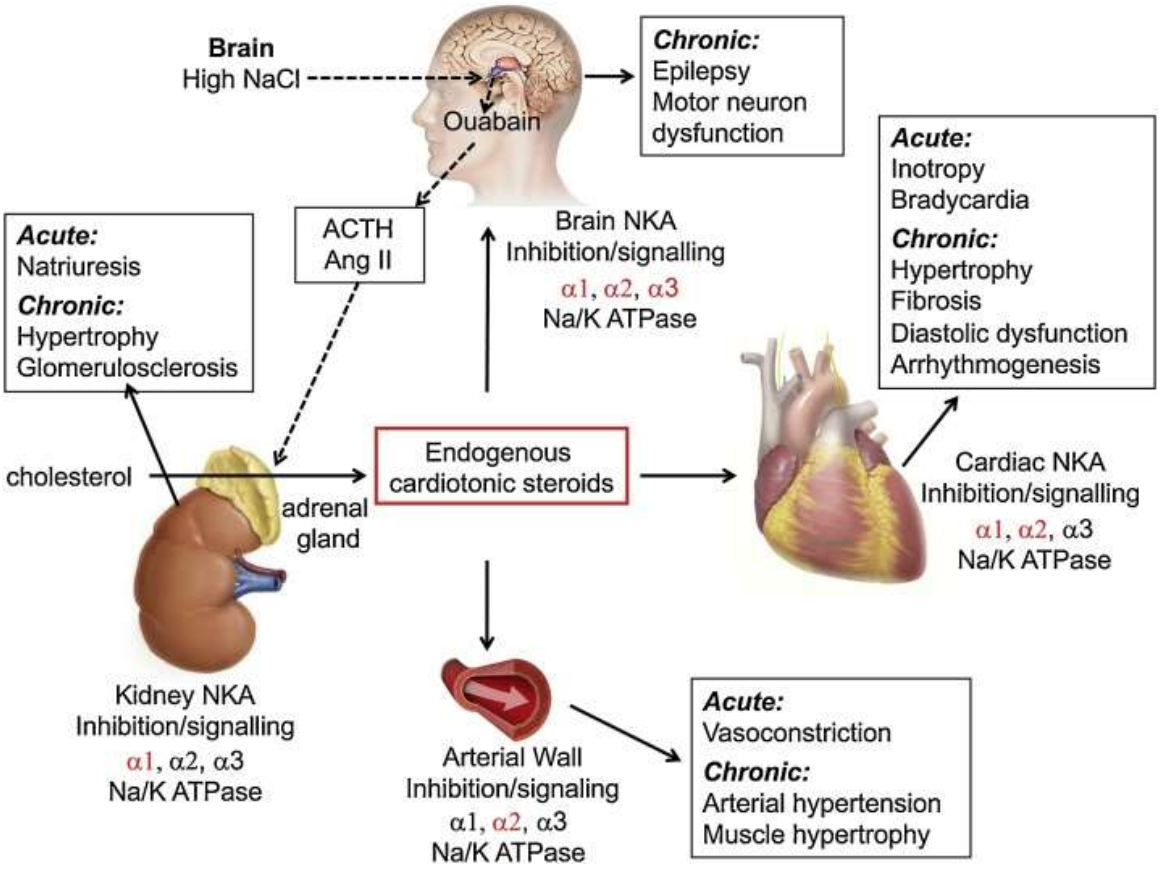


Figure 1.7 Proposed model of synthesis of CTS and acute and chronic effects on different tissues. Endogenous CTS are synthesised in the adrenal cortex from cholesterol regulated by adrenocorticotropic hormone (ACTH) and angiotensin II initiated by ouabain synthesis in the hypothalamus in response to high salt intake. Short-term endogenous CTS by inhibition of NKA increases cardiac output in the heart, excretion of more Na+ by the kidneys and vasoconstriction of the smooth muscle cells in the vasculature. Long-term related effects of endogenous CTS are remodelling in the tissue leading to hypertrophy, fibrosis, hypertension and even arrhythmogenesis through various mechanisms. ACTH = adrenocorticotropic hormone, Ang II =. Angiotensin II. Adapted from (87).

1.4.2 Effects of CTS on signaling

CTS have mainly two ways of interacting with NKA, via the ionic and the signaling pathway (Figure 1.8). The effect of CTS and sensitivity of NKA seem to be dependent on the localisation of NKA either in the plasma membrane or in caveolar domains. The ionic pathway describes an initial binding of CTS to NKA and thereby leading to inhibition of

the activity of NKA (70, 76). This results in an increase in Na^+ intracellularly, leading to NCX inhibition or even reversal of the NCX to favor Ca^{2+} accumulation or influx, respectively, leading to increase of intracellular Ca^{2+}(76). The increased intracellular Ca^{2+} mediates enhanced cardiac contraction but chronically high diastolic Ca^{2+} can also initiate activation of pro-hypertrophic or pro-fibrotic signaling pathways (76). There is evidence that these signaling pathways are Src dependent(70). Upon CTS binding to NKA the activation of Src leads further to transactivation of the epidermal growth factor receptor (EGFR)(70). It is proposed that small, sub-nanomolar, concentrations of CTS are needed to activate these signaling pathways leading to hypertrophic and fibrotic signaling cascades in the nucleus via activation of PLC, MAPK/ERK kinase (MEK)1/2, phosphoinositide 3-kinase (PI3K) and PKC among others(70). Finally, upon binding of CTS to the NKA-Src-EGFR complex an internalisation of the whole complex (CTS-NKA-Src-EGFR) can be initiated(88). Activation of these pathways was suggested to lead to hypertrophic growth of the heart(76).

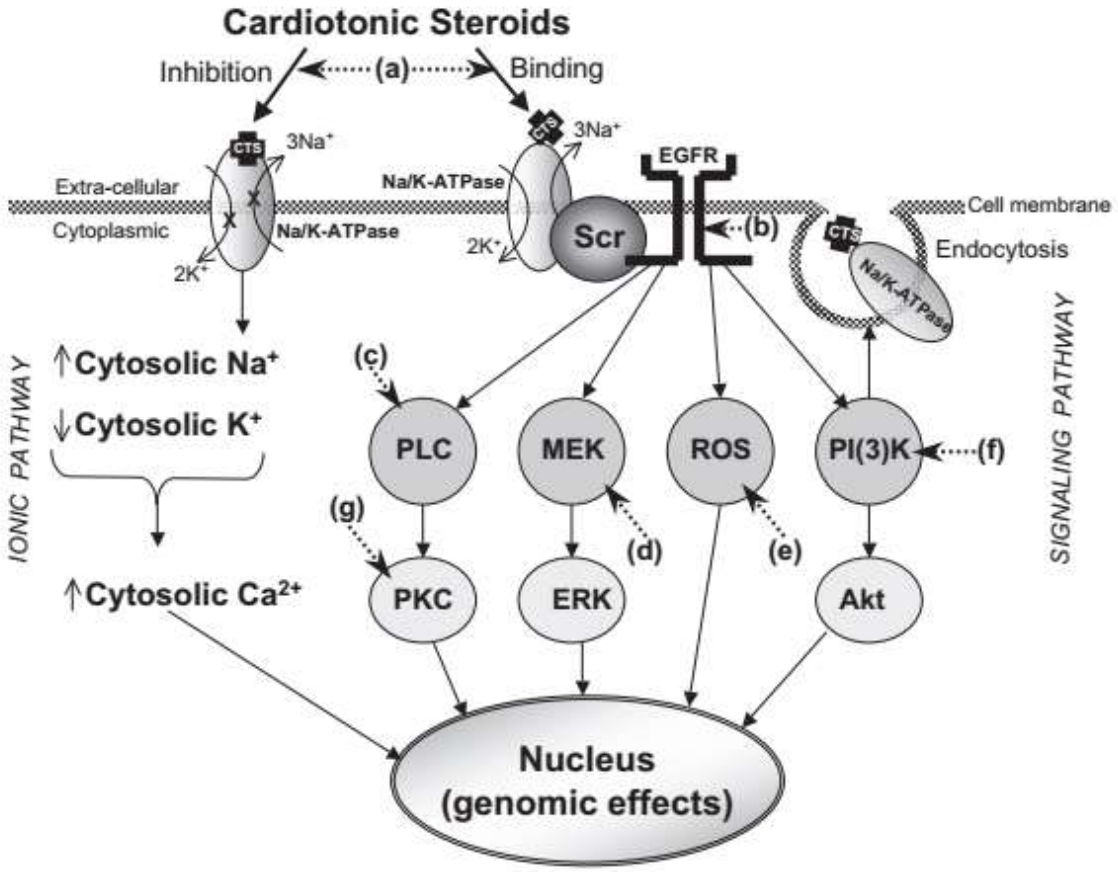


Figure 1.8 Schematic overview of the two pathways for the interaction between CTS and NKA i.e. the ionic and the signaling pathway. The ionic pathway via its inhibition of NKA leads to increase of Na^+ subsequently driving Ca^{2+} influx via NCX, leading to effects on contraction in CMs but also can exert genomic effects. CTS binding to NKA can also activate a signaling pathway via the activation of Src, which leads to transactivation of the epidermal growth factor receptor (EGFR). This leads to changes in pathways of hypertrophic and fibrotic signaling in the nucleus via activation of PLC, MAPK/ERK kinase (MEK)1/2, phosphoinositide 3-kinase (PI3K) and PKC. Adopted from (73).

1.4.3 Detection of CTS

Many studies have to date detected a number of CTS in circulation or urine, demonstrating elevated levels ofeither digoxin, ouabain, marinobufagenin, bufalin or telocinobufagin, in experimental animal models and in patients with various volume related diseases such as hypertension, preeclampsia and heart failure(89-198).

Particularly ouabain and marinobufagenin have received much attention. Although being from different CTS classes, both ouabain and marinobufagenin have been demonstrated to be involved in hypertrophy and fibrosis in both cardiac and renal tissue in several experimental animal models (76, 77, 175, 199, 200). Over the last few decades, endogenous ouabain (EO) has been detected by several research groups and demonstrated to affect cardiac, renal and vascular function (76, 195). EO was initially reported by Hamlyn and co-workers to have been measured in plasma from humans (116, 201). EO has over the years been shown to be increased in a number of physiological and pathological states, including after acute physical exercise (171), in pregnancy (202) in plasma of hypertensive patients (156), in patients with congestive HF (121) and those with chronic kidney disease (185). All these studies indicate EO may have a role in the development or sustaining various diseases as EO increases.

1.4.4 Interaction between CTS – Ouabain and Digoxin Antagonism

Digoxin and Ouabain, both cardenolides, initiate their effects via the binding to the α-subunit of NKA (73, 76). Ouabain-digoxin antagonism has been investigated in several studies over the years in different tissues. It has been shown that ouabain is able to attenuate the effects of digoxin or bufalin on the intracellular membrane traffic despite the interaction being via the NKA binding site (203). Furthermore, it was shown that ouabain could lower the cardiotoxicity of digoxin both in primary isolated heart muscle from guinea pig but also in an *in vivo* model (204). Ouabain-digoxin antagonism was also observed in a study by Song and colleagues, investigating the effects of various CTS including ouabain and digoxin in rat arteries and nerones (205). The interaction between ouabain and digoxin (34, 35, 121, 195, 206) has not been directly examined in healthy or

diseased cardiac cells/tissues. Thus, in patients with HF where digoxin is used as a treatment, and where increased endogenous CTS are detected, one could imagine a potential interaction between digoxin and the endogenous CTS. Furthermore, with HF a common co-morbidity in AF patients (up to 50 % of symptomatic HF patients will have been diagnosed with AF), it is of interest to examine whether endogenous CTS are elevated and whether digoxin-ouabain antagonism plays a role in varied response to digoxin in this patient population.

1.5 This Thesis

This thesis will investigate the potential interaction between endogenous CTS and digoxin and will examine whether endogenous CTS affect the response to digoxin in the RATE-AF cohort of patients. Thus, in this thesis experiments were set out to develop 1) a cellular assay able to detect changes in intracellular Na^+ in response to incubation with serum or serum/plasma extract and 2) an ELISA able to detect and quantify endogenous ouabain in patient serum/plasma. The intracellular Na^+ assay was used to explore the effects of different CTS on intracellular Na^+ and their interaction with digoxin. The ELISA was developed to enable measurements of endogenous ouabain from the plasma/serum of patients with AF and HF. The aim of the work described here is to provide novel information on the role of endogenous CTS in patients with AF and to uncover novel stratification methodologies for digoxin responsiveness of patients with AF.

CHAPTER 2. MATERIALS AND METHODS

The methodology utilised and developed in this thesis is divided into two parts, 1) cellular-based technology for measuring intracellular sodium and 2) antibody-based technology for measuring ouabain concentration. As both of these technologies are being developed and optimised in this thesis, many of the details for each assay will hence be discussed in more detail below and in subsequent chapters; see chapter 3 & 4 for full method development and validation of the cell-based assay and antibody-based assay respectively.

2.1. Fluorescent assay for measuring intracellular Na^+

2.1.1. Culture of the HEK293t cells

Human embryonic kidney 293t (HEK293t) cells were purchased (ECACC cat. No. 12022001) and thawed according to the manufacturer's instructions. HEK293t cells were chosen as they are very easy to handle in the laboratory and as they can tolerate changes to environment including change in pH and temperature. In brief, cells were thawed by heating for 2-3 minutes in a 37 ˚C water bath followed by careful 1:1 dilution in 37˚C prewarmed Dulbecco's Modified Eagle´s Medium (DMEM) (Sigma cat. No. D6429) supplemented with 100 U/mL Penicillin/Streptomycin (Sigma cat No. P4333) and 10% Foetal bovine serum (heat-inactivated) (Sigma cat No. F9665) prior to centrifugation at 1500 rotations per minute (rpm) for 5 minutes. DMEM supplemented with 100 U/mL Penicillin/Streptomycin and 10% foetal bovine serum (heat-inactivated) was used for maintenance of HEK293t cells. The cells were subsequently resuspended in 1 mL culture

media, transferred to a 25 cm^2 culture flask containing 8 mL of DMEM and moved to an incubator containing air comprised of 5% CO^2, and 95% atmospheric air with a temperature of 37 ˚C. The culture media was changed after 4hrs to remove dead cells. Cell cultures were checked every 24hrs until confluent prior to transfer to a 75 cm^2 culture flask.

Cells were cultured and split every 2-3 days after reaching 85-90 % confluency. Splitting was carried out by washing the cells twice in Phosphate-buffered saline (PBS) (Sigma cat No. D8662) followed by the addition of 5 mL of Trypsin-EDTA (Sigma cat No. T3924), for 5-7 minutes, in order to detach the cells. Thereafter, the suspension of cells was diluted in 10 mL of media and centrifuged for 5 min at 1500 rpm. After the supernatant was carefully removed, the cells were resuspended in 3-4 mL of culture media, transferred to a culture flask containing approximately 20 mL of culture media and cultured in the incubator.

2.2. The methodology of measuring intracellular Na^+

The methodology is described broadly with variables being optimised and validated further in the subsequent chapter. tyrode was used for all experiments. Calibration stock solution A and B were used to create calibration solutions containing 0, 11, 22, 45 and 90 mM Na^+. Each calibration solution also contained ouabain (100 μM) needed as a blocker of NKA and Gramicidin (10 μμM) used to allow control of intracellular ion

concentrations. Solutions utilised for the HEK293t cell-based experiments are summarised below in table 1.1.

HEK293t Intracellular Na^+ Solutions	**Composition**
tyrode Solution	mM/L: 137 NaCl, 5.4 KCl, 1 CaCl2, 0.5 MgCl2, 10 HEPES, 10 glucose, pH 7.4, 1 mM probenecid)
Calibration solution A	mM/L: 30 NaCl, 115 NaGluconate, 2 EGTA, 10 HEPES, 10 glucose, pH 7.4, 1 mM probenecid)
Calibration solution B	mM/L: 30 KCl, 115 KGluconate, 2 EGTA, 10 HEPES, 10 glucose, pH 7.4, 1 mM probenecid)

Table 1.1 Composition of the solutions utilised in the HEK293t cell-based intracellular sodium experiments.

2.2.1. Measurement of intracellular Na^+ in HEK293t cells

40000 HEK293t cells in 100 µL of culture medium were seeded per well in black/clear bottom 96 well ViewPlates (PerkinElmer Inc., USA) and incubated until ~90% confluency in the incubator (5% CO2, and 95% atmospheric air with a temperature of 37 ˚C). 96 well plates were removed from the incubator and the media was gently removed from the wells and exchanged with the tyrode solution containing Na^+-sensitive fluorescent dyes, either 5 µM (in tyrode solution) Asante Natrium Green 2 (ANG-2-AM) (Abcam cat No. ab142802) or Sodium-Binding Benzofuran Isophthalate (SBFI-AM)

(Thermofisher cat No. S1263). Both dyes are AM-ester forms allowing the dye to cross the membrane of the cells. The fluorescent dye incubation times are tested and validated in Chapter 3. All incubations with fluorescent dyes were done at room temperature and shielded from light using aluminium foil. ANG-2 and SBFI stock solution was prepared by dissolving 50 µg in 46 µL and 44 µL Dimethyl sulfoxide (DMSO) (Sigma cat No. D5879), respectively. ANG-2 and SBFI were dispersed by adding 46 or 44 µL, respectively, of 20% Pluronic F-127 (Sigma cat no. P2443) (in DMSO) prior to 100-fold dilution in tyrode solution. The ANG-2 or SBFI dyes were replaced with 100 µL/well of tyrode solution spiked with varying concentrations of commercially available CTS, extracted CTS from spiked serum or with patient plasma samples diluted in tyrode solution (Figure 2.1). The length of time of incubation for adequate change in fluorescence was validated in Chapter 3.

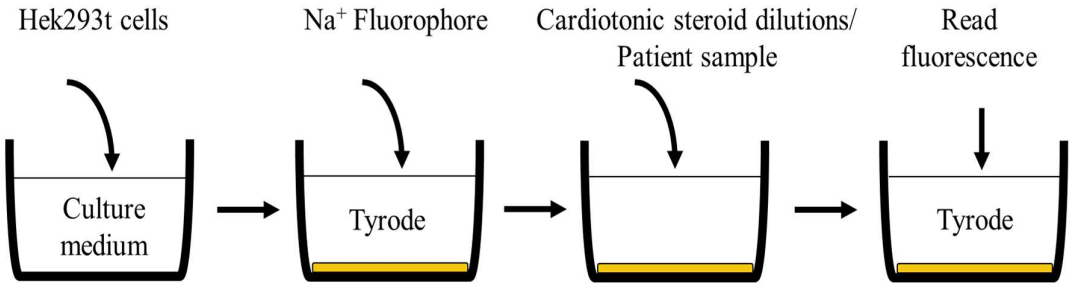


Figure 2.1 The general methodology of the developed intracellular sodium assay utilising HEK293t cells. HEK293t were seeded in 96 well plates and grown to ~90% confluency. The medium was exchanged with Na^+ fluorophore in tyrode. After 4 hours, the Na^+ fluorophore was exchanged with either cardiotonic steroids or patient samples diluted in tyrode, prior to measuring fluorescent changes after 3 hours.

For the Na^+ cellular assay, the concentrations of cardiotonic steroids (CTS) investigated ranged from 0.001 pM to 100 µM. All CTS were prepared in 1 mM stock solutions prior to dilution. Ouabain was prepared in tyrode solution. All other CTS were dissolved in

methanol, due to limited solubility in water. All further dilutions were made in tyrode solution. 1 mM probenecid (Thermofisher cat No. P36400) was added to limit the extrusion of the dye from the cells by blocking the activity of organic-anion transporters.

2.3. Detection and quantification of ouabain by ELISA

2.3.1. Primary antibody and Ouabain-BSA Coat

The primary antibody and the Ouabain-BSA coating are both a gift from Professor John Hamlyn (University of Maryland, Baltimore, Maryland). Both have been developed and described in full detail previously by Harris et al 1991(207).

2.3.2. ELISA methodology

The Enzyme-linked immunosorbent assay (ELISA) developed in this thesis is a competitive ELISA. The general protocol is shown below. The protocol employed in this thesis is adapted from the protocol developed by Harris et al 1991(207), but several steps have been optimised and validated (see chapter 4) prior to utilising the ELISA methodology on patient samples.

The composition of each of the buffers utilised in the ELISA methodology is summarised in table 2 below.

ELISA Buffer name	**Composition**
Coating solution	50 mM sodium carbonate buffer, pH 9.6, containing 11.4 mg/L thimerosal

Rinsing solution	50 mM sodium/potassium phosphate buffer, pH 7.4, 0.05% Tween 20 and 11.4 mg/L thimerosal
Blocking solution	50 mM sodium/potassium phosphate buffer, pH 7.4, 0.05% Tween 20, 11.4 mg/L thimerosal, and 10 g/L Bovine Serum Albumin (BSA)
Assay solution	50 mM sodium/potassium phosphate buffer, pH 7 with 2% Bovine Serum Albumin (BSA), 0.05% tween-20 and 0.1% chloroacetamide
Stop solution	1M H_3PO_4 (Mix 2 mL of 85% H_3PO_4 in 30 mL water)

Table 2 Composition of the solutions utilised in the ELISA

For the ELISA, the concentrations of cardiotonic steroids (CTS) investigated ranged from 0.01 pM to 10 nM. Most CTS were prepared in 1 mM stock solutions in methanol prior to dilution in assay buffer. Ouabain was prepared in assay buffer.

Firstly, the plates were coated with 50 µL of BSA-C6-Ouabain, added into each well in the plate(s) and kept at 4°C for 2 days. The concentration of the coating was optimised and validated as described in chapter 4. Plates were then washed by pipetting 100 µL of rinsing solution to each well three times to remove unbound BSA-C6-ouabain, prior to the addition of 100 µL blocking buffer to allow blocking unoccupied protein binding sites. The plates were incubated at room temperature with shaking (450 rpm). Appropriate blocking time is optimised in chapter 4. Prior to the addition of standards, samples and primary antibody, the plates were washed with 125 µL rinsing solution three times. For all experiments at least two replicates were treated as blanks and received 50 µL of assay

buffer with no primary antibody present. All standards and samples were diluted/reconstituted in assay buffer prior to addition in plates. This was to allow to background subtraction. 25 µL of standards and/or samples were added to at least two replicates followed by the addition of 25 µL primary antibody. The concentration of the primary antibody was tested and validated in chapter 4. The plate(s) were incubated for 1 hour at room temperature with shaking (450 rpm). Each plate was again washed with 125 µL rinsing solution three times. Next, the Goat Anti-rabbit horseradish peroxidase (HRP) conjugated (Merck Millipore, cat No AP370P) secondary antibody (1:1000 dilution in assay buffer) was added by pipetting 50 µL to each well followed by incubation for one hour. To allow detection of the horseradish peroxidase (HRP) activity, 50 µL of room temperature 3,3',5,5'-tetramethylbenzidine (TMB) (Thermo Scientific, cat No. 34028) were added to each well and incubated for 30 minutes for colour development, according to the manufacturer's instructions. The reaction was stopped by adding 50 µL stop solution (1M H_3PO_4). The plates were read at 450nm (also 650nm as a reference) on a flexstation plate reader (Molecular Devices, FlexStation 3 Multi-Mode Microplate Reader).

2.4. Samples from the BBC-AF Registry and the RATE-AF Trial

Samples from the Birmingham and Black Country Atrial Fibrillation (BBC-AF) registry were used to investigate the effects of different disease states (AF with/without HF vs Sinus rhythm) on intracellular Na^+ in HEK293t cells and ouabain levels detected by ELISA. Information about the collection process from BBC-AF patients including with or without anticoagulation were not known. These investigations were essential validation

of assays prior to RATE-AF trial samples. Treatments from either study of individual samples were blinded to avoid any bias of the investigator.

As a part of the RATE-AF trial, 160 patient blood samples were collected at the first visit as a baseline in EDTA tubes. Sample time between baseline and follow up are not known, but dependent on patient availability thus probably not same time during the day. Another blood sampling was carried out 6 months after the randomised digoxin or beta-blocker therapy. Samples from both time points were utilised in this thesis for analysis of 1) endogenous ouabain levels using ELISA and 2) effects on intracellular Na^+ in HEK293t cells.

2.5. Solid-phase Extraction methodology

In this thesis, the Sola Solid-phase extraction (SPE) method was compared with the original SPE method (Bond Elute C18)(207) utilised for CTS prior to this thesis. These 2 methodologies were tested and compared as part of the validation of both the HEK293t assay and the ELISA developed within this thesis. Both protocols are shown below and were carried out to the manufacturer's instructions.

2.5.1. C18 Bond Elute SPE Method

C18 Bond Elute column (200mg bedding/3mL singular columns) (Agilent Technologies, cat No. 12102025) was washed three times with 3 ml of 0.1% trifluoroacetic acid diluted in distilled water, in order to prime the column. To allow extraction of cardiotonic steroid material, 2 mL of spiked sample or patient sample was passed over the column. To

remove unbound material and potential contaminants, the column was washed twice with 3 ml of 0.1% trifluoroacetic acid, followed by 3 mL of 2.5 % acetonitrile diluted in 0.1% trifluoroacetic acid. Lastly, the bound cardiotonic steroid material was eluted with 3 mL of 25% acetonitrile/75% water containing 0.1% trifluoroacetic acid. The eluent was collected in silanised glass vials, dried under nitrogen airflow and stored at -80 degrees until use.

2.5.2. Thermo sola SPE Method

The Thermo SOLA (SOLA HRP 10mg/2mL 96 well plate) (Thermofisher, cat no. 60309-001) methodology was carried out in 96 well plates. A positive pressure manifold (Biotage, PRESSURE+ 96 Positive Pressure Manifold) was used at each step to ease transfer. Each column was primed by the addition of 500 µL methanol per well followed by a washing step with 500 µL distilled water. 1 mL of spiked sample or patient sample was passed through the column to allow extraction of cardiotonic steroid material. Each column was washed two times with 500 µL distilled water to pass through contaminants and unbound material. The collection of the bound cardiotonic steroid material in a plastic collection plate was done carried out by using 2x 200 µL methanol as eluting agent . The plate was dried using an automated nitrogen evaporation system (Biotage, TurboVap 96) and stored at -80 degrees until use.

2.6. Data analysis and statistics

All data were analysed and plotted using GraphPad Prism (GraphPad Prism ver. 8.4.1 Software, CA, USA).

The statistic tests used were also carried out using GraphPad Prism. The statistical test utilised for specific experiments are stated in the relevant figure legend. All graphs are plotted as mean ± standard error of the mean (SEM).

CHAPTER 3. METHOD DEVELOPMENT FOR DETERMINING THE EFFECTS OF CTS IN HEK293 CELLS

3.1. Introduction and aims

It is essential to maintain constant intracellular Na^+ concentration as it is involved in many cellular processes, including involvement in resting membrane potential, action potential generation and contractility. Thus a reliable tool for consistent measurements of intracellular Na^+ is required. Previously techniques have included at least 3 groups of detection methods each with their limitations(208). 1) Atomic absorption can be used to measure total sample Na^+ content, but are limited in use as the sample is destroyed in the process, and that the extracellular Na^+ usually is not distinguishable from the free intracellular Na^+(209, 210). 2) Nuclear magnetic resonance spectroscopy techniques are able to quantify intracellular from extracellular Na^+ in real time, but these are expensive, technically difficult to implement and cannot be applied to cells but only whole perfused hearts (211, 212). 3) Use of microelectrodes selective for Na^+ have been used by several group to assess the intracellular levels of Na^+(213-215). The drawback of this method is mainly the capability of only investigating one cell at the time thus limiting the use for screening as a high throughput assay.

Thus other methods are needed to allow for high throughput cellular experimentation. One option is the use of Na^+ sensitive fluorescent dyes. Over the years several Na^+ sensitive dyes have been tested for measurements of intracellular Na^+ during

physiological responses to changing environment in different experimental models. Most widely used is the sodium-binding benzofuran isophthalate (SBFI) dye(216-218), which is a ratiometric dye allowing corrections for baseline changes in experiments e.g. loss of cells during liquid change steps. SBFI has the limitation of excitation at UV range where cellular fluorescence and some pharmacological substances might interfere with the signal. More recently the Asante natrium green 2 (ANG-2) dye has been developed, with a slightly lower excitation energy resulting in potentially brighter signals and more amenable to use in living cells(219) however ANG-2 is not a ratiometric dye limiting corrections of baseline.

Both ANG-2 and SBFI were thus chosen to be assessed in this thesis for better suitability for potential use of measuring intracellular Na^+ in HEK293t cells.

The aims of this work are:

(i) To develop and validate a sensitive cell-based fluorescence methodology for detection of changes in sodium in response to cardiotonic steroids.

(ii) To test the effects of different cardiotonic steroids on intracellular sodium in HEK293t cells.

(iii) To assess changes in intracellular sodium in HEK293t cells following exposure to serum from patient samples from the BBC-AF registry.

(iv) To test and validate the use of solid-phase extraction methodology for cardiotonic steroid extraction from serum.

3.2. Additional methodology and data handling

3.2.1 Extraction and analysis of raw data

In this chapter, two sodium sensitive fluorescent dyes were used, i.e. Asante Natrium Green 2 (ANG-2) and sodium-binding benzofuran isophthalate (SBFI). The signal sensitivity for Na^+ is different between the two dyes with SBFI having the lower dissociation constant (SBFI Kd 11 mM vs ANG-2 Kd 34 mM). For ANG2 the relative fluorescence (RFU) measurements were done at excitation 490 nm and 550 nm emission. Emission cutoff at 530 nm was used to reduce bleed-through of the excitation into the emission spectrum. For SBFI, a ratio metric dye, excitation at both 340 nm and 380 nm was used with fluorescence emission collected at 505 nm, with 495 nm emission cut-off value. All data are presented as fold change unless otherwise noted. Fold change were calculated based on mean RFU of tested steroids divided by the mean RFU of either tyrode or monensin (see equation 1 below).

Equation 1:

$$Fold\ Change = \frac{Mean\ tested\ steroid\ (RFU)}{Mean\ Tyrode\ or\ Monensin\ (RFU)}$$

3.2.2 Analysis of dose-response curves

The dose-response curves of various steroids after normalisation were plotted in GraphPad Prism. The curves were subject to analysis using a 3-parameter logistic function, see equation 2 below.

Equation 2:

$$Y = Bottom + \left(\frac{Top - Bottom}{1 + 10^{(LogIC50 - X)}}\right)$$

Y = Response in fold change of either tyrode or monensin

X = Log(Concentration of steroid tested)

IC50 = Amount of X needed to get 50% of response of Y

Top = Plateau of response at the top end of dose-response curve

Bottom = Plateau of response at the bottom end of dose-response curve

3.3 Results

3.3.1 Development of an assay for intracellular Na^+ determination

Before using the Asante Natrium Green 2 (ANG-2) dye assay to measure changes in Na^+ for investigations of CTS, it is important to optimise the assay in terms of: dye entry, time of dye incubation, cell density and assay buffer. First, the entrance of the dye into the HEK293t cells was tested to make sure the assay could be used in these cells to measure changes in intracellular Na^+. Figure 3.1A shows the comparison between HEK293t cells with and without dye measured over a 3hr period. Cells with dye show a time-dependent increase in fluorescence over the time course while the cells without the dye show no increase in signal. Secondly, experiments were carried out to test whether inhibition if Na^+/Ca^{2+} exchanger (NCX), improves the sensitivity of the ANG-2 assay. The NCX transports Ca^{2+} in exchange for Na^+, thus the activity of the NCX could affect the intracellular sodium load and sensitivity of the assay. Ethylenediaminetetraacetic acid (EDTA) is a chelating agent which binds Ca^{2+}. Thus, two test solutions were used, tyrode

solution with or without EDTA instead of Ca^{2+} (See table 2.1 in methods). Figure 3.1B shows the comparison between the two test solutions: with or without EDTA and effect of ouabain (100 μM) measuring the changes in Na^+ using the ANG-2 dye in HEK293t cells. The tyrode without EDTA was observed to show a significantly reduced fold change in response to ouabain compared to all other conditions. The tyrode and ouabain (100 μM) are not significantly different from tyrode with EDTA, although it has a significantly higher fold-change compared to tyrode and significantly lower than the tyrode with EDTA when ouabain (100 μM) is added as well. Finally, the tyrode with both EDTA and ouabain (100 μM) shows a significantly higher fold-change than all other conditions. The effect of incubation time with the dye on the sensitivity of the Na^+ measurements was tested to ensure optimal use of the dye in experiments. As a positive control, gramicidin (10 μM) was used. Gramicidin (10 μM) is an ionophore, which produces a lot of channels allowing entry of Na^+ from the extracellular buffer. As the extracellular milieu has high amounts of Na^+, the use of gramicidin (10 μM) should increase intracellular Na and thus serve as a positive control for the dye. Ouabain (100μM) was also used as a positive control. In figure 3.1C at 2-6hrs of dye incubation both gramicidin (10 μM) and ouabain (100μM) significantly increase the intracellular Na^+ response compared to their controls with tyrode. At 2-4hrs gramicidin (10 μM) shows a significantly higher fold-change than the ouabain (100μM), while this difference is not present at 6hrs. The sensitivity of the assay is observed to increase significantly over time peaking at 4 hrs with either gramicidin (10 μM) or ouabain (100μM) and then decaying thereafter. At 8hrs the sensitivity of the assay is observed to be significantly reduced compared to all other time points, with especially the ouabain (100μM) showing lower sensitivity than the control. Finally, experiments investigating the effects of cell density

during the assay were carried out. Next, experiments were done to test how the confluency of cells used in the assay affects assay performance. Figure 3.1D show the effect of cell density ranging from 30-90% on measurements of intracellular Na+ in the presence or absence of gramicidin (10 μM) or ouabain (100 μM). The gramicidin (10 μM) with cells at 50-90% confluency is observed to significantly increase the fold-change in assay response compared to controls, with a tendency of the sensitivity to increase from 50% towards 90% confluency without being significantly different. Gramicidin (10 μM) at 50-90% confluency show a significantly higher response than at 30% confluency, where the sensitivity of the assay seems lost. The ouabain (100 μM) treatment in these experiments did not seem to have any effect in the assay, although at 30% ouabain (100 μM) is significantly lower compared to both 90 and 50%.

To summarise, figure 3.1A shows the ability of the dye to enter the cell over time. Figure 3.1B shows a small improvement in increases in intracellular Na^+ following ouabain exposure in the presence of EDTA. This effect can potentially be explained by the EDTA binding the Ca^{2+} which blocks NCX activity leading to accumulation of more Na^+ inside the cells. In figure 3.1C the sensitivity of the measurements of intracellular Na^+ rise and peaks at 4 hrs with both gramicidin (10 μM) and ouabain (100 μM). Lastly, figure 3.1D shows that 90% confluency leads to improvements in sensitivity of the assay.

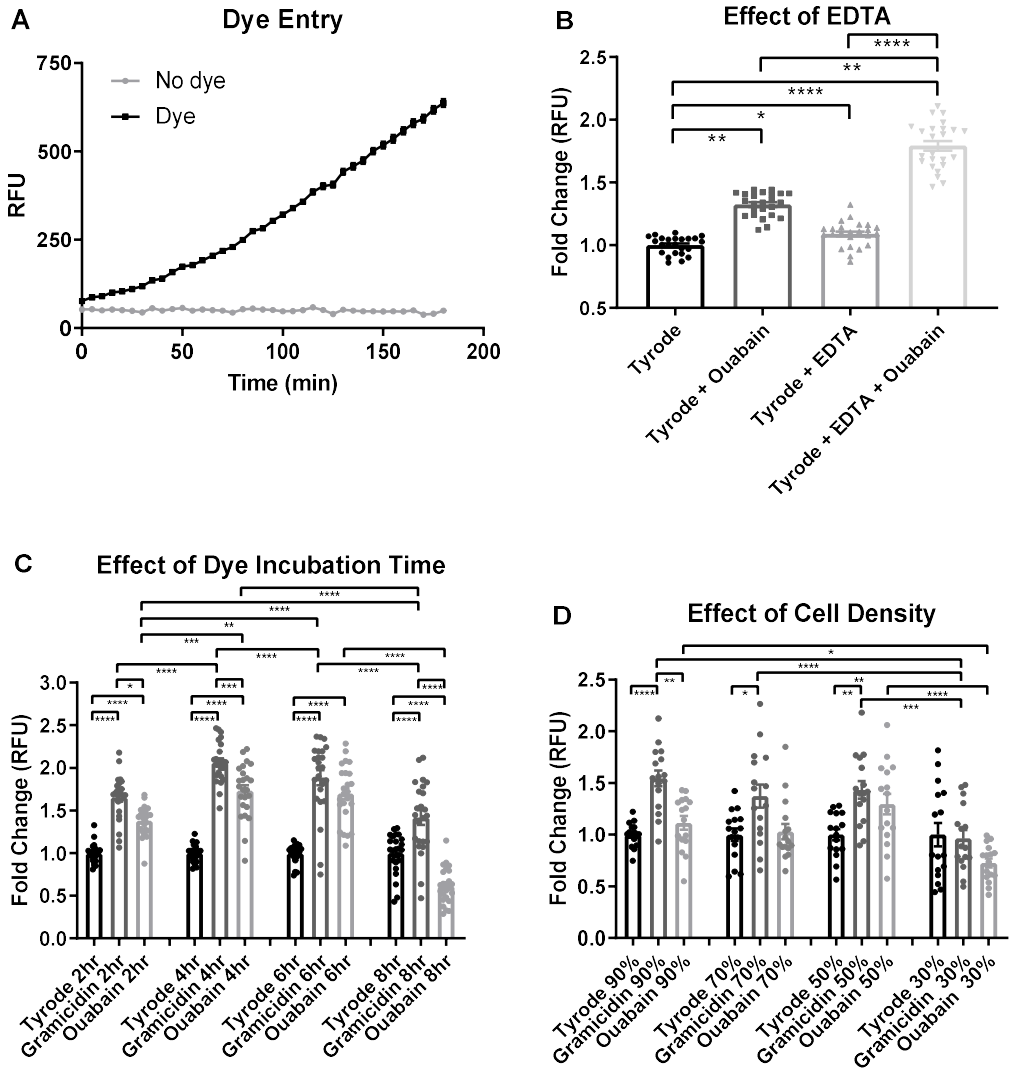


Figure 3.1 Optimisation of intracellular sodium assay in HEK293t cells. (A) represents intracellular Na^+ responses over a 3hr time course in HEK293t cells with/without dye. Both conditions represent 48 replicates from 1 experiment. (B) represents intracellular Na^+ responses normalized to control in response to a 1.5hr treatment with either tyrode, tyrode with ouabain (100 µM), tyrode with EDTA, tyrode with EDTA and ouabain (100 µM) in HEK293t cells. All conditions represent 32 pooled replicates from 4 experiments. (C) represents the effect of incubation time (2-8 hrs) on the sensitivity of the intracellular Na^+ measurements normalized to control in response to a 3hr treatment with either tyrode, tyrode with ouabain (100 µM) or tyrode with gramicidin (10 µM) in HEK293t cells. All conditions represent 24 pooled replicates from 3 experiments. Figure 6D shows the effect of cell density (30-90%) on the sensitivity of the intracellular Na^+ measurements were normalised to control in response to a 3hr treatment with either tyrode, tyrode with ouabain (100 µM)

or tyrode with gramicidin (10 μM) in HEK293t cells. All conditions represent 16 pooled replicates from 2 experiments. All data is presented as mean +/- SEM. Statistical test was a one-way ANOVA with Tukey post hoc test (Panel 5B) or Bonferroni post hoc test (panel 5C and 5D) for multiple comparisons, **** $p < 0.0001$, *** $p < 0.001$,** $p < 0.01$ and * $p < 0.05$ between the different tested groups.

3.3.2 Dose-Dependent Effects of Cardiotonic Steroids Using Asante Natrium Green 2 Dye

Dose-dependent response curves of different CTS at a range from 10 pM to 100 μM were generated using the ANG2 dye. CTS included cardenolides (digoxin, digoxigenin, ouabain, ouabagenin, digitoxin and digitoxigenin) and bufadienolides (marinobufagin, telocinobufagin and bufalin).

All the CTS tested demonstrated a robust dose-dependent increase in intracellular Na^+ (Figure 3.2A-I). This data was utilised to derive IC50 and maximal response (Imax) (Table 3.1). The bufadienolides demonstrate lower IC50 values compared to the cardenolides with the exception of ouabain having lower IC50 than marinobufagenin. Removal of the sugar groups from cardenolides, i.e. ouabagenin, digoxigenin and digitoxigenin leads to marked increase in IC50 values compared to ouabain, digoxin and digitoxin, respectively. Digoxin was observed to have considerably higher maximal response in comparison to the bufadienolides and all the other cardenolides except for the related digoxigenin. The Imax did not show any different for cardenolides with or without their sugar groups, as was the case for the affinities of binding, except for digitoxigenin (Table 3.1).

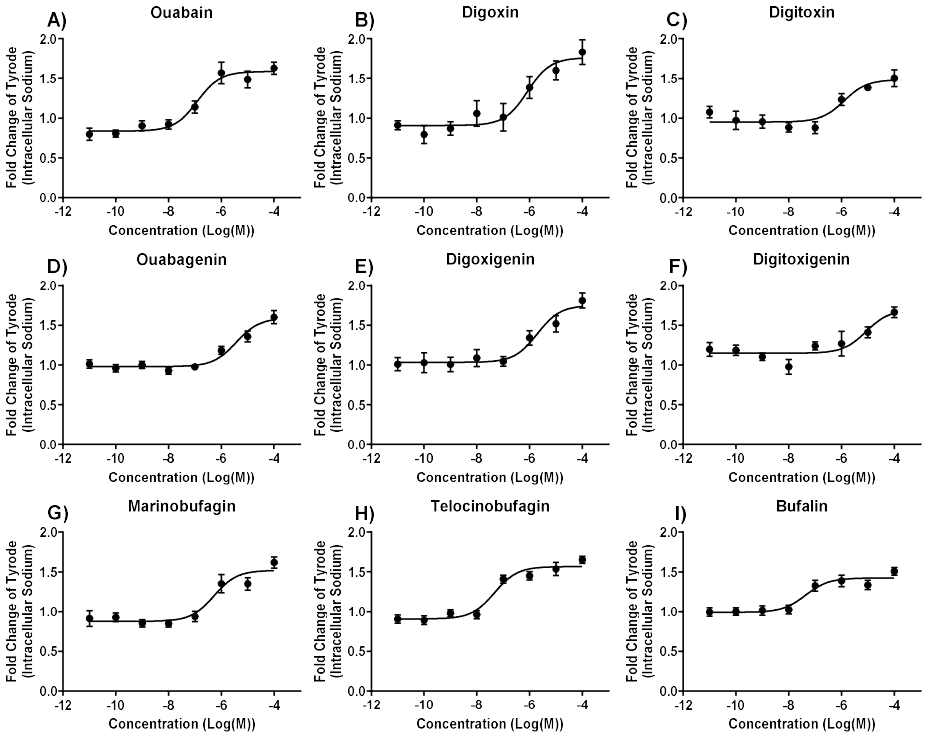


Figure 3.2 Dose response curves (3-parameter logistic regression) generated with various CTS. Cardenolides (digoxin, digoxigenin, ouabain, ouabagenin, digitoxin and digitoxigenin) and bufadienolides (marinobufagin, telocinobufagin and bufalin) were examined at a range of 0.01-100 μM. All experiments represented by mean +/- SEM of 4-16 experiments with 8 replicates of each concentration in each experiment.

Asante Natrium Green 2 (ANG2)						
Cardiotonic Steroid	**IC50 (nM)**	**Rank**	**Imax (Fold change)**	**Rank**	**Goodness of fit R^2**	**N (n)**
Bufalin	44 (+/- 28)	1	1.42 (+/- 0.04)	9	0.52	10 (80)
Telocinobufagin	47 (+/- 19)	2	1.57 (+/- 0.03)	6	0.78	8 (64)
Ouabain	124 (+/- 61)	3	1.58 (+/- 0.05)	5	0.50	16 (128)
Marinobufagin	528 (+/- 297)	4	1.52 (+/- 0.06)	7	0.49	13 (104)
Digoxin	834 (+/- 580)	5	1.76 (+/- 0.11)	1	0.49	9 (72)
Digitoxin	1256 (+/- 885)	6	1.48 (+/- 0.07)	8	0.59	5 (40)
Digoxigenin	1967 (+/- 1293)	7	1.75 (+/- 0.09)	2	0.44	11 (88)
Ouabagenin	3715 (+/- 1823)	8	1.59 (+/- 0.06)	4	0.65	9 (72)
Digitoxigenin	8616 (+/- 7852)	9	1.69 (+/- 0.14)	3	0.49	4 (32)

Table 3.1 Half maximal inhibitory concentration (IC50), maximal effect (Imax) and rank of the NKA inhibition by various cardiotonic steroids. CTS included Ouabain, Ouabagenin, Digoxin, Digoxigenin, Digitoxin, Digitoxigenin, Marinobufagin, Telocinobufagin and Bufalin inducing an increase in intracellular Na^+ in HEK293t (NKATPase) cells using Asante Natrium Green 2. Data displayed mean +/- SEM. N= plates, n=wells.

The above fitted curves was observed to have R^2 ranging between 0.44 – 0.78 with the best fits being telocinobufagenin and ouabagenin. Some of the lower fittings might be due to the ANG-2 not have the same properties as SBFI (with having a second fluorescence signal) to control for example loss of cells in different wells. This could increase the variability in the data acquired resulting in some of weaker fits observed above.

3.3.3 Potential Biphasic Effects of Cardiotonic Steroids Using Asante Natrium Green 2

The dogma in the field is that CTS inhibits NKA, although in recent years several studies suggest that at low physiologically relevant concentrations CTS can potentially stimulate the NKA(62, 220). In the Na^+ assay utilised here some of the cardiotonic steroids show a drop in intracellular Na^+ at subnanomolar concentrations, which led to a further investigation of the bimodality of the cardiotonic steroids tested in the assay. Figure 3.3A-I shows effects of different cardiotonic steroids at 10 pM - 10 nM on intracellular Na^+ in HEK293t cells. Ouabain demonstrated a significant lowering of intracellular Na^+ at 10-100 pM. Although not significant, digoxin shows a similar trend of lowering the intracellular Na^+ at 100 pM. Digitoxin, does not seem to exert this effect on intracellular

Na^+. Interestingly, neither aglycone form of ouabain, ouabagenin, or of digoxin, digoxigenin, lowers the intracellular Na^+ at sub-nanomolar concentrations. The aglycone forms of digitoxin, digitoxigenin, did not show any effect at these low concentrations at intracellular Na^+ even with the low N values considered. Three bufadienolides were tested for their effects at these low concentrations as well. Neither bufalin, marinobufagenin or telocinobufagin exert any effect on intracellular Na^+ in the concentration span used in these investigations.

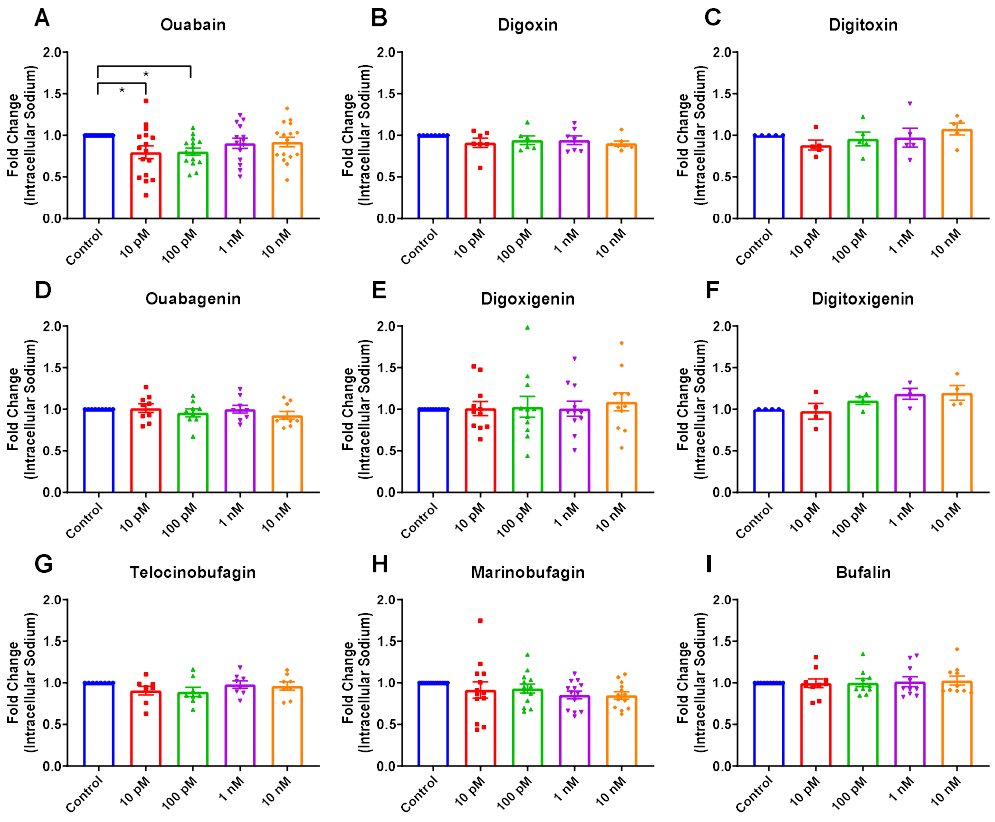
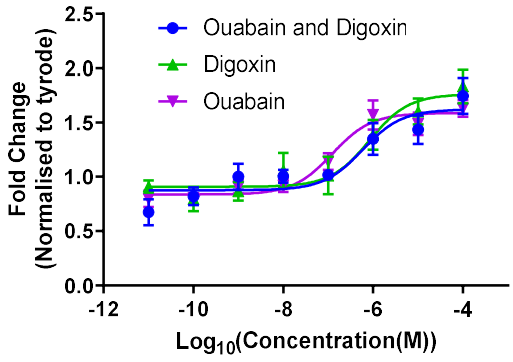


Figure 3.3 Investigations of biphasic responses with various CTS. Cardenolides (digoxin, digoxigenin, ouabain, ouabagenin, digitoxin and digitoxigenin) and bufadienolides (marinobufagin, telocinobufagin and bufalin) was investigated at range of 0.01-10 nMs. All experiments represented by mean +/- SEM of 4-16 experiments with 8 replicates of each concentration in each experiment. Statistical differences was assessed using a one-way ANOVA with tukey's post hoc test for multiple comparisons, * $p < 0.05$, between the different tested groups.

3.3.4 Investigating Antagonism of Cardiotonic Steroids Using the Asante Natrium Green 2

Cardiotonic steroids are very similar in structure and share the binding target, the NKA, thus logically they could potentially interact with one another. Indeed, a study by Song et al showed evidence of ouabain and digoxin antagonism in rat(205). Thus to investigate potential antagonism on intracellular Na^+, dose-response curves with either ouabain or digoxin alone and together, at equimolar doses were carried out at range of 0.01 – 100 µM (Figure 3.4A). To allow comparisons, the IC50s from each dose-response were derived from the standard curve and are listed in figure 4B. Ouabain alone shows a lower IC50 when compared to digoxin alone (Figure 3.4A-B). Interestingly, adding ouabain and digoxin together seems to decrease the IC50 suggesting an interaction of the two steroids and potential antagonism.

A)



B)

Cardiotonic Steroid	IC50 (nM)	N
Ouabain	124 +/- 45	19
Digoxin	834 +/- 580	8
Ouabain + Digoxin	585 +/- 450	4

Figure 3.4 Investigations of antagonism responses with ouabain and digoxin. The cardenolides were examined alone or equimolar together at range of 0.01-100 µM and presented as concentration-response curves (3-parameter logistic regression). All experiments represented by mean +/- SEM of 4-19 experiments with 8 replicates of each concentration in each experiment.

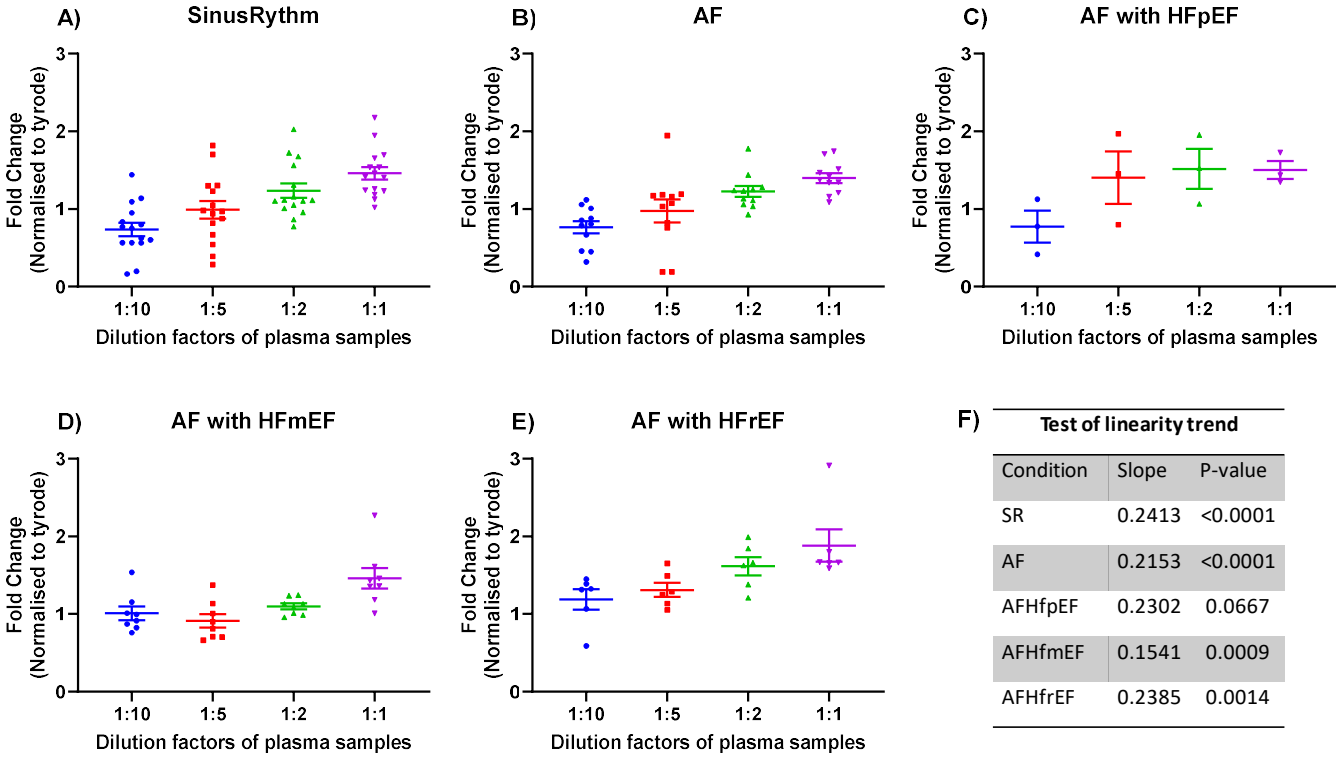
3.3.5 Effects of BBC-AF patient samples on intracellular Na^+

The second goal of the developed intracellular Na^+ assay was for it to be used as a functional assay to investigate the effects of serum sample incubation on intracellular Na^+. Samples from the Birmingham and Black Country Atrial Fibrillation (BBC-AF) registry was used to investigate the effects of atrial fibrillation (AF) with/without heart failure (HF) on intracellular Na^+ in HEK293T cells. Patient samples were divided into 3 groups, sinus rhythm, AF and AF with HF and reduced ejection fraction (rEF), treated with either digoxin or beta-blockers. The investigator was blinded to avoid any bias.

Firstly experiments were set out to investigate optimal conditions to utilise the patient samples in the cell-based assay. Experiments were thus carried out with patient samples at different dilutions (neat (1:1), 1:2, 1:5 and 1:10) with the 3 groups, sinus rhythm, AF and AF with HF, treated with beta-blockers. The patients having HF were further broken down into 3 groups depending on their ejection fraction. Preserved ejection fraction (pEF) patients equal to or above of 50%, mid-range ejection fraction (mEF) between 40-49% and patients with lower than 40% as reduced ejection fraction (rEF).

Figure 3.5 (A-E) shows the results of the investigations of different dilutions (1:1 – 1:10) of the patient groups described above. All groups were analysed for trending linearity (Figure 3.5F). Sinus rhythm, the AF group and the AF with HFrEF group all have a significant positive trend upwards going from 1:10 towards 1:1, which could indicate potential dilution of factors in the samples interacting with intracellular Na^+ via NKA. This trend was less evident in the AF group with HFmEF although still significant. The

trend was not observed in the AF group with HFpEF, but do also not have many samples. Onward we chose the 1:2 dilution for two reasons 1) 1:2 representing a more physiological ratio which should also be less stressful for the cells 2) limited dilution of factors such as CTS in the sample allowing a potential effect on intracellular Na^+ to be observed. These were initial experiments with extractions merely diluted in tyrode buffer, limiting the control of pH, which can stress the cells and not be ruled out to affect the results. All subsequent patient sample experiments were done using extraction methodology to limit the pH change and potential interference with the results achieved using this method.



F)

Test of linearity trend

Condition	Slope	P-value
SR	0.2413	<0.0001
AF	0.2153	<0.0001
AFHfpEF	0.2302	0.0667
AFHfmEF	0.1541	0.0009
AFHfrEF	0.2385	0.0014

Figure 3.5 Investigations of effects of BBC-AF samples. (A-E) Investigations of effects of different dilutions (1:1, 1:2, 1:5 and 1:10) of different patient sample groups (SR (A), AF (B), AFHFpEF (C), AFHFmEF (D), AFHFrEF (E)) on intracellular Na^+ in HEK293t cells. All experiments represented by mean +/- SEM of 5-15 patient samples. F) Results of linearity trend test using one-way ANOVA. SR – Sinus Rhythm; AF – Atrial fibrillation; HF – Heart failure; pEF – Preserved ejection fraction; mEF – Midrange ejection fraction; rEF – Reduced ejection fraction.

Next step was to compare results from patients treated with either beta-blockers or digoxin to see if the treatment affects intracellular Na^+. Serum from AF+HF+rEF patients on beta-blockers (Figure 3.5A) significantly increased intracellular Na^+ compared to sinus rhythm patients. No difference was observed compared to AF patients and no effects were observed when AF alone was compared to sinus rhythm patients. Serum from AF+HF+rEF patients treated with digoxin (Figure 3.6B) did not show significantly increased intracellular Na^+ compared to sinus rhythm patients. Similar to the beta-blocker treated patients, AF+HF+rEF vs AF alone or AF vs sinus rhythm do not show any significant changes in intracellular Na^+. No healthy were run, as samples were not available, thus comparisons are made to sinus rhythm patients.

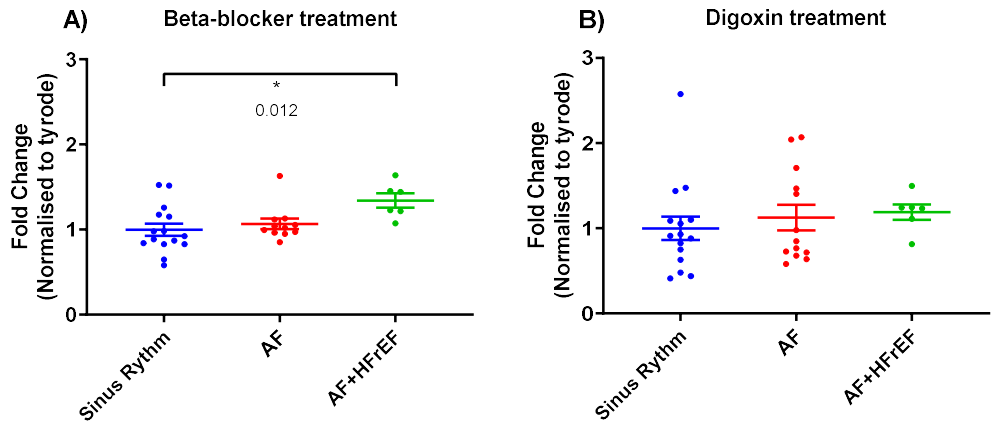


Figure 3.6 Comparison of BBC-AF patients treated with digoxin or beta-blockers. A) represents effects of beta-blocker treated and B) the digoxin treated patients with either sinus rhythm or atrial fibrillation with/without concomitant heart failure with reduced ejection fraction intracellular Na^+ responses after 1 hour's exposure individual patient plasma samples. Due to availability of plasma samples N varies among groups: 15 Sinus rhythm patients, 11-13 AF patients and 6 AF patients with concomitant heart failure with reduced ejection fraction. All data is presented as mean +/- SEM. Statistical differences was assessed using a one-way ANOVA with Dunnett's post hoc test for multiple comparisons, * $p < 0.05$ between the different tested groups.

3.3.6 Optimisation of the SBFI dye for Measurement of intracellular Na^+

In independent set of experiments, SBFI characterisation of the dye uptake in the HEK293T cells was carried out. SBFI was initially included as it was ratio metric which can reduce variability in the experiments, but after the first experiments with SBFI, the ANG2 dye became unavailable. All experiments were carried out using the same tyrode composition as previously.

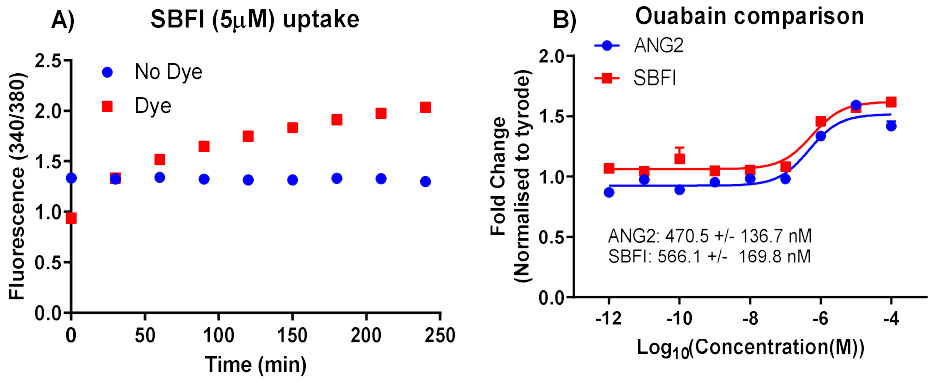


Figure 3.7 Optimisation of SBFI dye and direct comparison with ANG2 in HEK293t cells. (A) represents intracellular Na+ responses over a 4hr time course in HEK293t cells with/without dye. Both conditions represent raw data of 4 replicates from 2 plates. (B) represents intracellular Na^+ responses normalised to control in response to a 3hr treatment with Ouabain (100 μM) with either ANG2 or SBFI HEK293t cells presented as concentration-response curves (3-parameter logistic regression).. Dyes were directly compared in 4 plates with 4 replicates each. All data is presented as mean +/- SEM.

As seen in Figure 3.7A, the SBFI (5 μM) when added to the HEK293t cells increases the signal over time for up to 4 hours. Time beyond 4hrs was not assessed. Thus, similar incubation time (4hrs) as for the ANG2 dye was used for all the experiments presented in this thesis. Ouabain dose-response curves with SBFI and ANG2 were investigated, in order to directly compare the two dyes. As seen in figure 3.7B, ouabain produces a similar response using either dye as demonstrated from the very similar IC50 values (ANG2 470

nM vs SBFI 566 nM) derived from these experiments, thus demonstrating the validity of continuing with this dye.

3.3.7 Increasing sensitivity of the intracellular Na^+ cell-based assay using the SBFI

Utilising SBFI provided very consistent data with low variation but with no indications of changes at picomolar or nanomolar concentrations of CTS that were previously observed with ANG2. Experiments were thus carried out to increase the sensitivity of the assay with the SBFI dye. One option to increase sensitivity was to try and increase intracellular Na^+ within the cells allowing potentially detection of smaller changes. Monensin is a Na^+ ionophore, allowing transport of Na^+ ions across the membrane. In the presence of monensin, higher extracellular Na^+ will lead to increased intracellular Na^+, thereby potentially increasing the sensitivity allowing detection of lowering of intracellular Na^+ levels.

To assess the potential increase in sensitivity of the cell-based assay, experiments were carried out using monensin (1-100 µM) with ouabain concentrations (100pM or 100 µM) (See figure 3.8 below). 100 pM of ouabain reduced intracellular Na^+ in the experiments utilising the ANG2 dye (Figure 3.3), but these changes were not seen with SBFI (Figure 3.8). Several monensin concentrations were utilised 1, 10, 50 and 100 µM. In the absence of monensin, no intracellular Na^+ reduction is seen at 100 pM of ouabain. At 1 µM of monensin, 100 pM ouabain surprisingly lead to a small increase i intracellular sodium slightly. At 50 µM and 100 µM of monensin, a decrease in intracellular Na^+ was observed with the 100 pM ouabain. As expected, 100 µM of ouabain significantly increased

intracellular Na^+ at all monensin concentrations, though these were lower as the monensin concentration increases. Thus, as 50 µM monensin increases the sensitivity of the assay, this concentration was used for the experiments presented below and those in chapter 5.

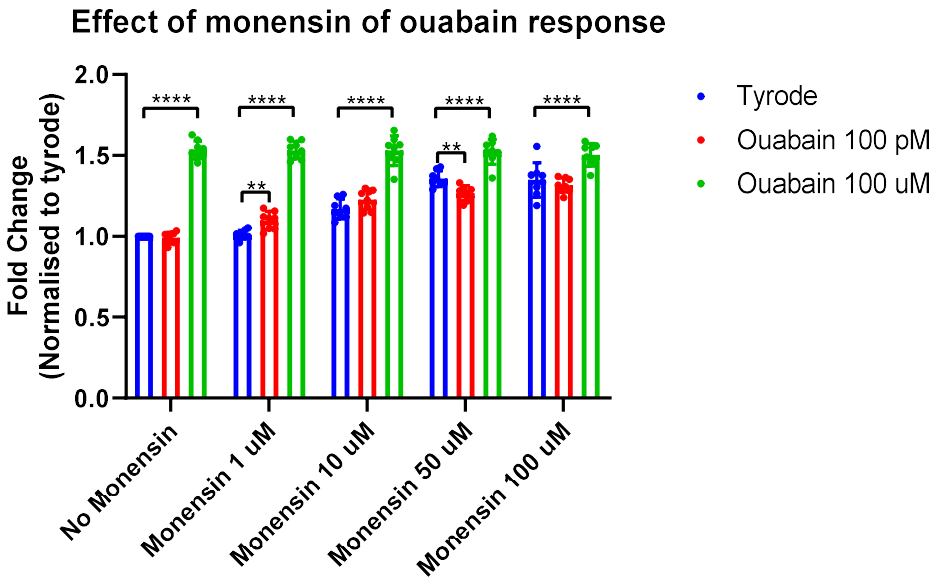


Figure 3.8 Investigation of effects of monensin. Monensin (1-100 µM) effects on sensitivity of ouabain (100 pM or 100 µM) induced intracellular Na^+ changes in HEK293t cells using SBFI dye. Data from 8 experiments of each condition. All data is presented as mean with SEM. Statistical differences was assessed using a one-way ANOVA with Dunnett's post hoc test for multiple comparisons, ** $p < 0.01$ and **** $p < 0.0001$ between the different tested groups.

3.3.8 Dose-dependent Effects of Cardiotonic Steroids Using the SBFI Dye

To allow comparisons with data using the ANG2 dye, dose-response curves were carried out with ouabain, digoxin and marinobufagenin with the SBFI. Dose-response curves were generated for each of these steroids using a similar concentration range (10 pM – 100 µM) as used in the ANG2 experiments above. Ouabain, digoxin and marinobufagenin all display dose-dependent increase in intracellular Na^+ (see figure 3.9). From each of the

curves, IC50s and Imax values were derived and are displayed in table 2 below. Ouabain and marinobufagenin exhibit very similar IC50 and Imax level. The ouabain IC50 is slightly higher than those in the experiments carried out with ANG2 (table 1), while marinobufagenin IC50 values were slightly lower. Digoxin, on the other hand, shows much higher IC50 than the other two steroids, although max responses (Imax) are higher than both ouabain and marinobufagenin (Figure 3.9 and Table 3.2). Digoxin unveiled more than 4.5 times higher IC50 and slightly lower Imax than the figures obtained using the ANG2.

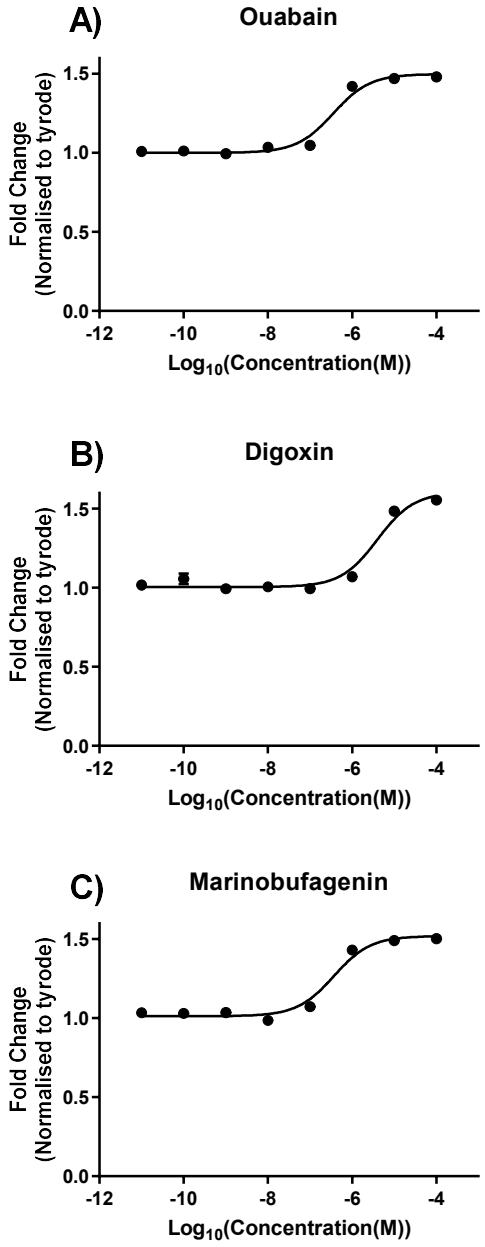


Figure 3.9 Dose response curves generated with various CTS. CTS included cardenolides (digoxin, ouabain) and bufadienolide (marinobufagin) at a range of 0.01-100µM and presented as concentration-response curves (3-parameter logistic regression). All experiments represented by mean +/- SEM of 8 experiments with 8 replicates of each concentration in each experiment.

Sodium-binding benzofuran isophthalate (SBFI)						
Cardiotonic Steroid	**IC50 (nM) Mean (+/- SEM)**	**Rank**	**Imax (Fold change) Mean (+/- SEM)**	**Rank**	**Goodness of fit R^2**	**N (n)**
Ouabain	357.8 (64.8)	1	1.499 (0.014)	3	0.94	8 (64)
Marinobufagenin	368.5 (67.8)	2	1.520 (0.015)	2	0.94	8 (64)
Digoxin	3983 (732.4)	3	1.604 (0.022)	1	0.94	8 (64)

Table 3.2 Half maximal inhibitory concentration (IC50), maximal effect (Imax) and rank of the NKA inhibition by various cardiotonic steroids with SBFI. CTS including ouabain, digoxin and marinobufagin inducing an increase in intracellular Na^+ in HEK293t (NKATPase) cells using Sodium-binding benzofuran isophthalate. Data displayed mean +/- SEM. N= plates, n=wells.

The above displayed data for ouabain, marinobufagenin and digoxin utilizing the SBFI dye generated curves with very strong fits with a R^2 of 0.94. This demonstrates a much lower variability with SBFI than seen from the experiments with the ANG-2 dye. Yet another reason for SBFI being the better dye forward.

3.3.9 Potential Biphasic effects and interactions of Cardiotonic Steroids with SBFI

Similar to ANG-2 dye experiments, the potential biphasic responses of different CTS was carried out with the SBFI dye. The experiments were carried out in without (Figure 3.10 A-C) or with (Figure 3.10 D-F) of monensin (50 μM). Ouabain, digoxin and

marinobufagenin were examined at 0.1-10 nM (Physiological and treatment relevant range). In tyrode solution none of the three CTS tested demonstrated any changes in intracellular Na^+ (Figure 3.10 A-C). With monensin (50 μM) present ouabain show significant reduction of intracellular Na^+ at the concentrations tested (0.1-10nM) when compared to monensin alone. This reduction was not observed with digoxin at sany of the concentrations tested. Marinobufagenin showed a decrease at 10nM, but not at either 100 pM or 1 nM.

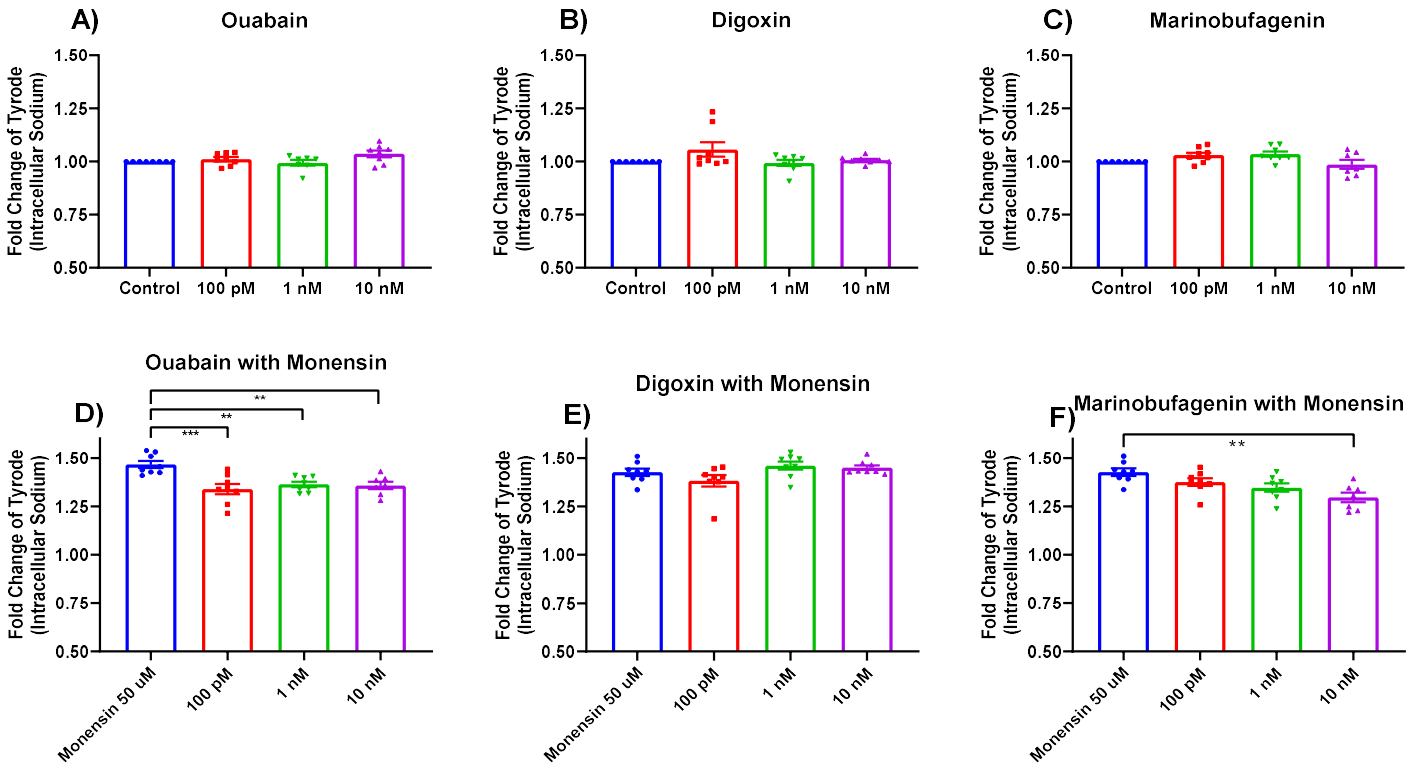


Figure 3.10 Investigations of biphasic responses with various CTS. Cardenolides (digoxin, ouabain) and a bufadienolide (marinobufagin) was investigated at range of 0.1-10 nM. All experiments represented by mean +/- SEM of 8 experiments with 4 replicates of each concentration in each experiment. Statistical differences were assessed using a one-way ANOVA with tukey's post hoc test for multiple comparisons, ** $p < 0.01$, *** $p < 0.001$, and **** $p < 0.0001$ between the different tested groups.

3.3.10 Investigating Antagonism of Cardiotonic Steroids Using the SBFI

Ouabain shows ability to potentially stimulate the NKA around 1 nM lowering intracellular Na^+ levels, which is similar to clinically relevant levels of digoxin for AF patients. Thus, investigations were carried out to examine the potential interactions between ouabain and digoxin at 1 nM. Figure 3.11 show ouabain and digoxin alone or equimolar in tyrode (Figure 3.11A) or in the presence of monensin (Figure 3.11B). In tyrode buffer without monensin present no difference was observed with either ouabain or digoxin alone or together at 1 nM (Figure 3.11A). In the presence of monensin (Figure 3.11B), ouabain (1 nM) led to a significant 6%reduction in intracellular Na^+ levels (1.51 +/- 0.006 vs 1.42 +/- 0.013). This reduction was not seen with digoxin (1.51 +/- 0.006 vs 1.50 +/- 0.015). Interestingly, in the equimolar levels of ouabain and digoxin, the significant reduction seems abolished indicating interaction between ouabain and digoxin (21.51 +/- 0.006 vs 1.48 +/- 0.028).

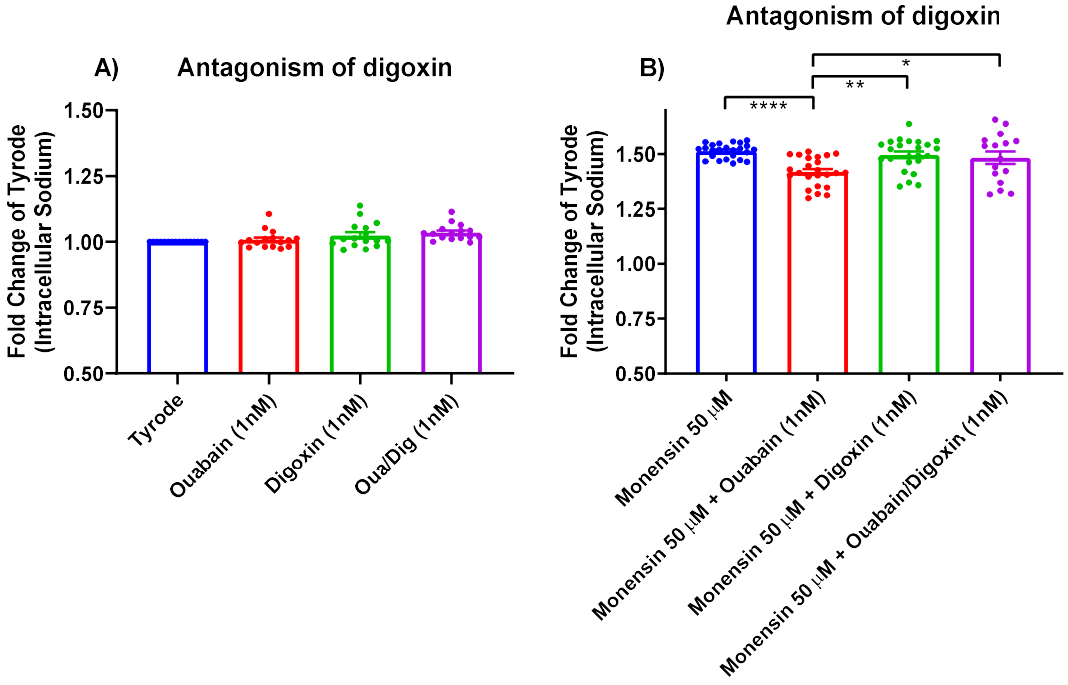


Figure 3.11 Investigations of interactions of ouabain and digoxin. Interactions of ouabain and digoxin examined in tyrode (A) and in presence of monensin (B) at 1 nM. All experiments represented by mean +/- SEM of 2-3 experiments with 8 replicates of each concentration in each experiment. Statistical differences was assessed using a one-way ANOVA with tukey's post hoc test for multiple comparisons, * $p < 0.05$, ** $p < 0.01$, and **** $p < 0.0001$ between the different tested groups.

3.3.11 Extraction of cardiotonic steroids and potential matrix effects with SBFI

A critical part of the validation of the use of SBFI in the assay was to examine the potential matrix effects on the SBFI measurements and whether extractions could be a way around potential matrix effect. Thus, the effect of FBS (Mimics matrix from samples) were initially examined (Figure 3.12A). Dose-response curves were generated for ouabain (1 pM-100 μM) in tyrode and mixed in FBS to see whether the FBS matrix changes the response. The experiments clearly demonstrated a steep reduction in the IC50 in presence of FBS (465.2 (+/-104) nM vs 2601 (+/-799.8) nM), thus indicating the matrix effects severely impair the binding affinity of ouabain to NKA (Figure 3.12A and Table 3.3). Therefore, as the matrix effects can be expected to possess a clear impact on the results with SBFI, a method to get around this interference had to be sought out.

Two extraction methodologies i.e. Bond Elute (Figure 3.12 B-C) and Thermo Sola (Figure 3.12 D-F) were used to rescue the severe impact on the binding affinity. Ouabain, digoxin and marinobufagenin were mixed up in human serum and extracted through extraction columns according to manufacturer's instructions. The extracted materials were then directly compared to neat mixed up CTS in tyrode. Using the Bond Elute methodology, the extractions for ouabain do not demonstrate any dose-response curve

(Figure 3.12A) which is also seen from the IC50 values (Table3.3). Digoxin extracts did demonstrate a dose-response curve, although still having IC50 values much higher than freshly used digoxin (2510 (552.4) nM vs 5810 (+/- 2984) nM or 9108 (+/- 2530) nM). The Thermo Sola methodology demonstrated a ~2.3 times worse in inhibition effect for ouabain when compared to ouabain mixed up neat in tyrode, (Table 3.3). Digoxin and marinobufagenin showed 1.77 and 1.26 times higher IC50 when compared to the respective tyrode neat solutions. All three CTS show a minor loss of inhibitory effect after extraction, but do also show very well-defined dose-response curves comparable to neat solutions.Thus, Thermo Sola methodology was used in the subsequent chapter 4 (ELISA) and chapter 5 (RATE-AF samples).

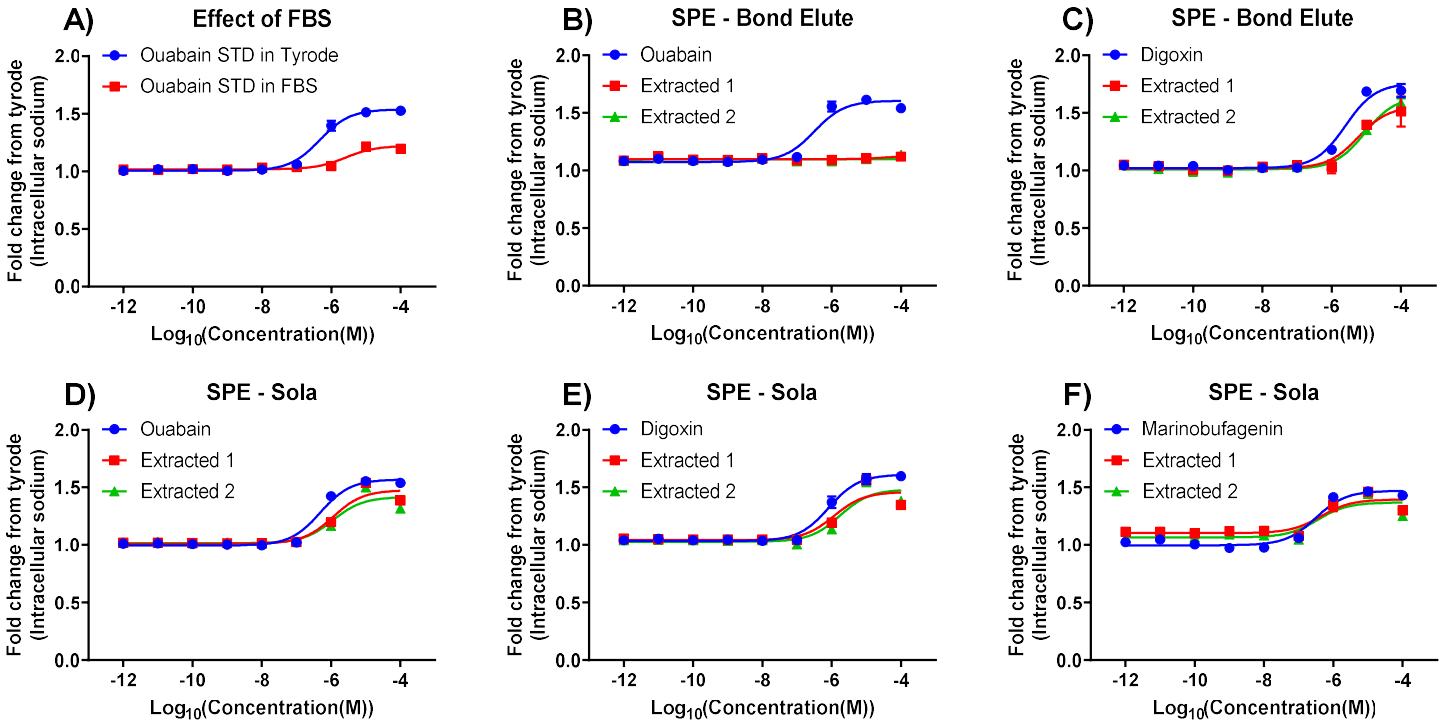


Figure 3.12 Concentration response curves (3-parameter logistic regression) generated with ouabain, digoxin and marinobufagenin and respective extractions. Bond elute (B-C) and Thermo Sola (D-F) extraction methods used and compared for cardenolides (digoxin, ouabain) and bufadienolide (marinobufagin) at a range of 0.01-100µM. All experiments represented by mean +/- SEM of 4-6 experiments with 8 replicates of each concentration in each experiment.

Matrix effects and extractions			
Matrix effect - FBS	**IC50 (nM) Mean (+/- SEM)**	**Goodness of fit R2**	**N(n)**
Ouabain in tyrode	465.2 (104.0)	0.91	8 (32)
Ouabain in FBS	2601 (800)	0.83	8 (32)
Solid phase extraction - Bond Elute			
Ouabain	319.3 (84.1)	0.91	6 (24)
Extracted ouabain 1	34860 (200)	0.03	6 (12)
Extracted ouabain 2	No fit available	0.01	6 (12)
Digoxin	2510 (552)	0.93	6 (24)
Extracted digoxin 1	5810 (2984)	0.68	6 (12)
Extracted digoxin 2	9108 (2530)	0.86	6 (12)
Solid phase extraction - SOLA			
Ouabain	492.2 (80.5)	0.97	4 (32)
Extracted ouabain 1	1137 (313)	092	4 (16)
Extracted ouabain 2	1140 (410)	087	4 (16)
Digoxin	822.6 (185)	0.95	4 (32)
Extracted digoxin 1	1166 (513)	0.81	4 (16)
Extracted digoxin 2	1751 (746)	0.83	4 (16)
Marinobufagenin	310.6 (81.4)	0.94	4 (32)

Extracted marinobufagenin 1	433.2 (241.5)	0.77	4 (16)
Extracted marinobufagenin 2	349.1 (189.1)	0.78	4 (16)

Table 3.3 Half maximal inhibitory concentration (IC50) of the NKA inhibition by CTS and extractions. Ouabain and digoxin, marinobufagenin with extracts from two extraction methodologies using ANG-2 and SBFI. Data displayed mean +/- SEM. N= plates, n=wells.

The majority of the fits for the data obtained from the extractions were very good (R^2>0.75) again demonstrating how repeatable and stable the assay is with SBFI. s

3.3.12 Calibration of Na^+ signals with SBFI dye

Last validation step of the the assay was to investigated the ability of fluorescent data to be calibrated to intracellular Na^+ levels. Na^+ calibrations have previously been carried out in rat and rabbit CMs(216, 221), using gramicidin (10 μM) and strophanthidin (100 μM) to allow for permeabilization of the cells and blocking the NKA activity, allowing for extracellular and intracellular Na^+ to equilibrise. Similar calibration protocol using stepwise increase of extracellular Na^+ was used in this thesis. In this thesis ouabain (100 μM) was used instead of strophanthidin (100 μM) as the two compounds are very similar. Calibration was carried out in presence of extracellular Na^+ steps at 0 mM, 11 mM, 22 mM, 45 mM and 90 mM. The data was fitted with a 3-parameter logistic function, see equation 3 below.

Equation 3:

$$Y = Bottom + (\frac{Top - Bottom}{1 + 10^{X - LogIC5}})$$

Y = Response in fold change of either tyrode or monensin

X = Log(Concentration of steroid tested)

IC50 = Amount of X needed to get 50% of response of Y

Top = Plateau of response at the top end of calibration curve

Bottom = Plateau of response at the bottom end of calibration curve

Bottom was set to 0 as suggested from the analysis program due to subtractions of 650nm and background from 450 values.

To assess whether the calibration works, experiments were conducted with ouabain, digoxin and equimolar of each at 1 nM. As previously shown, at 1 nM neither ouabain, digoxin or together when in tyrode changes the fluorescent signals indicating no change in intracellular Na^+ (Figure 3.13A). The generated calibration curve (Figure 13.3B) were then used to calibrate the fold changes of tyrode into intracellular Na^+. The calibrated levels show the HEK293t cells have intracellular Na^+ level of 15.4 mM at RT when not challenged with any CTS (Figure 13.3C). Ouabain (1 nM) show a 5.2% decrease (15.4 mM vs 14.6 mM) but without being significant. Although it was not significant, similar trends were not observed with either digoxin alone or equimolar with ouabain (Figure 3.13C).

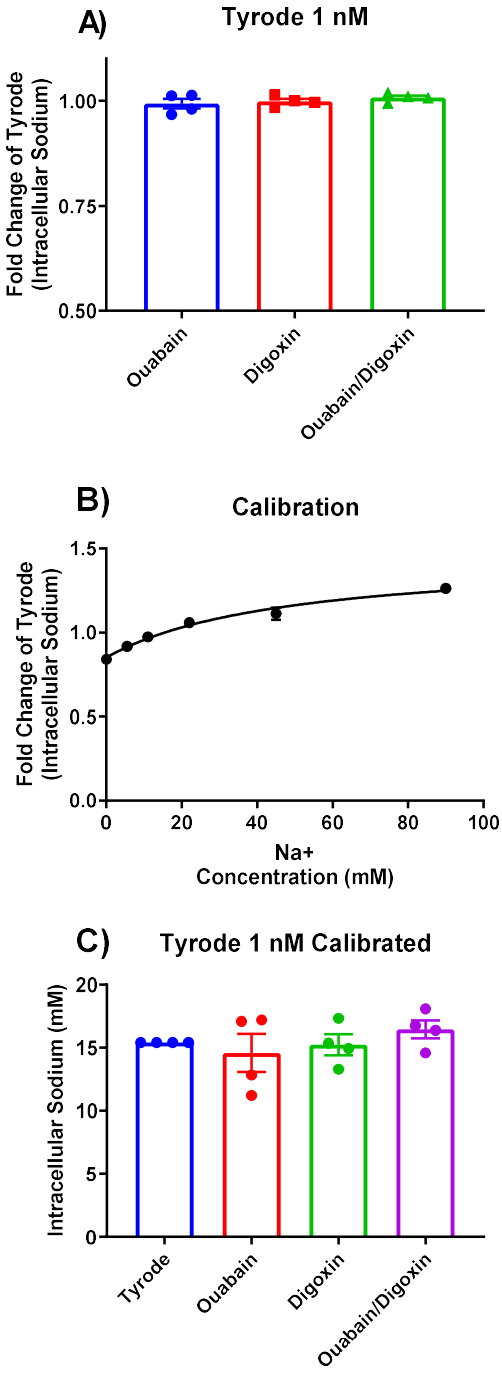

A)
Tyrode 1 nM
Fold Change of Tyrode (Intracellular Sodium)
1.00
0.75
0.50
Ouabain
Digoxin
Ouabain/Digoxin
B)
Calibration
Fold Change of Tyrode (Intracellular Sodium)
1.5
1.0
0.5
0.0
0
20
40
60
80
100
Na+ Concentration (mM)
C)
Tyrode 1 nM Calibrated
Intracellular Sodium (mM)
20
15
10
5
0
Tyrode
Ouabain
Digoxin
Ouabain/Digoxin

Figure 3.13 Calibration of Tyrode, 1 nM fresh ouabain, digoxin and equimolar of each. A) Freshly mixed up ouabain, digoxin and equimolar of both at 1 nM were used to test calibration. B) Calibration was done at 0-90 nM Na^+. C) Calibrated values for the three CTS combinations. Goodness of fit R^2=0.94. All experiments represented by mean +/- SEM of 4 experiments with 8 replicates of each concentration in each experiment.

3.4 Discussion

3.4.1 Development of intracellular sodium assay

Firstly, the ability of the dye to enter the Hek293T and provide measurements of changes in intracellular Na^+ were tested and are shown is figure 3.1. The dye is over time observed to increase the signal in Hek293T cells compared to cells without the dye. Together with the experiments with CTS, this confirms the ANG-2 is a suitable tool for measurements of intracellular Na^+ in the Hek293T cells.

Secondly, the effect of changing the extracellular Ca^{2+} with EDTA in the tyrode instead was used to investigate the effects of Ca^{2+} on the intracellular Na^+. The tyrode used in this report was comprised of 137 NaCl, 5.4 KCl, 1 $CaCl_2$, 0.5 $MgCl_2$, 10 HEPES, 10 glucose (all in mM), pH 7.4. This was chosen based on previously published data using tyrode solution for very similar experiments (222). The comparisons between the tyrode with or without EDTA are seen in figure 3.1B. Exchanging the Ca^{2+} with EDTA in the tyrode is observed to increase the intracellular Na^+ signal significantly. A similar difference is observed between tyrode with ouabain and the tyrode with EDTA and ouabain. The EDTA leaves no extracellular Ca^{2+} to limit the NCX extrusion of Ca^{2+} and import of Na^+, which could explain the slight rise although the NCX have not been observed to be present in Hek293T cells. As the use of EDTA increases the sensitivity

slightly it was used for the rest of data presented in this thesis and should be considered for future experiments as well, when working on HEK293t cells at least.

Experiments looking at the effect of incubation time with the dye were carried out and are shown in Fig.5C. The other experiments in this report were made with an incubation time of >2 hours, which was based on previously published data(222). The test of incubation time shows the sensitivity of the assay to measure changes in intracellular Na^+ increases up to 4 hours. After 4 hours, the sensitivity is observed to decrease ending with low sensitivity at 8hrs compared to the other time points. Although 4 hour incubations with the dye have significantly higher sensitivity in these experiments compared to the 2 hour, a practical perspective also has to be considered. Thus, using a timepoint in between could be considered for future experimentation.

Lastly, the confluency of the HEK293T cells used for experimentation was tested to optimise conditions under which the changes in intracellular Na^+ are measured (Fig. 5D). In experiments cells are usually grown to confluency prior to starting the experimentation(222). Although it is worth noting the density of cells could potentially play a role in the response to CTS. Thus, experiments using confluency ranging from 30-90% were used to evaluate potential effects of the density on the sensitivity of the assay like previously published work (223). The sensitivity of the measurements of Na^+ is observed highest at 90% confluent cells and slowly decreases with very limited response at 30%. As the confluency seems optimal around 90%, future experiments should be continued carried out with cells grown to 90% confluency prior to experimentation.

3.4.2 Dose-response effects of cardiotonic steroids

The effect of different CTS on NKA measured as intracellular Na^+ changes was investigated in HEK293t cells. All cardiotonic steroids investigated inhibited NKA dose dependently and grouped into cardienolides and bufodienolides in terms of IC_{50}s except for ouabain (see Figure 1B). Limited studies have compared numerous different cardiotonic steroids in the same assay as has been carried out in this report.

Ouabain inhibited NKA with an IC_{50} of 123.9 45 and 465 +/-104 nM withANG-2 and SBFI, respectively. Compared to previously published work ouabain show similar results as a shark NKA inhibition assay (224), 4-6 times lower IC_{50} than shown in a rabbit erythrocyte NKA inhibition assay(225), 4-6 times higher than experiments carried out inhibiting the NKA of human cardiac membranes(226) and slightly higher IC_{50} when compared to investigations carried out in NKA from pig kidneys(220) and NKA from human erythrocytes(220).

Marinobufagenin and bufalin show similar inhibitory effect to investigations using NKA of human cardiac membranes(226). No comparisons available for telocinobufagin from the reviewed literature. Digoxin showed a slightly higher affinity than experiments in rabbit erythrocyte NKA(225) although 6 times weaker than results show from the NKA of human cardiac membranes(226). Digitoxin show a worse IC_{50} when compared to previous experiments in both rabbit erythrocyte NKA(225) and NKA of human cardiac membranes(226). Ouabain, digoxin and digitoxin show a weaker affinity with their sugar

groups removed demonstrated by ouabagenin, digoxigenin and digitoxigenin, respectively. Similarly observed in both rabbit erythrocyte NKA(225) and NKA of human cardiac membranes(226) that each cardiotonic steroid loses a lot of the inhibitory effect by cutting of the sugar groups, indicating the importance of these for the functionality.

This together show indications of the validity of our functional assay but also demonstrates the inherent variability of different assays. As the measurements of intracellular Na^+ are indirect measures of the effects of the CTS on NKA, many factors can influence the sensitivity. Although with varied number of experiment for each cardiotonic steroid the assay still provides information on the inhibitory effects of different CTS of NKA and thus still a useful tool for comparison, although having lower sensitivity than NKA of human cardiac membranes(226). As the sensitivity of the assay seems lower than the human NKA assay a consideration could be to use of primary cell lines like hiPSC CMs, which have beating activity and thereby higher turnover of Na^+.

3.4.3 Bimodality of cardiotonic steroids

Investigation of a two-sided low/high concentration dependent effect (Bimodal effect) on NKA was investigated as indications of lowered intracellular Na^+ was observed with ouabain. Only ouabain and digoxin show trends of a bimodal effect leading to a reduction in intracellular Na^+. Neither the aglycone forms or the bufodienolides show this effect. This again indicates the importance of the structure of the individual cardiotonic steroids for their affinity and effects both at high but also at low concentrations. Investigations of these low physiological relevant levels has not been explored much although CTS have

been around for decades. Nesher et al(62) have previously shown that nanomolar concentrations of ouabain, similar to the ones used in this thesis, demonstrate an increase of the NKA activity in rat heart membranes. Although with limited papers on the topic there are indications of a bimodality of ouabain although more cardiotonic steroids and also the use in different functional experiments have to be sought out to provide answers for the effects of the cardiotonic steroids at low concentrations.

3.4.4 Extraction necessity and effects of patient samples on intracellular Na^+

In many different patients and various experimental animal models endogenous cardiotonic steroids are increased and extractions are suggested by most studies . With the potential of cardiotonic steroids present in the patient samples utilised in this chapter provided an opportunity to further validate the assay for its relevance to investigate the effects of cardiotonic steroids in a functional assay. Thus samples were tested on the HEK293T cells with and without extraction.

In this chapter the results showed patient samples with AF with concomitant severe HF led to an increase of intracellular Na^+ when patients were treated with beta-blockers. Interestingly, this increase was not observed in patients treated with digoxin. This could indicate a potential interaction between digoxin and the endogenous levels of cardiotonic steroids present in the plasma samples. Interactions between not only ouabain and digoxin, but a wider range of cardiotonic steroids have previously been observed. Nesher et al(204) demonstrated bufalin and ouabain interacted leading to increased contractile force and lower cardiotoxicity, compared to bufalin alone in different cardiac tissues. The contractility was reduced in the presence of ouabain and digoxin, compared to digoxin

alone. In another study Song et al(205) observed both digoxin, digitoxin, digoxigenin and bufalin antagonised the effects of low concentrations of ouabain on calcium levels in rat arteries and neurons. Similarly, digoxin was able to antagonise the effects of ouabain, ouabagenin, dihydro-ouabain and strophanthidin. These studies and the results presented in this report indicate that ouabain might interact with different cardiotonic steroids differently highlighting the need for further investigations to improve the understanding of potential interactions and potential implications for patients.

Two extraction methods were tested in this project. The Bond Elute and the Thermo Sola columns. At the time of experiments using the Bond elute columns, information regarding how to proper prime the columns with organic solvent was not available. Thus, it cannot be ruled out the not proper priming of the columns might affect some of the extractions especially the polar ouabain and thus affect the conclusion on what column to use forward for the ELISA and the RATE samples. The disadvantage of the Thermo Sola columns used in this project is the sorbent to sample ratio, which is much lower than the Bond Elute columns (10mg bedding/2mL vs 200mg bedding/3mL). Even though the extractions with Sola columns looked superior to the Bond Elute columns, the low sorbent to sample ratio might underestimates the actual content of endogenous CTS in the sample, as the bedding might not be able to bind it all. This could be followed up with Thermo Sola columns with containing more bedding to assess this problem.

3.4.5 Calibration to intracellular Na^+ concentration

The acquired resting levels for the Hek293t cells around 15.4 mM Na^+ is slightly lower than what was observed in HeLa cells(228) but slightly higher than CMs tested previously to this work (216, 218). In this chapter a 3-parameter logistic function was chosen to be fitted to the calibration values. This was based on the observation of the different levels

of Na^+ did not display a linear relation when examined at the range of 0-90 nM of Na^+. This is slightly different from the previous work, as commonly calibration data was fitted with linear functions instead although that is based on the use of cardiomyocytes (221, 229, 230). These calibrations were mainly carried out between 0-30 nM Na^+, which is a shorter span than the one used in this thesis. Looking at figure 3.13B from 0-25 nM Na^+ also look linear, but as this was extended to 90 nM it was decided to use a 3-parameter logistic function instead as this fits the data better.

3.5 Conclusions

Based on the data in this chapter the following can be concluded. Firstly, an assay able to measure small changes in intracellular Na^+ was accomplished utilising both the ANG-2 dye, but also the SBFI dye, when in presence of monensin (50 μM). This tool was further more able to evaluate various CTS and compare their inhibitory effect and maximal binding effect with both dyes. Importantly, using patient samples from the BBC-AF, the developed assay demonstrated ability to see difference between severe AF patients with HF and sinus rhythm patients dependent on treatment. This provides evidence that the assay is useful for patients and potentially help improve stratification of these patients. The Thermo Sola SPE method also demonstrated very good extractions of CTS and was comparable to fresh mixed up of CTS. Lastly, the assay were able to be calibrated to Na^+ levels which enables easier comparison to previous data but also provides essential information for the patient work.

CHAPTER 4. DEVELOPMENT OF A COMPETITIVE ELISA FOR THE MEASUREMENT OF OUABAIN CONCENTRATION

4.1. Introduction and aims

Since the early 1980s researchers have been looking for ways to quantify the endogenous levels of cardiotonic steroids (CTS)(90). Numerous studies since have also focused on understanding the role of cardiotonic steroids in physiology and pathophysiology with focus on quantifying CTS levels (73, 84, 89, 90, 92-94, 96, 98, 101-105, 107, 110, 111, 113-119, 121, 122, 125-127, 129-132, 134-140, 142, 145, 146, 148-153, 155, 156, 158-161, 163-167, 169-171, 173, 174, 176, 179, 182, 183, 185, 186, 188, 189, 194-196, 207, 231-246). Commonly utilised quantification methodology for measurement of endogenous cardiotonic steroids, primarily endogenous ouabain, relies on the use of radioimmunoassays (RIA)(89, 92, 139). RIA methodologies utilise the competition of the radioactive antigen to the same binding site on the primary antibody by the non-radioactive antigen, which was preincubated with the primary antibody. Thus, the more antigen present in the sample the less the radioactive antigens are able to compete for binding(247). The use of RIA methodologies has some drawbacks as it relies on utilising radioactive labelling of the antigen of interest, which requires specialised training and specialised equipment, thus limiting its wider use. Enzyme-linked immunosorbent assay (ELISA) methodology that relies on the use of non-radioactive detection methods is required. Validity and application of antibody-based methodologies is however dependent on the specificity of a primary antibody, necessitating limited cross-reactivity.

The aims of this work are:

(v) To develop and validate a competitive ELISA for measurement of ouabain in blood of patients and animals.

(vi) To quantify cross-reactivity with other structurally similar steroids.

(vii) To examine whether endogenous ouabain levels correlate with age, disease progression, and other selected cardiovascular variables (See Chapter 5).

4.2. Analysis of ELISA data

4.2.1 Extraction and analysis of raw data

After being measured on the Flexstation (FlexStation 3, Molecular Devices, San Jose, Ca, USA), data were extracted as notepad files and imported into Excel. Optical density measurements were done at 450 and 650 nm for all plates. Reading at 650nm is the reference background. Values recorded at 650nm for each well were subtracted from its respective 450 nm values. Within each plate, blanks without primary antibody were carried out to further eliminate antibody background and mean blank value were subtracted from all individual values of both standards and samples. To allow comparison, all values were normalised to standard 0 (Std 0), which is the assay buffer without any ouabain added. This was done by dividing all the values with the mean of Std 0 and multiplying by 100 to get % off 0 Std (See equation 4.1 below).

Equation 4.1:

$$Change\ of\ Standard\ 0\ (\%) = \left(\frac{Mean\ [Standard/Sample]}{Mean[Standard\ 0]}\right) * 100$$

4.2.2 Analysis of Standard curves

Standard curves were performed with concentrations of ouabain ranging from 0 to 10 nM. After normalisation to Std 0, all the standards were plotted in GraphPad Prism. Calibration curve was performed for each plate, using a 4-parameter logistic function, see equation 4.2 and 4.3 below.

Equation 4.2:

$$Y = Bottom + \left(\frac{[Top - Bottom]}{1 + (\frac{X^{HillSlope}}{IC50^{HillSlop}})} \right)$$

Y= Bottom + (Top-Bottom)/(1 + ((X^HillSlope)/(IC50^HillSlope)))

Y = Response in normalized value as % of Std0

X = Concentrtion of standard

HillSlope = Slope factor of the Std curve

IC50 = Amount of X needed to get 50% of response

Top = Plateau of response at the top end of Std curve

Bottom = Set to 0

This function was developed to allow calibration of sample data to calculate cardiotonic steroid levels from each sample utilised in the assay as described below. To allow for

estimation of X from the gathered Y values, equation was rearranged to isolate X (see Equation 3). Bottom was set to 0 as background absorbance was subtracted.

Equation 4.3:

$$X = ((\frac{Top}{Y} - 1) * (IC50^{HillSlope}))^{\frac{1}{Hillslope}}$$

4.2.3 Sample analysis

The normalised Y values from each sample were averaged. Each of the sample means was inputted into the Std curve function (see above), which were then used to calculate the amount of cardiotonic steroid in each of the samples. All levels of cardiotonic steroid levels were plotted both as % of Std 0 values and as calibrated nM values for comparisons.

4.3. Results

4.3.1 Development of ELISA

Below are shown different variables being validated and optimised including incubation time, antibody concentration and plate selection. This was done prior to experiments investigating cross-reactivity of ELISA with other steroids and extraction efficiency.

4.3.1.1 Primary antibody and coating concentration

First experiments carried out investigated the optimal dilution factor of the primary antibody (sera) and the optimal concentrations for coating the wells. Thus, combinations of coat concentration (1-100 ng/mL) and the primary antibody dilution ($1:10^4$-$1:10^6$) were carried out (see figure 4.1A-F). Data was plotted both as the raw absorbance values and

the normalised values. The raw absorbance values show whether the amount of antibody and coat maxes out the signal on the plate reader (Flexstation maximal signal is 4 OD units) thus leading to little or no change in the standard curve as seen when looking at the normalised values.

10 and 100 ng/mL coating show similar results, regardless of the primary antibody dilution (1:10000-1:1000000). The absorbance raw values are maxed out, leading to little or no change observed in the standard curves (Figure 4.1C-F). At 10 ng/mL coating, the primary antibody dilutions at 1:10000 – 1:100000 still both maxes out the absorbance leading to no change in the normalised values as seen below (Figure 4.1A-B).

Similar experiments were carried out with a lower coating ranging from 0.01-1 ng/mL with primary antibody dilution at either 1:1 000 000 or 1:10 000 000 (Figure 4.2A-F). The data are presented both as the raw absorbance values, but also the normalised % changed from standard 0. The absorbance values are included to assess the signal achieved with the ELISA, as the % change from standard could potentially hide a very low signal (See Figure 4.2A-B). The standard curves from 0.01 and 0.1 ng/mL, no matter the primary antibody dilution (1:1000 000 -1:10 000 000), leads to a big decrease in absorbance and leads to increased variation (Figure 4.2C-F). At 1ng/mL the standard curves from both primary antibody dilution (1:1000 000 -1:10 000 000) are similar when compared at normalised values (Figure 4.2B). But when comparing the standard curves (Figure 4.2A) the 1:10 000 000 dilution of the primary antibody still leads to a low signal.

From both figure 4.1 and figure 4.2 the standard curve with the primary antibody dilution at $1:10^6$ at the 1ng/ml coating demonstrates a concentration-dependent decrease as ouabain concentration increases from 0.01 – 5 nM. Thus, the 1ng/ml coat and $1:10^6$ dilution of the primary antibody was chosen for all the subsequent experiments.

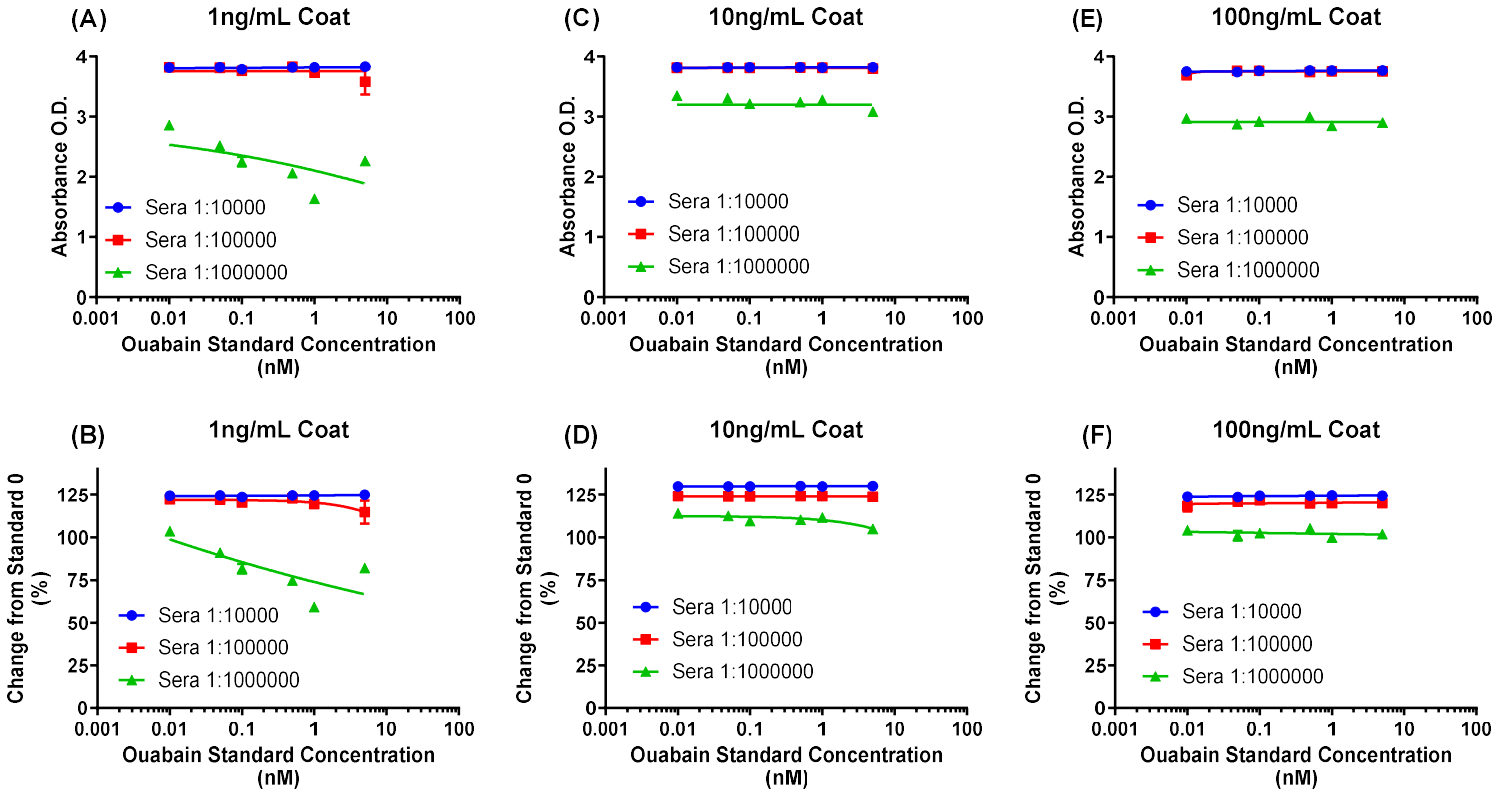


Figure 4.1 Effects of varying the primary antibody dilution factor and coating concentration. Absorbance values (A, C, E) and normalised (B, D, F) standard curves derived from 0.01-5 nM of ouabain with different coatings (1-100 ng/mL) and different primary antibody concentrations ($1:10^4$-$1:10^6$)(N/n=2/16 each). Data are presented as mean +/- S.E.M

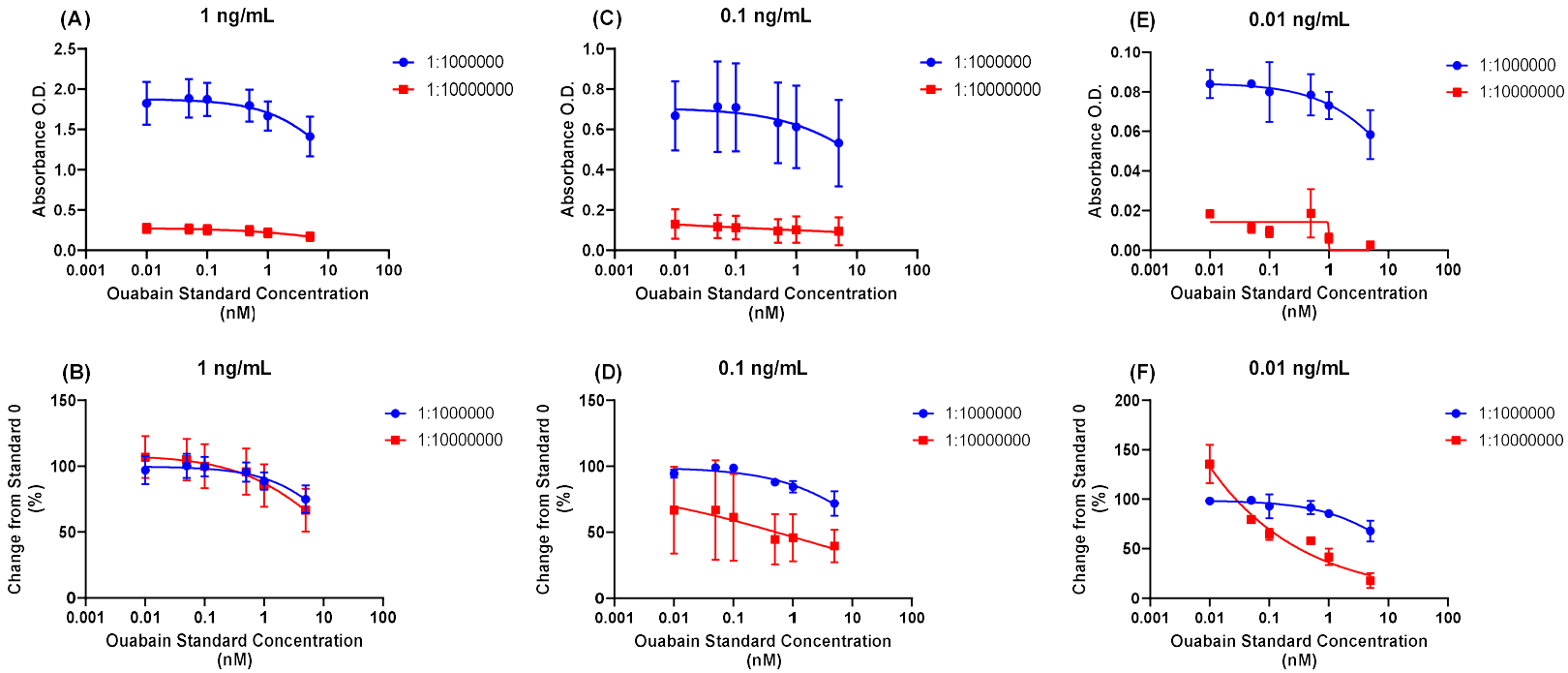


Figure 4.2 Effects of varying the primary antibody dilution factor and coating concentration. Absorbance values (A, C, E) and normalised (B, D, F) standard curves derived from 0.01-5 nM of ouabain with different coatings (0.01-1 ng/mL) and different primary antibody concentrations ($1:10^6$-$1:10^7$)(N/n=2/12 each). Data are presented as mean +/- S.E.M.

4.3.1.2 Primary antibody incubation time

Primary antibody incubation time optimisation is needed for optimal measurements with the ELISA. Thus incubation time with the primary antibody was carried out for 1 hour or 2 hours (see Figure 4.3A-C).

Standard curves of ouabain from 0.01 to 5 nM were done with either primary antibody incubation for 1 hour or for 2 hours (Figure 4.3A). The two standard curves do not look different and both show similar dose-dependent relationship. To allow direct comparison, the 0.1, 1 and 5 nM standards from both conditions were plotted both as normalised data (Figure 4.3B) and calibrated data (Figure 4.3C). Even though the standard curves are quite similar, at 0.1 nM the 2-hour incubation data point is significantly lower than the 1-hour incubation. These differences were not seen after calibration, and also neither the 1 or 10 nM standards showed any differences between incubation times. Because of the limited difference between conditions, the 1-hour incubation of the primary antibody was chosen forward.

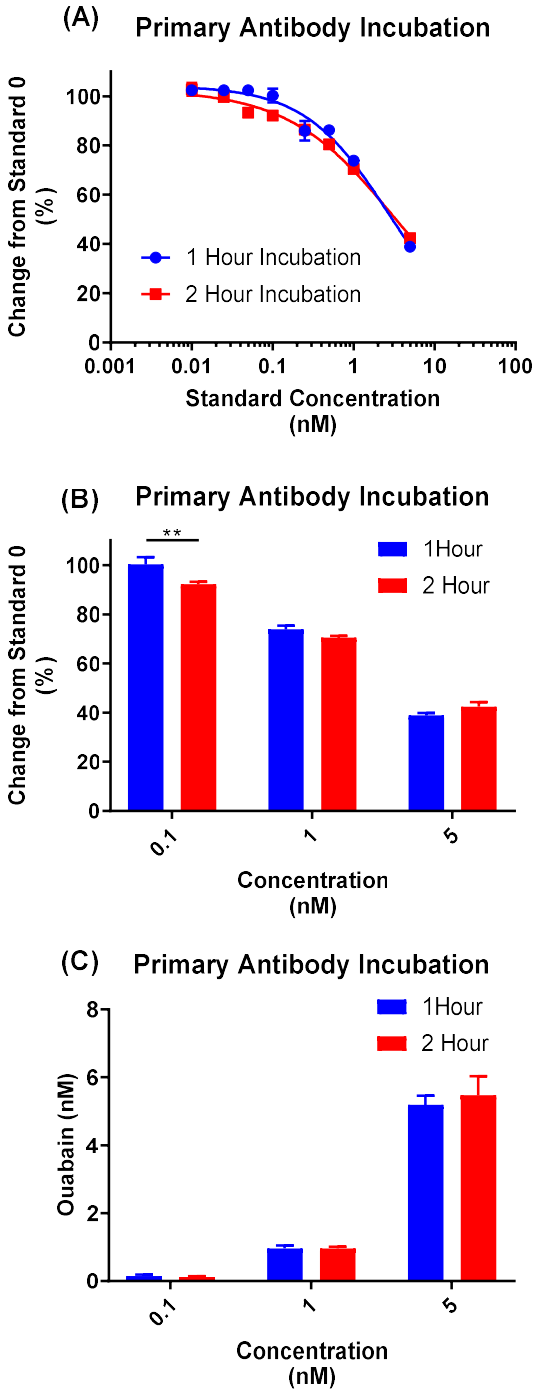


Figure 4.3 Incubation time of primary antibody. (A) Standard curves derived from 0.01-5 nM of ouabain with 1-2 hour incubation of primary (N/n=1/8 each). Normalised (B) and Calibrated

(C) data from ouabain (0.1-5 nM) at 1 or 2 hours of primary antibody incubation (N/n=1/8 each). Data were analysed by repeated Measures Two-way ANOVA with sidak post hoc test, ** $p < 0.01$. Data are presented as mean +/- S.E.M.

4.3.1.3 Choice of BSA as a blocking agent

The choice of blocking agent and its purity are known to be essential for optimal measurements with an ELISA. A molecular grade BSA has higher purity than regular grade and could potentially interfere less with the ELISA sensitivity. Hence molecular grade BSA was compared to regular grade BSA in terms of ELISA performance and sensitivity (see figure 4.4A-C).

Ouabain standard curves were generated ranging from 0.01 to 10 nM using regular or molecular grade BSA as blocking agent (Figure 4.4A). The standard curve of the molecular grade BSA have a less steep curve (Hill slope 0.647 vs 0.927) but seems more sensitive in the range of 0.025 – 10 nM ouabain. Thus to allow direct comparison, the normalised (Figure 4.4B) and calibrated data (Figure 4.4C) was plotted from 0.1, 1 and 10 nM standards from both conditions. The differences in the standard curves were also observed with both 1 nM and 10 nM of calibrated being significantly lower in the molecular biology grade BSA. These differences were not seen after calibration with the standard curves. Although a difference was observed at 0.1 nM with a significant decrease in the molecular biology grade. Because of the slight improvement in sensitivity the molecular biology grade BSA was chosen forward.

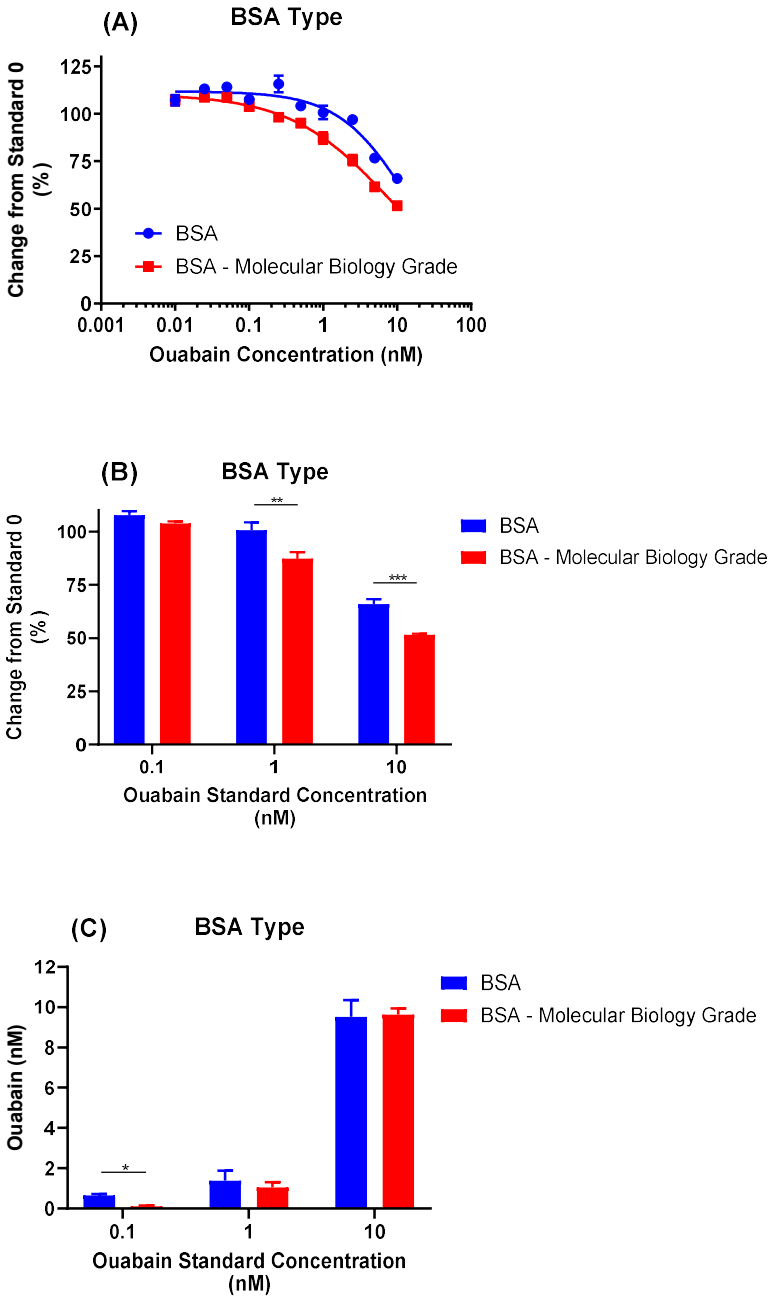


Figure 4.4 Choice of BSA type as blocking agent. (A) Standard curves derived from 0.01-10 nM of ouabain BSA at molecular biology grade or not (N/n=1/4 each). Normalised (B) and Calibrated (C) data from ouabain (0.1-10 nM) using BSA at molecular biology grade or not (N/n=1/4 each). Data were analysed by mixed-effects model with sidak post hoc test, * $p < 0.05$, ** p

< 0.01, *** p < 0.001. Data are presented as mean +/- S.E.M.

4.3.1.4 Choice of plates

Here, the 96-well half area plates and normal 96-well full area plates were assessed in terms of sensitivity for ouabain. Using half-area plates has the benefit of reduced volume and thus reduced costs, but must ensure that this alteration in methodology does not compromise the sensitivity of the ELISA.

Ouabain standard curves ranging from 0.01 to 10 nM were carried out in both half-area and full-area plates and compared as shown in figure 4.5A-C. The two standard curves were similar, both demonstrating a dose-dependent decrease in response with increasing ouabain concentration (Figure 4.5A). To further examine for potential differences the values from 0.1, 1 and 10 nM were plotted for direct comparison. No significant differences were found between half-area and full-area plates either in the normalised data or after calibration (Figure 4.5B-C).

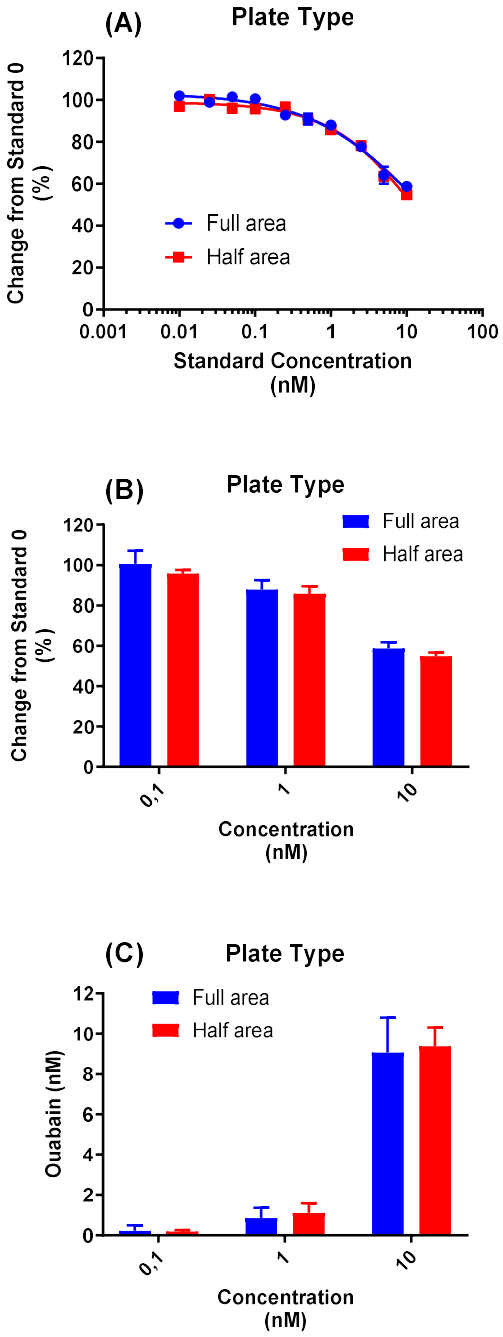


Figure 4.5 Choice of plate type. (A) Standard curves derived from 0.01-10 nM of ouabain from half and full area plates (N/n=1/8). Raw (B) and Calibrated (C) data from ouabain standards in half and full area plates at

concentrations of 0.1, 1 and 10 nM (N/n=1/8 each). Data are presented as mean +/- S.E.M.

4.3.2 Validation of cross-reactivity of primary antibody

In this thesis, the investigations of cross-reactivity included 4 compounds. Ouabain is a cardiotonic steroid belonging to the cardenolides. Hence cross-reactivity with digoxin, another cardenolide in clinical use for patients with AF and HF, was assessed for its potential to interfere with the ELISA. Marinobufagenin was chosen as it belongs to the other group of cardiotonic steroids, the bufadienolides. Marinobufagenin has been detected endogenously by a number of independent studies(175, 188, 197, 199, 248-250) and may therefore cross react with the ELISA. Dexamethasone and testosterone are both unrelated to cardiotonic steroids but were included as they both share the same steroidal core as ouabain. Testosterone is also present in circulation and dexamethasone is used as treatment for many patients, hereby covering both endogenous and exogenous steroids with similarity. . The results below are presented both as normalised raw values and also as calibrated values.

4.3.2.1 Cross-reactivity of Digoxin

The cross-reactivity of digoxin is displayed in figure 4.6 below. Standard curves were generated (Figure 4.6A). Digoxin and ouabain show a dose-dependent decrease in response to the standards added (0.01-10nM). The data from digoxin and ouabain alone or together at equimolar concentrations of 0.1, 1 and 10 nM are depicted in figure 4.6B as % of Std 0. It is clear that digoxin does affect the ELISA results and will potentially interfere with measurement of endogenous ouabain.

At 0.1 nM the digoxin group neither alone (98.75 (+/- 3.71) vs 94.91 (+/- 1.99), ns) nor together with ouabain (98.75 (+/- 3.71) vs 93.52 (+/- 2.29, ns) show siginificant change from standard or ouabain concentration. 1 nM digoxin group alone did not show any siginificant difference compared to the ouabain alone but did show significant change compared to the digoxin and ouabain group (Figure 4.6B). This therefore substantially affected the final ouabain concentrations, see figure 4.6C.

10 nM ouabain alone (51.64 (+/-2.17) vs 84.29 (+/- 3.21), <0.0001) and when equimolar with digoxin (44.52 (+/-2.34) vs 84.29 (+/- 3.21), <0.0001) shows a significant decrease in change of standard (%), compared to the 10 nM digoxin group. Following calibration with the ouabain standard curve, 10 nM digoxin, overestimates the ouabain concentration by circa 55% (Figure 4.6C). Thus, digoxin significantly cross react with the ouabain ELISA and may potentially substantively affect the results from patients treated with digoxin.

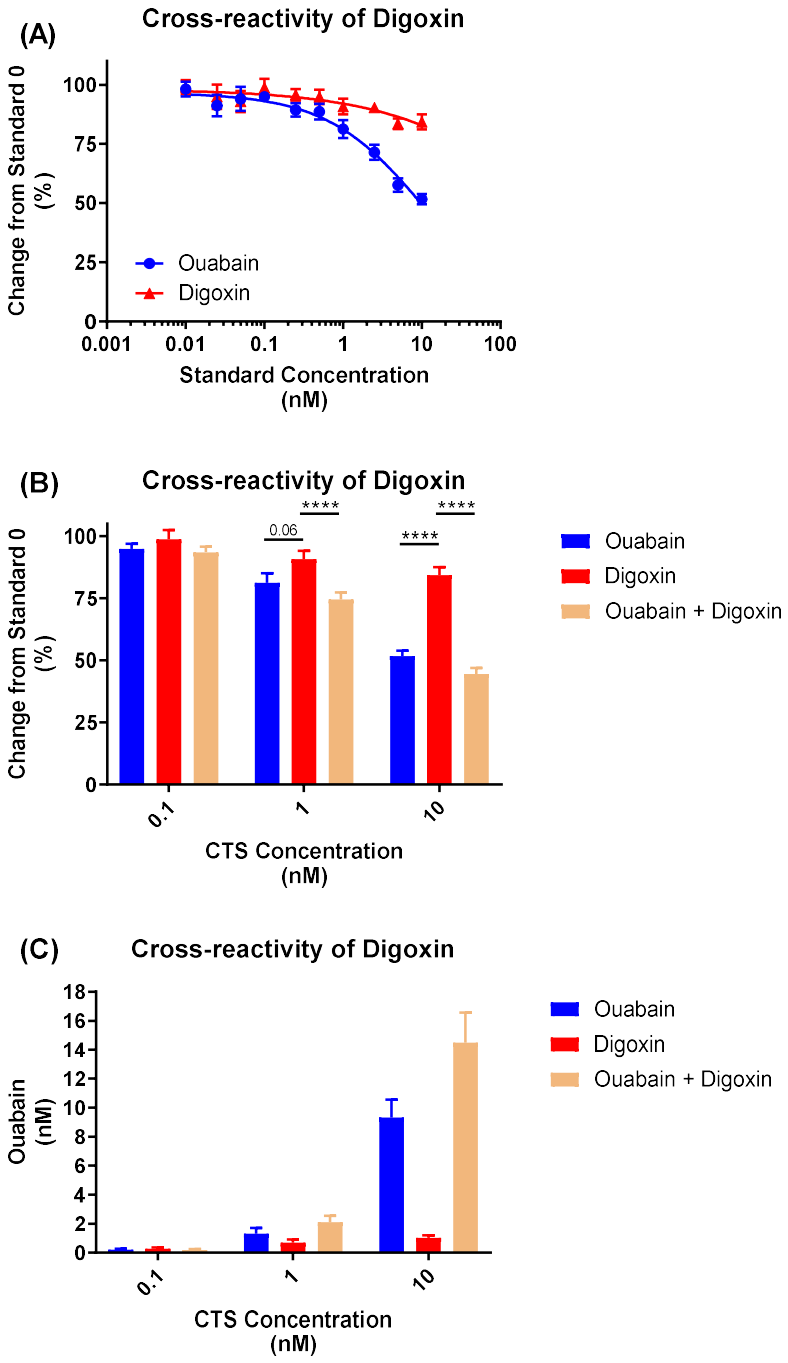


Figure 4.6 Cross-reactivity assessment of digoxin. (A) Standard curves derived from 0.01-10 nM of ouabain and digoxin (N=8 each). Raw (B) and Calibrated (C) data from ouabain or digoxin alone or at equimolar concentrations of 0.1, 1 and 10 nM (N=8 each).

Repeated Measures Two-way ANOVA with Tukey post hoc test, **** $p < 0.0001$. Data are presented as mean +/- S.E.M.

4.3.2.2 Cross-reactivity of marinobufagenin

The cross-reactivity of marinobufagenin was investigated and shown below in Figure 4.7. The standard curve was generated for ouabain only as marinobufagenin did not meet requirements for fitting with the development logistic function (Figure 4.7A). The ouabain standard curve demonstrates a dose-dependent relationship throughout the concentration range (Figure 4.7A). The data in figure 4.7 are presented as ouabain alone or together with marinobufagenin at equimolar concentrations of 0.1, 1 and 10 nM and depicted as % of Std 0 or ouabain concentration.

At 0.1 nM marinobufagenin group alone did not show significant difference when compared to ouabain alone (91.80 (+/- 1.24) vs 88.43 (+/- 0.91), ns) or when compared to the ouabain together with marinobufagenin group (91.80 (+/- 1.24) vs 95.62 (+/- 2.42), ns). Surprisingly, the ouabain group alone was lower compared to marinobufagenin and ouabain together (88.43 (+/- 0.91) vs 95.62 (+/- 2.42), <0.05) as seen in figure 4.7B.

Marinobufagenin group alone at 1 nM, was significantly higher than both ouabain alone (88.75 (+/-1.55) vs 71.38(+/-1.73), p=0.0001) and ouabain and marinobufagenin together (88.75 (+/-1.55) vs 66.3 (+/-2.42), <0.0001). No difference was observed between the ouabain alone when compared to ouabain and marinobufagenin together (71.38(+/-1.73) vs 66.3 (+/-2.42), ns).

The 10 nM marinobufagenin shows similar results to the 1 nM, being significantly higher than ouabain alone (86.97 (+/-0.82) vs 51.68 (+/-1.55), <0.0001) and ouabain and marinobufagenin together (86.97 (+/-0.82) vs 50.13 (+/-1.42), <0.0001). Again, the ouabain group alone is not significantly changed when compared to the ouabain with marinobufagenin group at 10 nM (51.68 (+/-1.55) vs 50.13 (+/-1.42), ns).

The ouabain standard curve was used to calibrate the raw data, shown below figure 4.7C without displaying any significant changes. It is clear that marinobufagenin does not significantly cross-react with the ouabain ELISA, as maribobufagenin did not change over concentrations used and also did not interfere with ouabain.

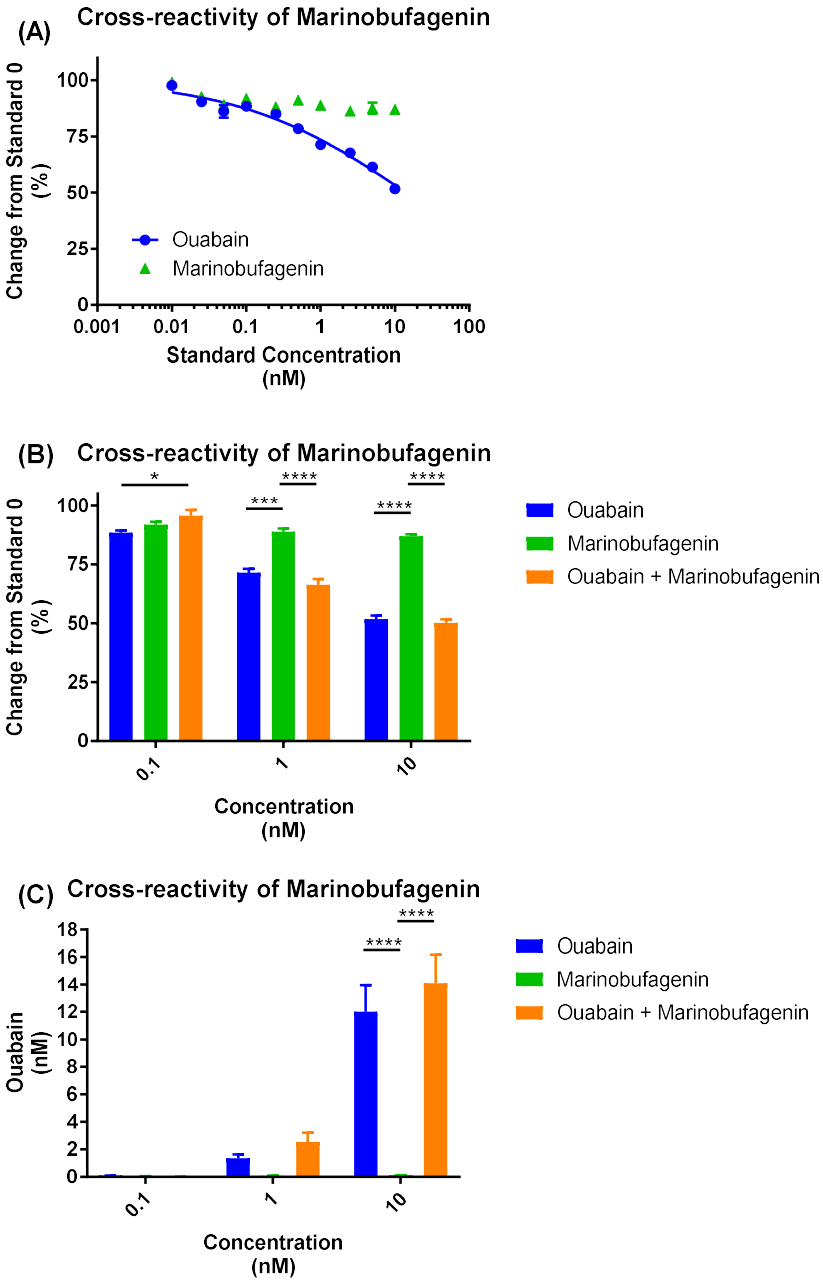


Figure 4.7 Cross-reactivity assessment of marinobufagenin. (A) Standard curves derived from 0.01-10 nM of ouabain and marinobufagenin (N=2 each). Raw (B) and Calibrated (C) data from ouabain or marinobufagenin alone or at equimolar concentrations of 0.1, 1 and 10 nM (N=2 each). Repeated Measures Two-way ANOVA with Tukey

post hoc test, * p < 0.05, *** p < 0.001, **** p < 0.0001. Data are presented as mean +/- S.E.M.

4.3.2.3 Cross reactivity of Testosterone

Figure 4.8 below shows the investigations of cross-reactivity of testosterone presented as ouabain alone or together with testosterone at equimolar concentrations of 0.1, 1 and 10 nM and depicted as % of Std 0 and ouabain concentration. Similarly, to marinobufagenin, the testosterone standards did not meet the requirements for fitting with the development logistic function, thus only ouabain standard was fitted. After fitting, ouabain

displays a dose-dependent relationship throughout the concentration range (Figure 4.8C).

At 0.1 nM the testosterone together with ouabain did test significantly higher when compared to ouabain alone (102.25 (+/- 1.04) vs 94.45 (+/- 0.37), p=0.021) or when compared to testosterone alone (102.25 (+/- 1.04) vs 95.49 (+/- 0.87), p=0.047). No difference was observed between ouabain and testosterone alone when compared at 0.1 nM (94.45 (+/- 0.37) vs 95.49 (+/- 0.87), ns). No differences were observed after calibration.

At 1 nM significant decreases in change from strandard (%) are observed between ouabain alone (82.83 (+/- 2.72) vs 99.32 (+/-3.52), <0.0001) or ouabain together with testosterone (81.07 (+/- 1.11) vs 99.32 (+/-3.52), <0.0001) when compared to the testosterone alone group. However, no changes were observed between ouabain with and

without testosterone present (82.83 (+/- 2.72) vs 81.07 (+/- 1.11), ns). The changes observed were no longer present after calibration.

At 10 nM, testosterone shows significant changes to both ouabain alone (58.40 (+/- 1.32) vs 100.19 (+/- 1.50), <0.0001) and to ouabain with testosterone (49.00 (+/- 1.95) vs 100.19 (+/- 1.50), <0.0001), indicating that testosterone does not interfere with the ouabain ELISA. However, a significant decrease is observed when comparing ouabain with testosterone to ouabain alone (58.40 (+/- 1.32) vs 49.00 (+/- 1.95), p= 0.006), 16% reduction in response (Figure 4.8B). After using the ouabain standard curve for calibration, testosterone when equimolar with ouabain leads to a 114% increase (Figure 4.8C). This indicates that whilst testosterone alone does not cross-react with the ouabain ELISA, together with ouabain, it substantively affects the assay at higher concentrations.

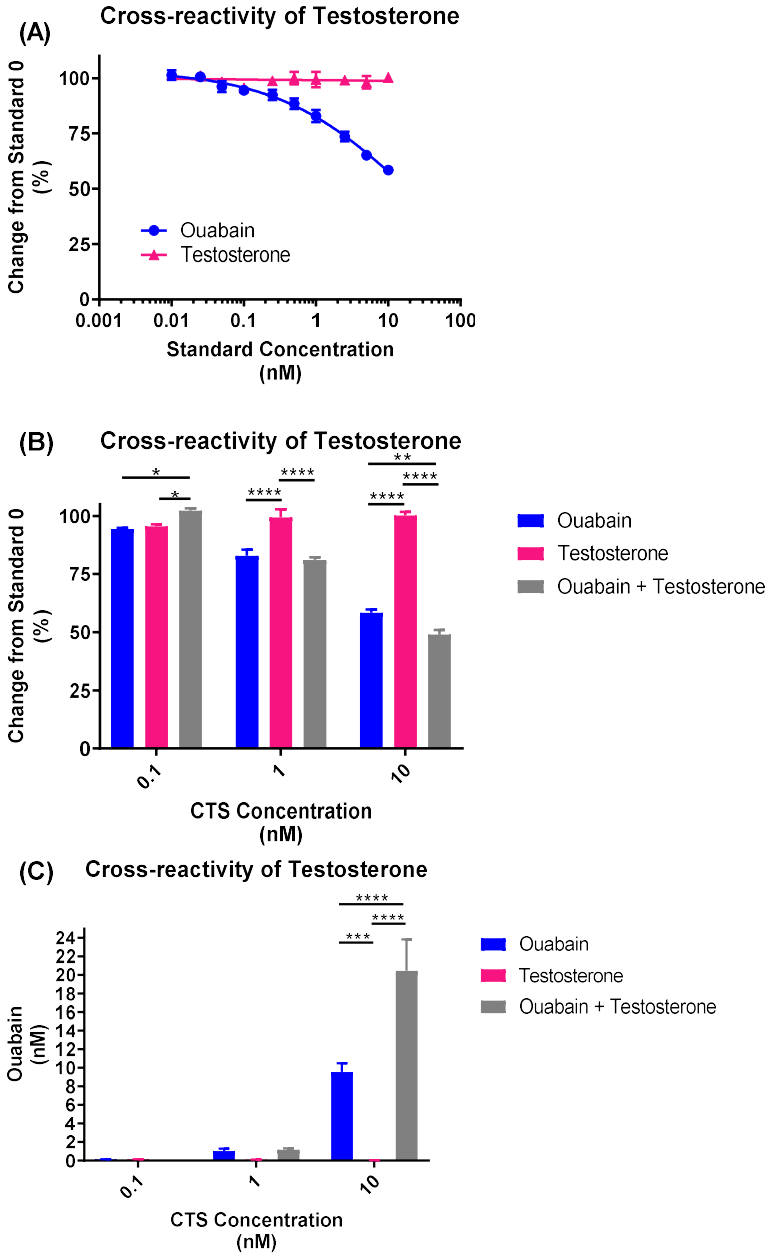


Figure 4.8 Cross-reactivity assessment of testosterone. (A) Standard curves derived from 0.01-10 nM of ouabain and testosterone (N=3 each). Raw (B) and Calibrated (C) data from ouabain or testosterone alone or at equimolar concentrations of 0.1, 1 and 10 nM (N=3 each). The raw data was analysed using repeated measures Two-way ANOVA with Tukey post hoc test, * $p < 0.05$, ** $p < 0.01$, **** $p < 0.0001$. The calibrated data was analysed by a mixed-effects analysis with Tukey post hoc test, ***

$p < 0.001$, **** $p < 0.0001$ Data are presented as mean +/- S.E.M.

4.3.2.4 Crossreactivity of Dexamethasone

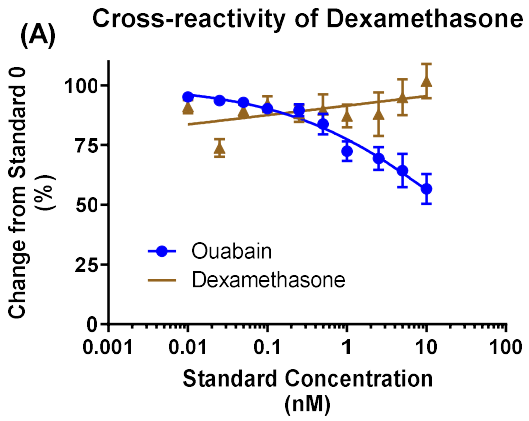
Dexamethasone was tested for cross-reactivity with the ouabain ELISA. Below in figure 9 data of dexamethasone alone or together with ouabain at equimolar concentrations of 0.1, 1 and 10 nM are presented. Similarly, to both testosterone and marinobufagenin above, the dexamethasone standards were not suitable for fitting with the logistic function developed earlier this chapter. Ouabain standards were still fitted with the logistic function creating the standard curve utilised for the calibration of the normalised raw values. ouabain displays a dose-dependent relationship throughout the concentration range (Figure 4.9A).

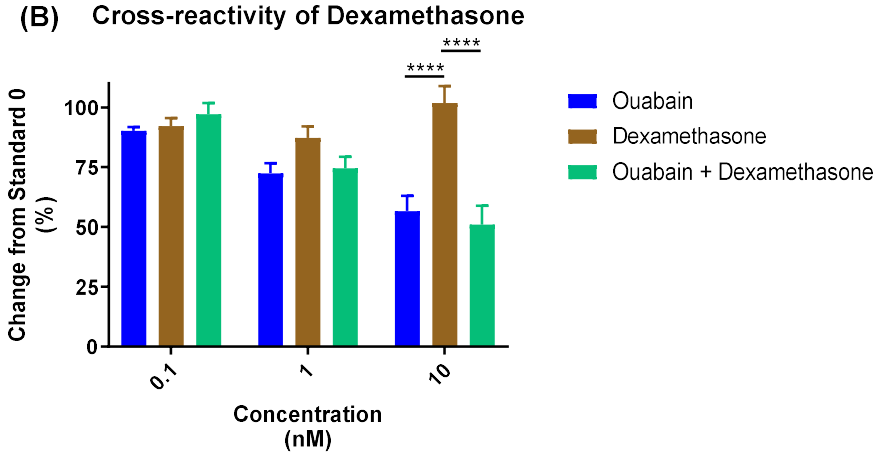
Both at 0.1 and 1 nM dexamethasone shows no observable differences between any of the tested groups. However, both 1 nM ouabain with/without dexamethasone has a trend of being lower than dexamethasone alone, without being significantly different.

The 10 nM dexamethasone level is significantly higher and thus closer to Std 0 than both ouabain alone (56.74 (+/- 6.28) vs 101.77 (+/- 7.17), <0.0001) and ouabain with dexamethasone (51.03 (+/- 7.87) vs 101.77 (+/- 7.17), <0.0001) (Figure 4.9B).

Lastly, the calibrated values trended higher at both 1 and 10 nM for ouabain with/without dexamethasone compared to dexamethasone alone as seen in figure 4.9C. It is important

to emphasise that in this set of experiment, the large variability of data may have affected the conclusions. Nevertheless, dexamethasone did not significantly affect the ouabain ELISA and thus shows limited cross-reactivity.





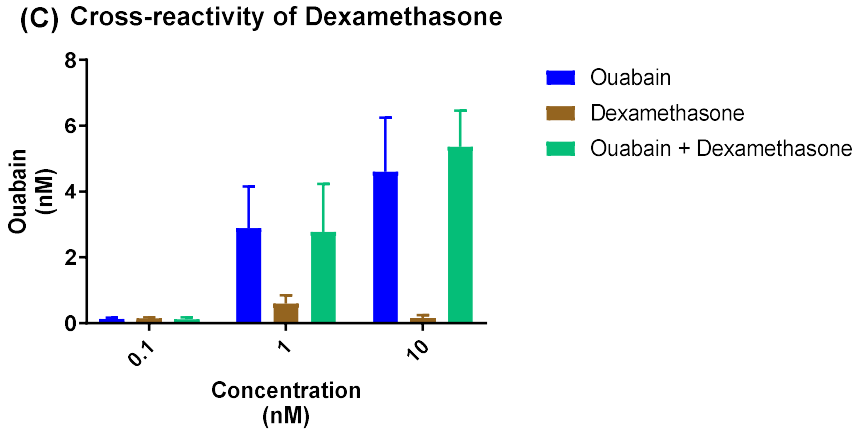


Figure 4.9 Cross-reactivity assessment of dexamethasone. (A) Standard curves derived from 0.01-10 nM of ouabain and dexamethasone (N=6 each). Raw (B) and Calibrated (C) data from ouabain or dexamethasone alone or at equimolar concentrations of 0.1, 1 and 10 nM (N=6 each). Repeated Measures Two-way ANOVA with Tukey post hoc test, **** $p < 0.0001$. Data are presented as mean +/- S.E.M.

4.3.2.5 Table of cross-reactivity

Cross-reactivity calculation (%) was based on the 10 nM measurements between ouabain and steroids tested, see formulas below (Equation 4.4 and 4.5 below). The calculated cross-reactivity based on both raw and calibrated numbers is summarised below in Table 4.1.

Equation 4.4:

$$Raw\ \ cross-reactivity(\%) = \left(\frac{100 - \%STD\ [Tested\ Steroid]}{100 - \%STD\ [Ouabain]}\right) * 100$$

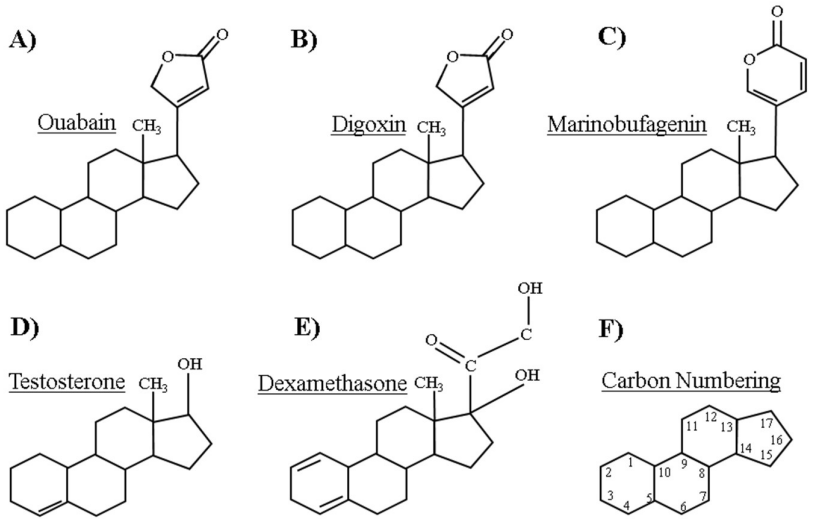
Equation 4.5:

$$Calibrated\ cross-reactivity(\%) = \left(\frac{100 - \%STD\ [Tested\ Steroid]}{100 - \%STD\ [Ouabain]}\right) * 100$$

	Raw Cross-reactivity (%)	**Calibrated Cross-reactivity (%)**	**N Values**
Digoxin	32.47	10.94	8
Marinobufagenin	26.96	0.89	2
Testosterone	-0.46	0.24	3
Dexamethasone	-4.09	3.47	6

Table 4.1 Table of calculated cross-reactivity from both raw and calibrated values of Digoxin, Marinobufagenin, Testosterone and Dexamethasone.

The 4 tested steroids in this section of the thesis all have similarities with ouabain and were chosen for different reasons as a validation of the primary antibody (See Figure 4.10 below). Using the above-explained methodology to calculate the cross-reactivity of the four tested steroids, digoxin demonstrates the highest cross-reactivity towards the primary antibody. Marinobufagenin shows a more modest reaction with the primary antibody leading to the second-highest cross reactivity percentage of the tested steroids. Both testosterone and dexamethasone show very low levels of cross-reactivity with the primary antibody in comparison to the two cardiotonic steroids tested shown both by raw data and calibrated data.



G)

	1	3	5	9	10	11	12	14	17
Ouabain	OH	Rhamnose	OH		CH_2OH	OH		OH	5 membered lactone ring
Digoxin		$(D\text{-}Digitoxose)_3$					OH	OH	5 membered lactone ring
Marinobufgenin		OH	OH		CH_3			14-O-15	6 membered lactone ring
Testosterone		O							OH
Dexamethasone		O		F	CH_3	OH			COCOH + OH

Figure 4.10 Steroid structure of the steroids included in the cross-reactivity investigations. For clarity not all groups are shown on the compounds, but rather compared in figure 4.10 G. The cardiotonic steroids have lactone rings while testosterone and dexamethasone have alcohol. The specific changes in the commonly shared steroidal structure on various positions are shown. Created by the author of the thesis.

4.3.3 Detection of Cardiotonic steroids from spiked serum/plasma samples

The main aim of this chapter is to develop and validate the ELISA methodology for measurement of endogenous ouabain in the blood of patients enrolled into the BBC-AF, RATE-AF and potentially other clinical trials. It is likely that patient serum or plasma will contain many other compounds that are similar in structure to ouabain. These potential contaminants and the matrix they are in could interfere with the ELISA measurements. Thus a key element was to assess the validity of using an extraction methodology to isolate the compounds of interest, in this case being the cardiotonic steroids. To examine this, ouabain standards and extracted serum spiked with ouabain and then extracted using the Thermo Sola solid-phase extraction methodology were utilised. The ouabain standards show an expected dose-dependently decreased response (Figure 4.11A). This standard curve created was used to normalise the raw data.

Neat ouabain and extracted material from spiked samples at 1 nM, 10 nM and 100 nM were compared and shown as raw and calibrated data in figure 4.11B and 4.11C, respectively. At both 1 and 10 nM, the neat ouabain values were significantly lower when compared to extracted samples, in raw measurements (Figure 4.11B). The significant difference between the two was still observed when the data were calibrated using the standard curve. These results indicate that as expected, extraction of ouabain from plasma

is possible in a dose dependent manner, though extraction itself does result in some loss of the spiked ouabain. At 100 nM no difference was observed between the predicted response and the extracted material looking at either the raw or calibrated data (Figure 4.11B-C).

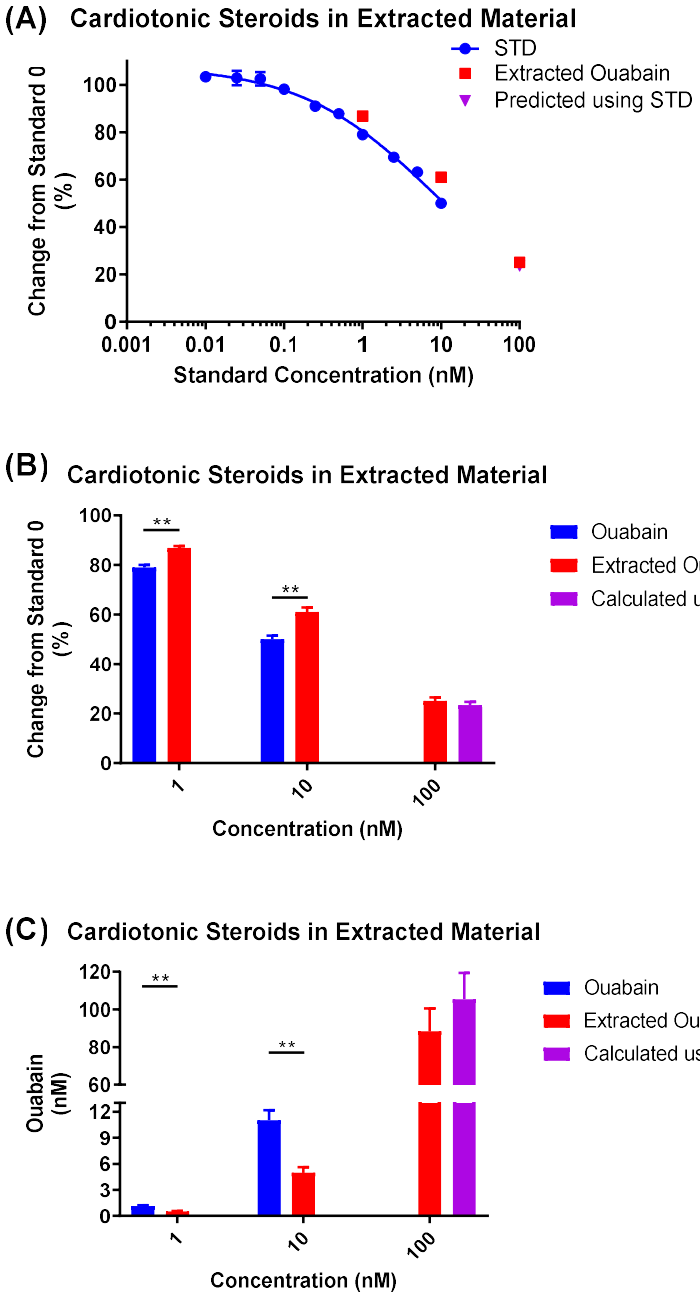


Figure 4.11 Detection of cardiotonic steroids in extracts from spiked samples. (A) Standard curves derived from 0.01-10 nM of ouabain with extracted ouabain (10-100nM) and calculated ouabain for 100 nM based on the standard curve (N=3 each). Raw (B) and Calibrated (C) data from ouabain (1-10 nM), extracted ouabain (10-

100 nM) and predicted ouabain level for 100 nM based on the standard curve (N=3 each). Data were analysed by multiple t-tests with Holm-Sidak correction method for multiple comparisons. Data are presented as mean +/- S.E.M.

4.4. Discussion

4.4.1 Development of ELISA

The goal of this chapter was to develop a methodology not based on radioactivity to allow for quantification of endogenous ouabain from patient samples. An HRP antibody-based methodology was chosen and prior to using the developed ELISA for patient samples (chapter 5), it was assessed for its sensitivity, stability and cross reactivity. The ELISA developed in this chapter is quick to perform (<5 hrs) and demonstrates consistent sensitivity to ouabain.

The primary antibody is highly important for the sensitivity of any methodology. Using the validated ELISA methodology, the sensitivity of the ELISA was very similar to the previously published work of around 0.1 nM(207). Other studies using either RIA(130, 139, 241) or ELISA(239, 240, 242) based methodologies have observed slightly better sensitivities between 0.01-0.076 nM. These differences could be due to the primary antibody difference used by different groups. The two main factors having an impact are 1) differences in ouabain conjugates used for immunisation (BSA-Ouabain, OVA-Ouabain, Ouabain-Keyhole limpet hemocyanin, Ouabain-succinyl dihydrazide-OVA) (See table 2 below for summary) and 2) most groups using immunisation in rabbits (125, 130, 133, 142, 144, 148, 153, 155, 161, 207, 239-242) while a few in other species like

goats(139, 141, 241), sheep(171) or rats(138, 140). These slight changes in the primary antibody and the choice of methodology could explain the small changes in sensitivity was observed.

4.4.2 Structural effects on cross-reactivity of the ouabain primary antibody

An essential part of the validation was to validate the cross-reactivity of the ouabain primary antibody both against 1) other cardiotonic steroids which might be in circulation and 2) also compounds known to have a steroidal backbone and be either in circulation (testosterone) or used as a treatment for some patients (dexamethasone).

Assessing the cross-reactivity in this thesis as described above is slightly different than what other studies have done(96, 139, 207, 239, 240, 242). Usually, the calculations were based on differences in IC50s rather than a specific concentration. In this thesis, it is calculated on the basis of a 10 nM as some steroids react minimally with the primary antibody. This could lead to overestimating the cross-reactivity and could explain potential differences.

Dexamethasone, a corticosteroid, has a much similar steroidal core to ouabain with main differences being the absence of rhamnose group on carbon 3 and having an ester on C17 instead of the 5-membered ring (See Figure 4.10 A, E and G). In the investigation in this thesis, the primary antibody displayed very limited cross-reactivity with dexamethasone (Figure 4.9 and Table 4.1). No other studies were found to investigate cross-reactivity of

dexamethasone. A few studies using a similar primary antibody (ELISA or RIA methodology) investigated two other corticosteroids, deoxycorticosterone(133, 207, 239, 240) and corticosterone(133, 139, 207, 239, 240, 242), which demonstrated a limited amount of cross-reactivity as well. Together these findings indicate that the primary antibody has limited binding affinitity to these two corticosteroids.

Testosterone shares some structural similiarity with dexamethasone and ouabain. Main differences being the lack of the rhamnose group at C3 but also having very few hydroxide groups in comparison (See Figure 4.10 A, D and G). Testosterone did not demonstrate any noteworthy cross-reactivity either calculated of raw or calibrated data (see table 4.1). Testosterone does at higher doses demonstrate potential interference with the ELISA. The very low observed calculated cross-reactivity is very similar when comparing to available literature, which demonstrates testosterone having very low cross-reactivity with the primary antibodies used for cardiotonic steroids(133, 139, 207, 239, 240, 242). Another steroid similar to testosterone, progesterone, has also previously been shown to exert low cross reactivity(96, 133, 139, 207, 239, 240, 242). So in line with previously published work, regardless of either being ketone/hydroxyl group replacements of the lactone rings and also missing the sugar moiety, the steroids display very limited cross-reactivity.

So the fact that dexamethasone (and other corticosteroids) but also sex steroids like testosterone and progesterone (not tested in this thesis) show limited cross-reactivity

could imply that steroids missing the lactone ring (5 or 6 membered) and/or the sugar moiety exert very low cross-reactivity towards the primary antibody.

Marinobufagenin is a bufadienolide, which has a 6-membered lactone ring instead of the 5-membered ring and the sugar moiety is replaced by a hydroxyl group (see figure 4.10). These differences change the interaction enough with primary antibody utilised in this ELISA, that the primary antibody does not seem to cross-react substantively with marinobufagenin. The literature was examined for other studies investigating the cross-reactivity of marinobufagenin. No such studies were found leading to no comparisons the previous work. Two studies(139, 239) did test another bufadienolide, bufalin, which is very similar apart from a replacement of the ketone on C14-15 with a hydroxyl group. Both studies found some cross-reactivity with their ouabain primary antibodies (see table 4.2 below).

Cross-reactivity with digoxin was assessed for several reasons 1) it is still being used as a treatment for atrial fibrillation and heart failure in the UK and could be present endogenously and 2) it is structurally similar to ouabain. These patients are usually treated with digoxin levels between 0.6 – 1.2 nM, which is close to the investigated concentrations used in this and the chapter prior to this. The interference of digoxin showed from the data in this chapter seems lower at 1 nM than at 10 nM. But it cannot be ruled out some interference will be seen in potential samples with digoxin present around 1 nM, which as it is close to this level for many patients, will have to be considered strongly when used for patient samples. As the reported levels of endogenous CTS could

be affected by digoxin concentrations present in the individual patient. Main differences between ouabain and digoxin are the sugar moiety change from a rhamnose group on ouabain, being replaced with a much longer chain of sugars (3 D-Digitoxose). There are also changes in the number of hydroxyl groups (see details in figure 4.10). In the chapter presented here, based on the concentrations used of digoxin, medium (10-36%) cross-reactivity was observed. This would imply cross-reactivity and thus interference in all the studies where patients were treated with digoxin. Previously, studies(130, 133, 139, 144, 207, 239-242) have found lower levels of cross-reactivity for most studies ranging <0.0001 - 9.2% as summarised in table 2 below. These variations can partly be due to the differences observed between ouabain and digoxin, with the rhamnose group or the hydroxyl groups potentially be important for interaction with the primary antibody. But could also be due to either the differences immunisation process or methodology used for these measurements.

Another way to assess cross-reactivity is by using the IC50s for cross-reactivity calculation. Of the steroids tested only ouabain and digoxin, in the concentration range used, were able to utilise the IC50 calculation method. Thus standard curve fitting was used to estimate the IC50 values of both ouabain (10.75) and digoxin (441.7nM). From these values, the cross-reactivity calculated for digoxin would be 2.43 %. This seems more comparable to what other studies have reported (see table 4.2).

There are many other cardiotonic steroids that could potentially influence the assay, although these have not been investigated in the presented work. Most structurally related to ouabain is ouabagenin and dihydro-ouabain (see table 2 below). Dihydro-ouabain

surprisingly does not demonstrate any noticeable interference in other studies. Interestingly ouabagenin seems to have relatively high cross-reactivity with the primary antibodies used, especially with the antisera based on conjugates with either BSA or OVA. Ouabagenin is a degradation product of ouabain, missing the rhamnose group. The importance of the rhamnose group was discussed above and suggested to be a possible factor contributing to the overall determining reactivity with the primary antibody. Hence the investigations showing high cross-reactivity of ouabagenin is both surprising but also interesting and needs to be considered as a potential interferant.

Lastly, the degradation product of digoxin but also digitoxin (used in Germany instead of digoxin) and its degradation product could in some patient groups be present. A few studies (see table 4.2 below) show that degradation products of digoxin (digoxigenin) and digitoxin (digitoxigenin) demonstrate no or limited cross-reactivity with ouabain quantitative assays. Interestingly, digitoxin unlike digoxin show at least in the OVA-ouabain immunisation based antisera quite high cross-reactivity (see table 4.2 below). But this observation is true only for ELISA studies, while the RIA method-based studies show no cross reactivity. The difference between digoxin and digitoxin is one hydroxyl group on C12. That hydroxyl group is also present in ouabain and ouabagenin and could potentially explain some of the difference as well as the different methodologies.

Comparison of cross-reactivity in studies investigating cardiotonic steroids									
	Harris et al(207)	Doris(130)	Gomez-Sanchez et al(239)	Lewis et al(240)	Naruse et al(241)	Komiyama et al(133)	Semra et al(139)	Harwood et al(242)	Worgall et al(144)
Assay method	ELISA	RIA	ELISA	ELISA	RIA	ELISA	RIA	ELISA	RIA
Primary Antibody	Ouabain rabbit antisera	Ouabain rabbit antisera	Ouabain rabbit antisera	Ouabain rabbit antisera	Ouabain rabbit antisera	Ouabain rabbit antisera	Ouabain goat antisera	Ouabain rabbit antisera	Ouabain rabbit antisera
Immunisation	1 OVA-C6-Ouabain 2 Poly-D-Lysine-ouabain 3 OVA-SDH-Ouabain	BSA-Ouabain	Jack bean urase-ouabain or Thyroglobulin-Ouabain	OVA-C6-Ouabain	BSA-Ouabain	OVA-C6-Ouabain OVA group removed prior to assay use.	1. OVA-C6-Ouabain 2. Keyhole Limpet hemocyanin-Ouabain	OVA-C6-Ouabain	BSA-Ouabain
Dehydro-Ouabain	0.16	-	0.015	-	-	0.82	2	0.3	-
Ouabagenin	40	56.2	2.2	77.24	-	72	4	55	88
Digoxin	5.2	<0.025	<0.0001	1.25	9.2	6.4	0.4	5.3	<0.1
Digoxigenin	-	-	<0.0001	-	-	-	0.1	-	-
Digitoxin	28	-	-	-	-	84.6	0.67	78	<0.1
Digitoxigenin	-	-	0.12	-	-	-	1.5	-	-
Bufalin	-	-	<0.0001	-	-	-	1.3	-	-

Table 4.2 The studies found to investigate the cross-reactivity of cardiotonic steroids are compared in the table above. Including information of assay type, primary antibody type, immunisation differences and the cross-reactivity % from various steroid.

4.5. Conclusion

The sensitivity of the developed competitive ELISA is comparable to previous shown work for similar polyclonal primary antibodies. The primary antibody did demonstrate some cross-reactivity with other steroids, mainly digoxin, but potentially also testosterone. Nevertheless, the assay was able to detect and quantify ouabain from spiked human serum. Thus, the next step was assessing ouabain concentrations in patient samples (see chapter 5).

CHAPTER 5. UTILISATION OF VALIDATED ASSAYS FOR RATE-AF PATIENT PLASMA SAMPLES

5.1. Introduction and aims

The RATE-AF trial was the first randomised clinical trial comparing head-to-head digoxin and beta-blocker treatment in permanent AF patients. The trial was a prospective study with open labels randomization and blinding of the major endpoints. Furthermore, the trial and all subsequent work was carried out according to Good Clinical Practice(251). 160 patients were invited to participate in the trial. The trial was carried out as seen below in figure 5.1. Briefly, patients were recruited and firstly assessed for quality of life, walk distance, full echocardiographic analysis of the heart. Blood samples were also collected for measurements of biomarkers including endogenous CTS. The patients were then randomised into either digoxin or beta-blocker treatment arm. Every patient had a follow-up visit after 6-months of treatment with similar tests as baseline. The plasma samples from each visit were collected and stored in the human biomaterials resource centre at the University of Birmingham. Samples were collected as according to Human Biomaterials Resource Centre (HBRC) protocol and stored at -80 degrees until use for extractions.

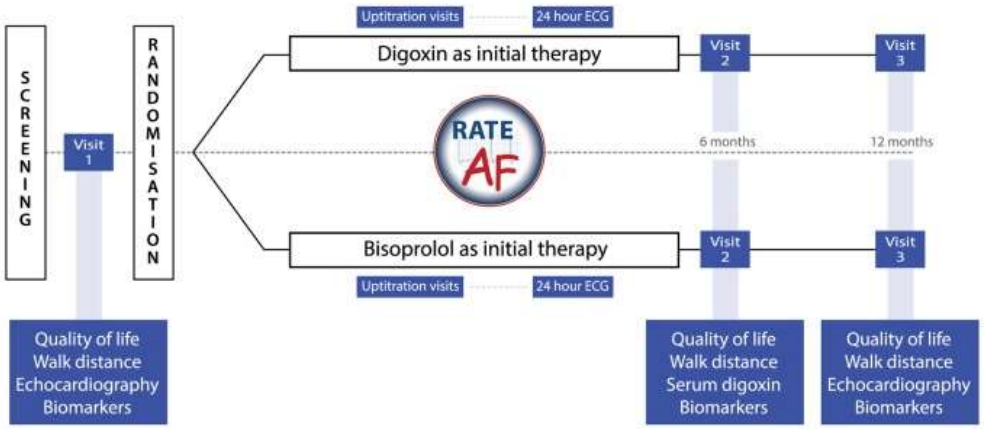


Figure 5.1 Flow chart of the RAte control Therapy Evaluation in permanent Atrial Fibrillation (RATE-AF) trial. Adapted with permission from Kotecha et al 2017(252).

Each of the collected samples were utilised in the ELISA and cell-based methodologies as described in Chapter 3 and Chapter 4.

(i) To examine whether changes in intracellular sodium levels correlate with disease stage, kidney function, cognitive function, age.

(ii) To examine whether endogenous ouabain levels correlate with disease stage, kidney function, cognitive function, age.

(iii) To examine whether endogenous ouabain levels affect digoxin treatment response in patients with atrial fibrillation enrolled in RATE-AF trial.

5.2. Analysis of RATE-AF trial data

Important to note is the data displayed below is from baseline values only, as the RATE-AF clinical trial was still not closed during the write up of this thesis. Inclusion of treatment arms risk compromising the clinical trials randomisation and were therefore not

allowed in this thesis. The baseline data allows comparison of different disease stages of disease and for correlation with HEK293t cell based and ELISA assays. It also allows comparisons between the two randomised group arms prior to treatment.

For each patient age, gender and total of 189 clinical variables were collected during the trial. Our primary focus is to examine the correlation of endogenous ouabain and effects on intracellular sodium at baseline and key variables such as gender, heart failure stage, atrial fibrillation classification score etc. Secondary aim is to broaden these correlations to other relevant cardiovascular variables of interest. The included variables can be divided into subgroups and are displayed below in table 5.1. In this chapter, raw data of HEK293t cell base assays and calibrated ELISA data have been used to examine potential correlation of endogenous ouabain and other CTS and clinical variables in RATE-AF patients.

General characteristics	Clinical Characteristics	Blood parameters	Electrocardiogram	Echocardiography
Age	Years in AF	Magnesium	HR	Left Ventricular End-diastolic volume
Gender	Modified EHRA score	Potassium	QRS duration	Left Ventricular End systolic volume
Height	Diagnosed with HF	Hb	QT duration	Left Ventricular ejection fraction
Weight	NYHA class	Hct	Estimated EF	LA volume
BMI	MI	NT-proBNP		E/e'
Waist circumference	Years since last MI	Sodium		Global longitudinal strain
Total distance walked	Stroke	Calcium		Systolic velocity of tissue Doppler at lateral annulus
	Years since last stroke	Creatinine		Systolic velocity of tissue Doppler at septal annulus

	Type 1 diabetes			Diastolic velocity of tissue Doppler at lateral annulus
	Type 2 diabetes			Diastolic velocity of tissue Doppler at septal annulus
	Insulin			Mitral valve inflow max velocity
	BP systolic			Mitral flow deceleration time
	BP diastolic			Average e' taken from the lateral and septal annulus
	Nephropathy			
	Neuropathy			
	Vascular disease			
	Previous cardioversions			
	Cardioversion			
	AF ablation			
	How many AF ablation			

	Peripheral edema			
	Hospitalisations			
	Digoxin (yes/no)			
	Years since last digoxin			
	Pulmonary hypertension			
	LV hypertension			
	Mini-Mental State Examination			
	Atrial Fibrillation Effect on QualiTy-of-life			

Table 5.1 List of variables of interest measured/recorded in RATE-AF patient cohort. AF, Atrial fibrillation; BMI, Body mass index; EF, Ejection fraction; HR, Heart rate; LV, Left ventricular; mEHRA, modified European Heart Rhythm society Atrial fibrillation score; NTpro-BNP, N-terminal prohormone of brain natriuretic peptide; NYHA, New York Heart Association.

The 61 variables were chosen prior to analysis thus excluding selection bias. Numerical variables were analysed with correlations. The categorical data could not be analysed by correlations, but were analysed as grouped comparisons instead. Some variables (Type 1 diabetes, insulin, nephropathy, neuropathy, vascular disease and peripheral edema, how many AF ablations, previous cardioversions, Cardiovert number, AF ablation, digoxin, years since last digoxin, pulmonary hypertension, LV hypertension) had limited patients with data hence they were excluded from analysis.

5.3. Results

Patients characteristics within the RATE-AF are listed in Table 5.2.

5.3.1 Population characteristics of RATE-AF patients

160 patients were included in the RATE-AF cohort. The collective characteristics of the patients at baseline prior to randomisation are displayed in the table 5.2 below. Of the patients included the mean age was 75.6 years (SD: +/-8.2) with 46.3% being women. The mean ECG heart rate was 99.7 beats/min (SD: +/- 18) with mean systolic blood pressure of 135.6 mmHg (SD: +/- 16.1). All the patients recruited were only included if rate control therapy was appropriate, which rules out patients better suited for rhythm control therapy. Many patients had presence of comorbidities which included diabetes mellitus, hypertension, history of strokes or transient ischaemic attacks and HF (clinical diagnosis). Most of patients had hypertension (72.5%) with more than half of the population showing signs of HF (52.5%) at baseline.

Characteristic		Total (n=160)
Age, mean years (SD)		75.6 (8.2)
Gender, n women (%)		74 (46.3%)
Diabetes mellitus, n (%)		38 (23.8%)
Airway disease, n (%)		42 (26.3%)
Previous stroke or TIA, n (%)		28 (17.5)
Treatment for hypertension, n (%)		116 (72.5)
Unplanned admission for either AF or heart failure in the last 12 months, n (%)		31 (19.4%)
Previous diagnosis of heart failure, n (%)		59 (36.9%)
Signs of heart failure at baseline, n (%)		84 (52.5%)
NTpro-BNP, median pg/mL (IQR)		1057 (744-1522)
Echocardiogram LVEF, mean % (SD)		56.9 (9.7)
Echocardiogram LVEF <50%, n (%)		30 (18.8%)
NYHA class, n (%)	I	0 (0%)
	II	99 (61.9%)
	III	56 (35%)
	IV	5 (3.1%)
	mean (SD)	2.4 (0.6)
Previous use of anti-arrhythmic drugs, n (%)		13 (8.1%)
Previous AF cardioversion, n (%)		15 (9.4%)
Previous AF ablation, n (%)		3 (1.9%)
mEHRA class, n (%)	1	0 (0%)
	2a	6 (3.8%)
	2b	74 (46.3%)
	3	65 (40.6%)
	4	15 (9.4%)
ECG heart rate, mean beats/min (SD)		99.7 (18)
Systolic blood pressure, mean mmHg (SD)		135.6 (16.1)
Creatinine, median μmol/L (IQR)		86 (73-101)

Table 5.2 Population characteristics of the RATE-AF patient cohort. AF, Atrial fibrillation; ECG, Electrocardiogram; IQR, interquartile range; LVEF, left-ventricular ejection fraction; mEHRA, modified European Heart Rhythm society Atrial fibrillation score; NTpro-BNP, N-terminal prohormone of brain natriuretic peptide; NYHA, New York Heart Association; SD, Standard deviation; TIA, Transient ischemic attack.

.

5.3.2 Correlations of basic research parameters with calibrations

Prior to the analysis of any other variables, the raw data from the HEK293t experiments with/without monensin and from the ELISA was correlated with calibrated data (See figure 5.2 below). The calibrated data from the HEK293t assay without monensin was transformed with natural logarithm to achieve normal distribution prior to analysis. Evaluating the correlation of the raw HEK293t assay data with its calibrated data (Figure 5.2A), a significant correlation was observed ($r=0.396$; $p=0.0085$). Considering that calibration process resulted in negative intracellular sodium values only the raw data were chosen for analysis.

Similar experiments were carried out in the presence of monensin. As monensin is an ionophore allowing inflow of Na^+ via pores in the membrane, which increases intracellular Na^+ in the cells. At this new higher baseline (Figure 3.8), further increases in intracellular Na^+ will be difficult to be observed, but on the other hand, could potentially increase the sensitivity in detecting small decreases in intracellular Na^+. The correlation between the raw and calibrated data from the HEK293t with monensin experiments demonstrated a very strong significant correlation coefficient ($r=0.811$; $p<0.0001$) (See figure 5.2B). Again, calibration conversion resulted in negative values hence only the data are used for further analysis.

Lastly, the raw data from the ELISA experiments were correlated with the calibrated data (Figure 5.2C). The calibrated data from the ELISA was also transformed with natural logarithm to achieve normal distribution prior to analysis. The correlation demonstrates a good correlation (r=-0.603) and was also significant (p<0.0001). Therefore the calibrated data will be used forward in the analysis of the variables of interest below.

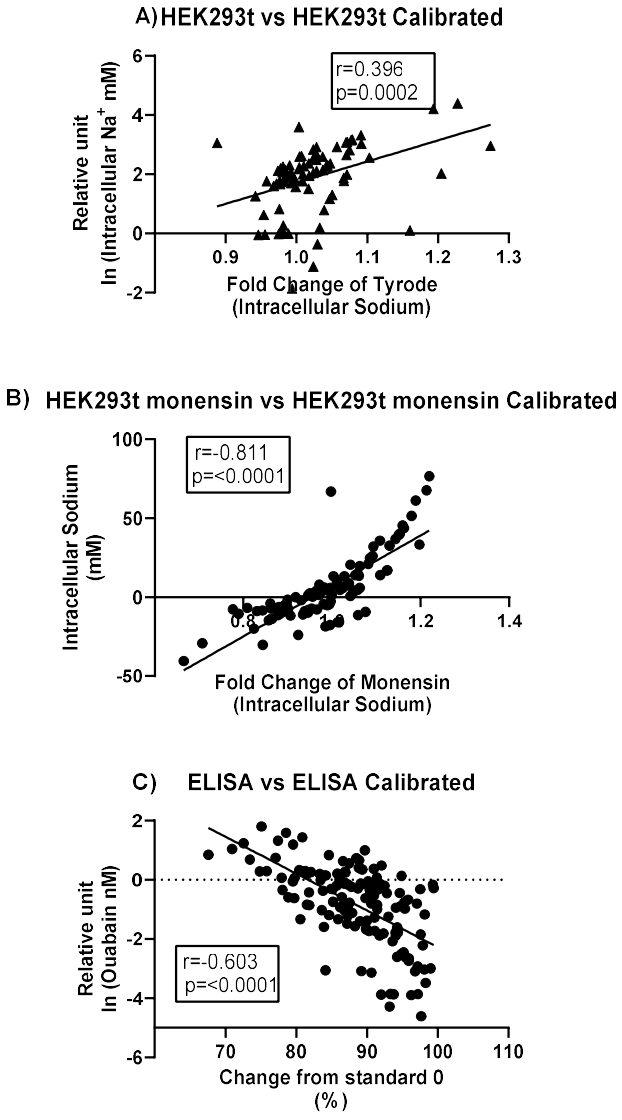


Figure 5.2 Correlation data from basic research parameters measure from 160 patients from the RATE AF trial. Correlations of the raw data

with the calibrated data from HEK293t (A) experiments, with monensin present (B) and from the ELISA (C). Pearson rank correlations were used and natural log were used to achieve normal distribution where appropriate as indicated on graph A and C. Analysis was followed by linear regression to fit best line of fit. Each data point represents one patient.

5.3.3 Correlations of basic research parameters with numerical RATE-AF variables

All the numerical variables from table 5.1 (Including the personal variables, some of the clinical variables, blood parameters, the electrocardiogram data and the echo data) were all tested for normality prior to analysis. Most of the parameters were discovered not to be normally distributed, and for most parameters natural logarithmic transformation did not result in a normal distribution. Thus a spearman ranked correlation were made between these variables and the HEK293t with/without monensin and the ELISA (See figure 5.3 below). Figure 5.3 shows the correlated data of each of the variables with one another on a scale going from bright green (strong negative correlation) to bright red (strong positive correlation). Most of the tested variables do not demonstrate good correlations with r coefficients less than +/- 0.3. They are therefore not plotted individually as the data indicates minimal relationships with the basic laboratory parameters.

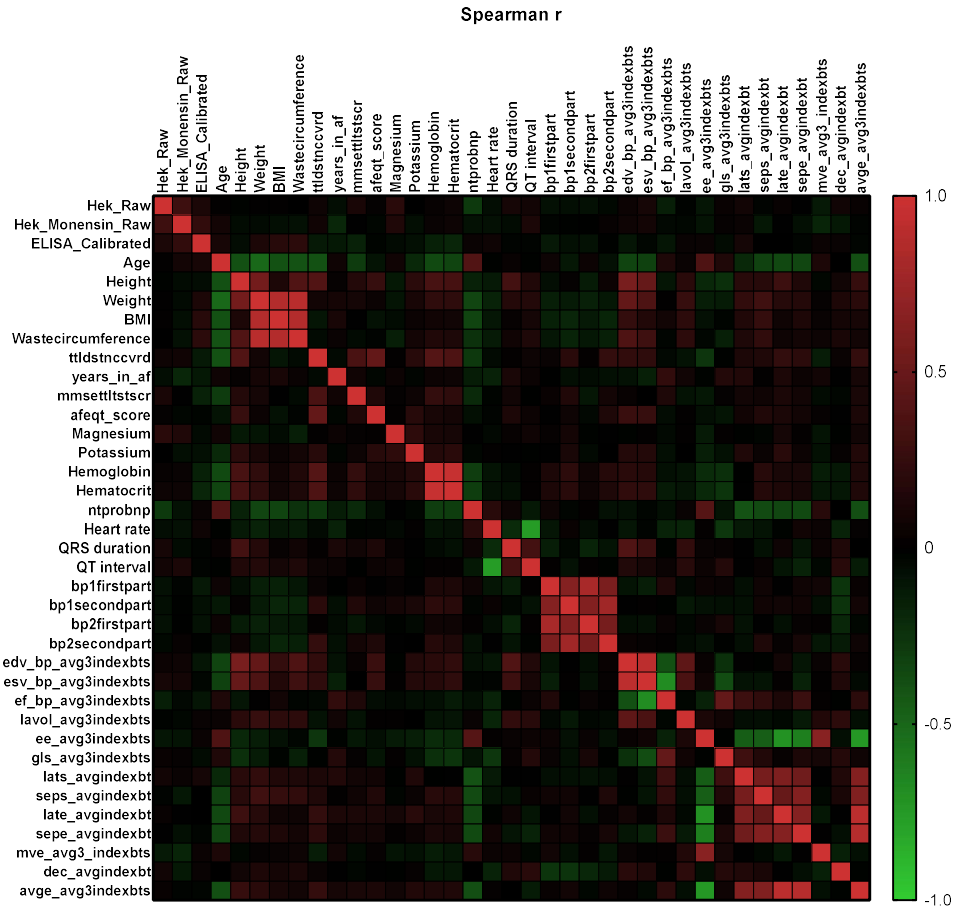


Figure 5.3 Correlation matrix of HEK293t raw data, HEK293t Monensin raw and ELISA calibrated data with the included variables from the 160 patients from the RATE-AF trial.

From the spearman correlations (Figure 5.3) NT-proBNP showed a weak correlation with HEK293t with a coefficient r of -0.279 but with strong significance (p=0.0003). Hence to investigate this relationship further the data was plotted individually and linear regression was used to fit a curve to the data (See figure 5.4 below). The fitted line showed a weak correlation between the variables with a r of 0.232, although still significant (p=0.0029). So even though the correlation is weak, surprisingly the data indicates that as NT-proBNP levels increase the intracellular Na^+ decreases. However, no correlation was shown

between NT-proBNP levels and HEK293t cells with monensin or the endogenous ouabain levels.

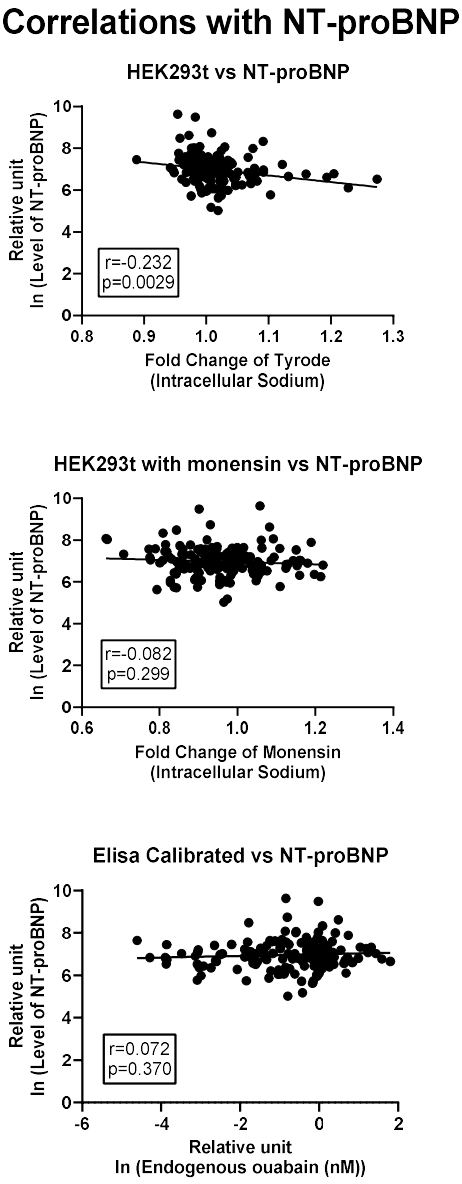


Figure 5.4 Correlation of HEK293t without or with monensin and calibrated ELISA response vs the NT-proBNP levels from 160 patients. Linear regression was used to fit the data. Pearson rank correlations were used and natural log were used to achieve normal distrubtiuon where appropriate as indicated on graph A-C for NT-proBNP and in graph C for ELISA. Analysis was followed by linear regression to fit best line of fitEach data point represents one patient.

5.3.4 Analysis of categorical variables

Below analysis of the selected clinical parameters from table 5.1 some of the variables were excluded due to low n numbers. For variables with two outcomes, the groups are directly compared. If three or more groups, the data was analysed for significant trends. The variables are plotted for each of the 3 selected experimental measurements (HEK293t raw, HEK293t monensin raw and ELISA Calibrated).

Figure 5.5 below investigates the difference between male and female participants from the RATE-AF trial. From the HEK293t experiments, no differences between genders was observed from either the raw data in the absence (Figure 5.5A) or presence of monensin (figure 5.5B). Lastly, no difference in endogenous ouabain levels is seen between males and females (Figure 5.5C).

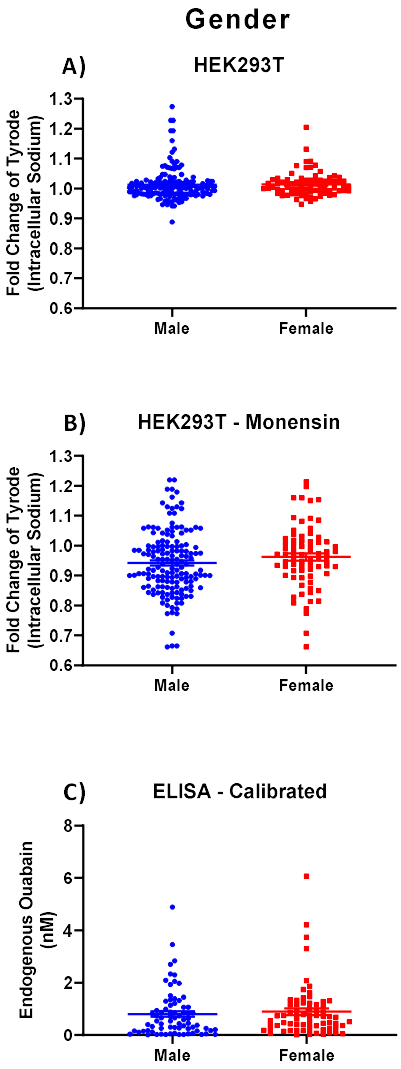


Figure 5.5 Gender specific differences investigated. Experiments inldcuded using intracellular sodium assay with HEK293t raw data (A) or HEK293t with monensin raw data (B) and ELISA calibrated data (C). Data is presented as mean +/- S.E.M with each data point representing one patient.

Endogenous ouabain has been implicated in diabetes(169) and type 2 diabetes is a common comorbidity in this cohort of patients (23.8 %), making it interesting to include in the analysis (Figure 5.6A-C). The HEK293t raw data without monensin show a small

but non-significant reduction in intracellular sodium in patients with type 2 diabetes compared to controls (Figure 5.6A). In HEK293t monensin experiments patients with type 2 diabetes demonstrate a significant reduction ($p=0.03$) in intracellular sodium, indicating potentially the presence of endogenous CTS (Figure 5.6B). Experiments using the ELISA was carried out to see whether the patients with type 2 diabetes have elevated endogenous CTS levels compared to patients without type 2 diabetes. The patients with type 2 diabetes show a small non-significant increase in endogenous ouabain compared to non-diabetic patients (1.07 +/- 0.22 nM vs 0.77 +/- 0.079 nM; SEM) (Figure 5.6C).

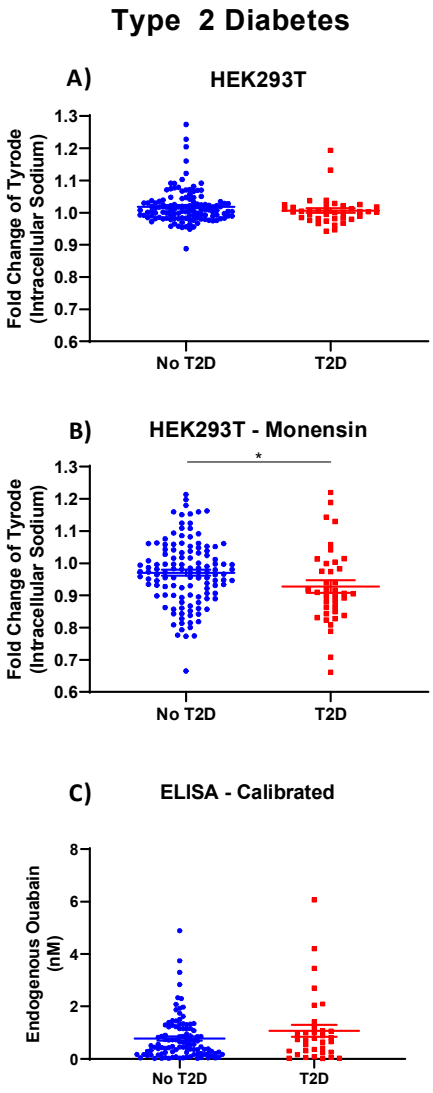


Figure 5.6 Effect of type 2 diabetes. Investigations intracellular sodium assay with HEK293t raw data (A) or HEK293t with monensin raw data (B) and ELISA calibrated data (C). Data is presented as mean +/- S.E.M with each data point representing one patient. Statistical analysis: Two tailed unpaired t-test *P<0.05 vs No T2D. Endognous ouabain data are not normally distributed so a non-parametric unpaired one-tailed mann-whitney test *P<0.05 vs No hospitalisations was used for the ELISA data.

Patients in the trial have all been diagnosed with varying levels of heart failure. Previous work showed that endogenous ouabain is negatively correlated with ventricular function(191, 195). Here we examined whether endogenous CTS are altered at different stages of heart failure, according to the NYHA I-IV classification. Most patients in RATE-AF are either NYHA class II or III. There were no differences or trends seen with the HEK293t cell-based data between any of the NYHA classifications (Figure 5.7A). Similarly, utilising the monensin for higher sensitivity did not show any difference between any of the groups as well and no trends was observed (Figure 5.7B). The ELISA experiments revealed a significant trend of increasing endogenous ouabain with increasing heart failure severity class (Slope = 0.5147; p=0.0002) (Figure 5.7C). Although only a few patients are classed in NYHA IV it does show a significant increase compared to NYHA II.

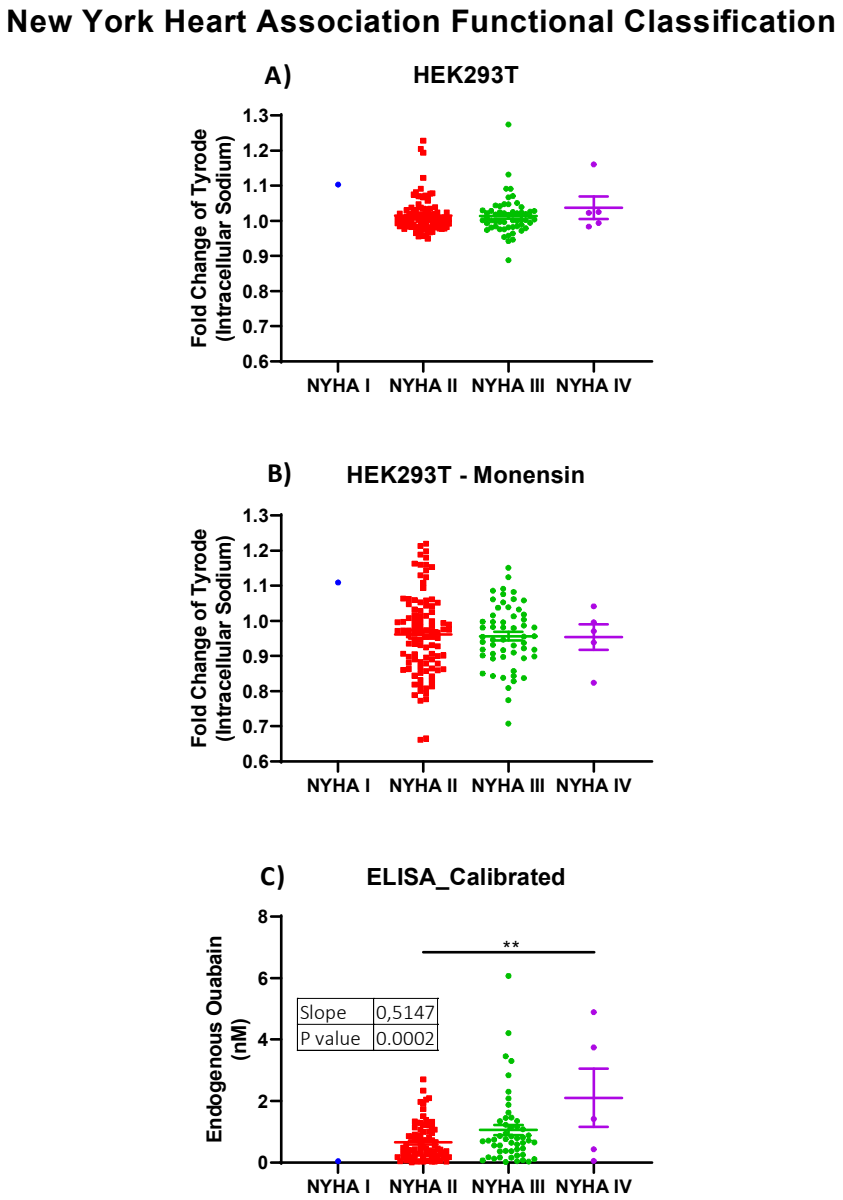


Figure 5.7 Classification of NYHA investigated. Experiments included intracellular sodium assay with HEK293t raw data (A) or HEK293t with monensin raw data (B) and ELISA calibrated data (C). Data is presented as mean +/- S.E.M with each data point representing one patient. Statistical analysis: One-way ANOVA with tukey post hoc test for mutipla comparisons **P<0.01 NYHA II vs NYHA IV. One-way ANOVA for trend analysis NYHA I -> NYHA IV ***P<0.001.

Patients were assessed and assigned into the mEHRA scores 2a, 2b, 3 or 4 depending on atrial fibrillation severity. Again, most patients are mainly distributed in 2b and 3 groups on the mEHRA score. Neither the HEK293t cell data or the monensin condition showed any differences between groups or having any trends of significance (Figure 5.8A-B). The ELISA data demonstrates significant trend (slope=0.2329; p=0.033) of increasing endogenous ouabain with disease severity (Figure 5.8C). mEHRA score 2b was significantly lower than the mEHRA 4 group (0.68 +/- 0.09 vs 1.414 +/-0.42), again indicating an increase of endogenous ouabain with severity of AF.

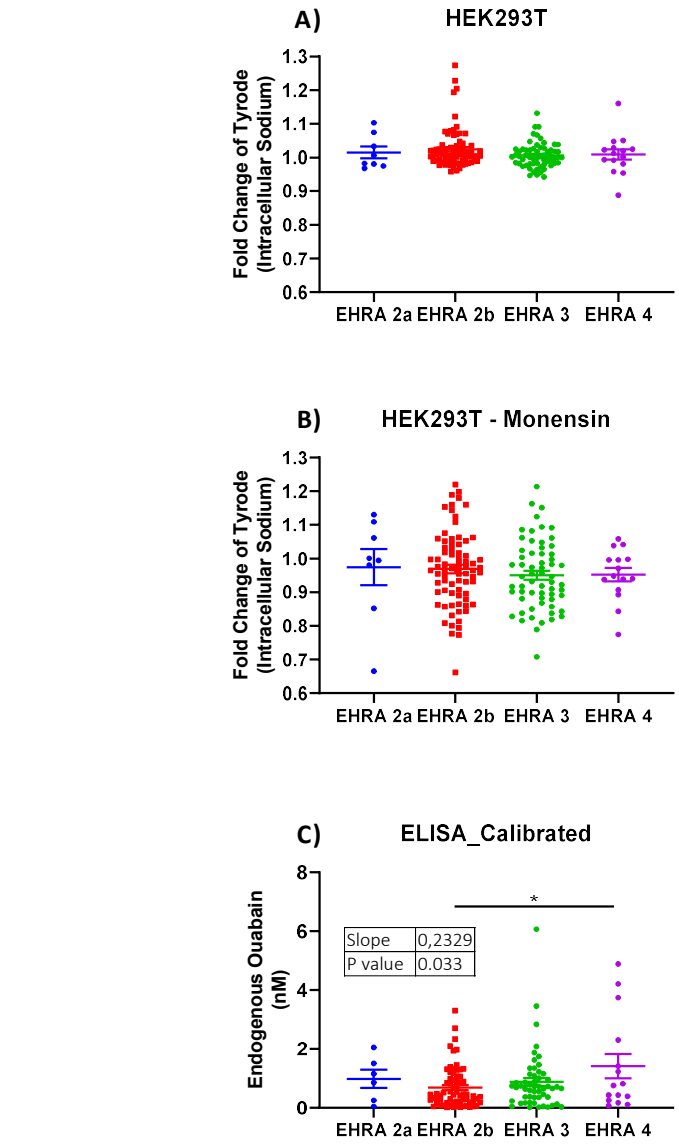


Figure 5.8 Classification of mEHRA. Investigations using intracellular sodium assay with HEK293t raw data (A) or HEK293t with monensin raw data (B) and ELISA calibrated data (C). Data is presented as mean +/- S.E.M with each data point representing one patient. Statistical analysis: One-way ANOVA with tukey post hoc test for multiple comparisons *P<0.05 vs NYHA IV. One-way ANOVA for trend analysis NYHA I -> NYHA IV *P<0.05.

Another clinical parameter of interest was whether or not the patients have had any myocardial infarctions (MIs). Previous work identified elevated levels of marinobufagenin in the urine of patients with MI(145). Most patients involved in the trial have not had any MIs leaving only a small group of patients for comparisons. The data from the HEK293t experiments did not show any changes in intracellular sodium (Figure 5.9A). The monensin data reveals a 7.1% significant decrease ($p=0.027$) in patients that have had MIs compared to patients without any prehistory of MIs (Figure 5.9B). This indicates the presence of potentially CTS or another factor that alters intracellular sodium. To investigate whether the change was caused by endogenous ouabain, the ELISA was performed on the samples. No changes between groups in endogenous ouabain were observed (Figure 5.9C).

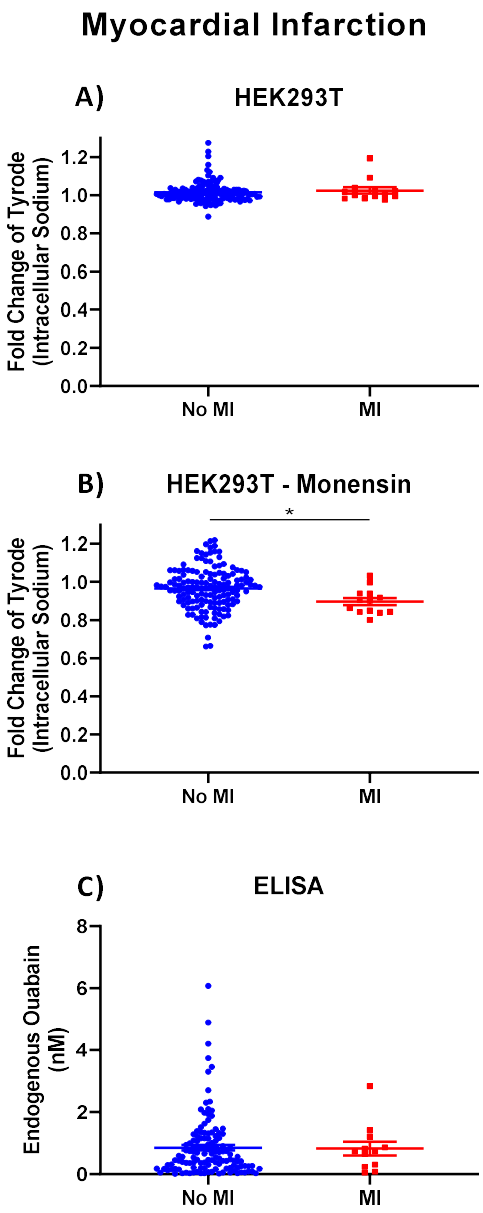


Figure 5.9 History of myocardial infarctions. Investigated using intracellular sodium assay with HEK293t raw data (A) or HEK293t with monensin raw data (B) and ELISA calibrated data (C). Data is presented as mean +/- S.E.M with each data point representing one patient. Statistical analysis: Two tailed unpaired t-test *P<0.05 vs No MI.

AF and HF are big risk factors for strokes. A small group of patients have had previous strokes in the RATE-AF cohort. No changes in intracellular sodium with the HEK293t with or without monensin were observed in patients with previous strokes when compared to patients without stroke history (Figure 5.10A-B). There was an increase in endogenous ouabain in patients with history of strokes compared to patients without any stroke history (1.14 +/- 0.27 nM vs 0.81 +/- 0.08 nM, SEM), although this was not significant (Figure 5.10C).

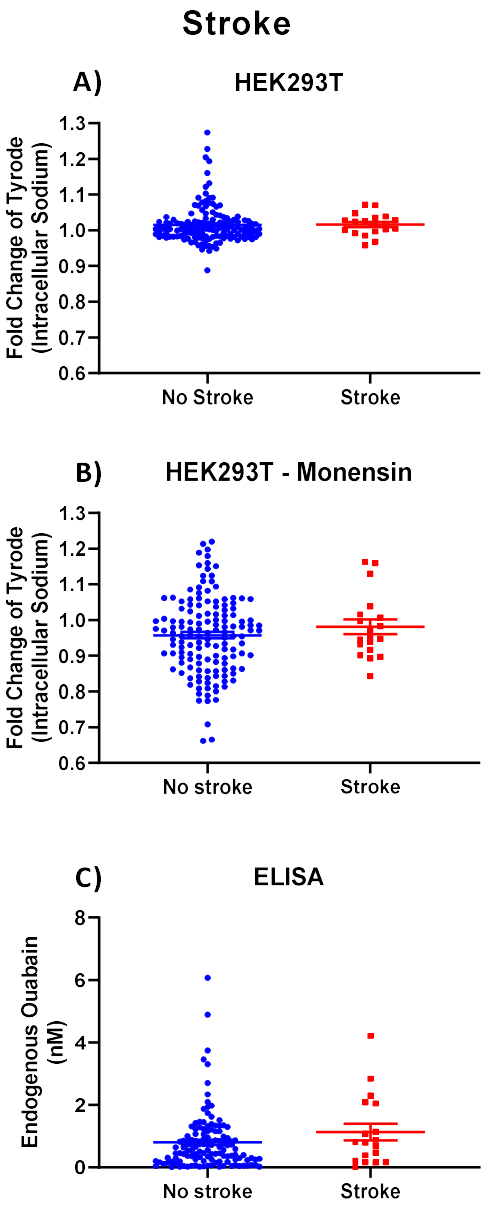


Figure 5.10 History of strokes investigated. Experiments used intracellular sodium assay with HEK293t raw data (A) or HEK293t with monensin raw data (B) and ELISA calibrated data (C). Data is presented as mean +/- S.E.M with each data point representing one patient.

Patients with either AF and/or HF are commonly experiencing unplanned hospital admissions and are known to have big impact on the patients health and could potentially affect overall mortality over time. Thus, we investigated whether cardiotonic steroids are altered in this patient group. Intracellular sodium in HEK293t cells without monensin were similar in patients that had higher rate of hospital admissions (Figure 5.11A). Using the HEK293t with monensin a significantly lower intracellular sodium is observed in the patients that have had unplanned admissions to hospital, compared to patients with no unplanned admission history (Figure 5.11B). This could be due to the presence of increases endogenous ouabain, so to examine this possibility the same patient samples were tested for the presence of endogenous ouabain. Interestingly, the ELISA demonstrated a 82.76 % significant ($p=0.0037$) increase in endogenous ouabain in patients with history of hospital admissions when compared to patients with no history (Figure 5.11C).

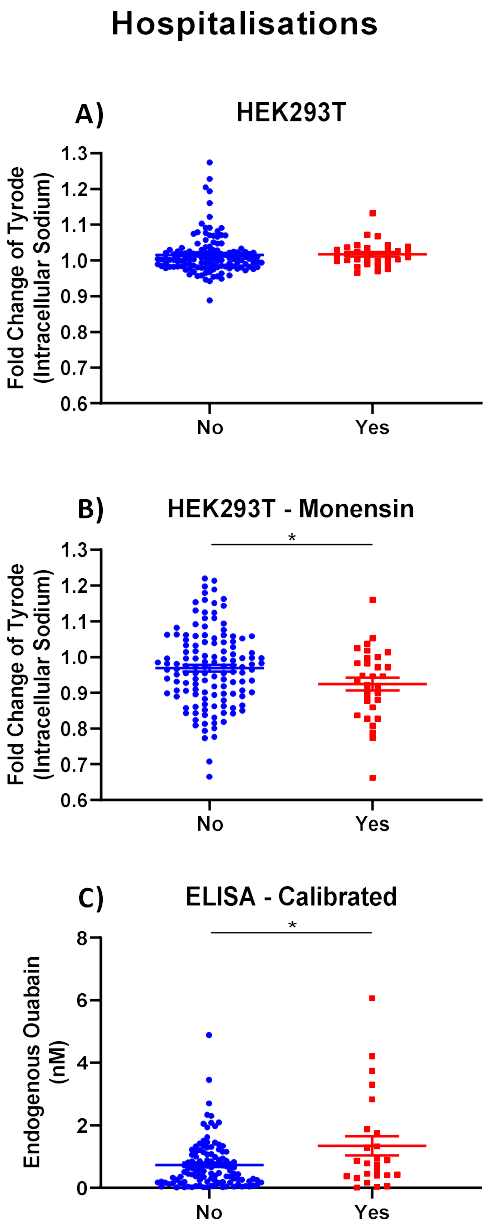


Figure 5.11 History of unplanned hospitalisations investigated. Experiments included intracellular sodium assay with HEK293t raw data (A) or H3k293t with monensin raw data (B) and ELISA calibrated data (C). Data is presented as mean +/- S.E.M with each data point representing one patient. Statistical analysis: Two tailed unpaired t-test *P<0.05 vs No MI were used for HEK293t with monensin and unpaired one-tailed Mann Whitney

test *P<0.05 vs No hospitalisations was used for the ELISA data.

5.3.5 The two treatment arms at baseline

It is important to evaluate whether there are any differences between the two RATE-AF treatment groups at baseline. Thus the last data set included in this thesis was investigating whether the two treatment arms of patients show any differences in intracellular sodium or endogenous ouabain levels at baseline (See figure 5.12). It is evident from both the HEK293t with or without monensin, that the two treatment groups do not display any differences in intracellular sodium (Figure 5.12A-B). No differences were observed in endogenous ouabain levels when interrogated with the ELISA (Figure 5.12C). Together the data suggest, the two treatment groups overall are very similar prior to treatment with either beta-blockers or digoxin.

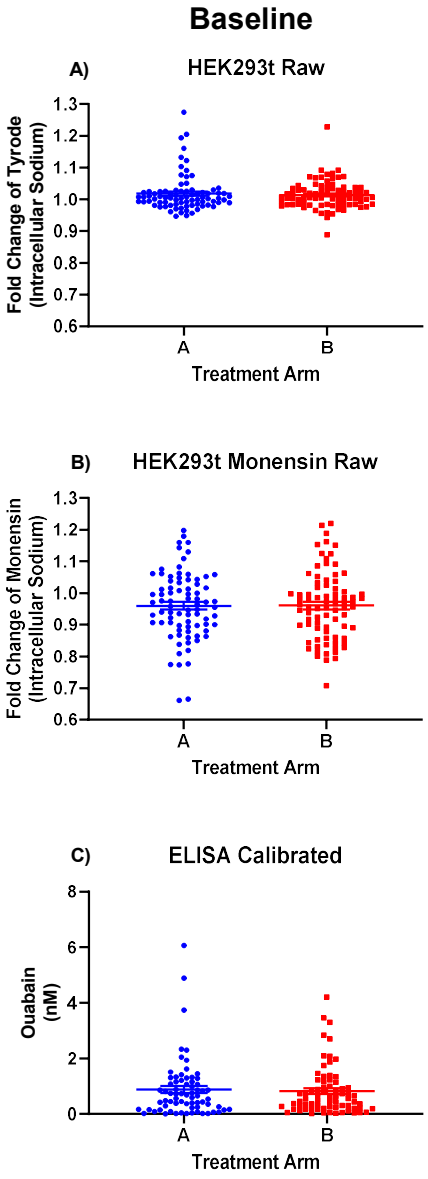


Figure 5.12 Comparison of baseline from RATE-AF treatment arms. HEK293t raw data (A) or HEK293t with monensin raw data (B) and ELISA calibrated data (C) from each treatment arm at baseline. Data is presented as mean +/- S.E.M with each data point representing one patient.

The 6-month treatment data were not allowed to be included in this thesis, as the RATE-AF was not concluded prior to this write-up and thus could potentially compromise the

randomisation of the trial. After the trial is closed the aim of my PhD thesis is to examine whether intracellular sodium or endogenous ouabain levels affect treatment (digoxin) outcomes.

5.4. Discussion

5.4.1 Correlations with NT-proBNP

Prior to the RATE-AF trial NT-proBNP have been linked to both AF and HF as potential prognostic biomarker and increasing with disease(253-255). Also previously published links between endogenous CTS with HF and AF, made it worth exploring in this cohort of patients. Perhaps surprisingly no corelation was found between NT-proBNP and endogenous ouabain (Figure 5.4). High inherent variation(256) in NT-proBNP levels is likely to require higher patient numbers. Our data demonstrate a weak negative correlation between NT-proBNP and intracellular sodium in HEK293t cells exposed to CTS extracted from the patient sera. However, contrary to this most studies report increased intracellular sodium in failing hearts(218, 257). It is likey that a consistent reduction in intracellular sodium, observed in pathiological states in this chapter is a consequence of our cellular model, whereby sub-nanomolar levels of ouabain actually lead to reduction in intracellular sodium, see Chapter 3.

5.4.2 Endogenous ouabain and intracellular sodium in disease states

The patients with type 2 diabetes in this cohort demonstrated lowering of intracellular sodium, which could indicate the presence endogenous CTS. This was weakly supported

by small, non-significant increase in endogenous ouabain. The decrease of intracellular sodium demonstrated in these experiments are quite surprising and could perhaps be due the NKA stimulation by CTS. This is opposite to the discoveries previously published by two independent groups (126, 169, 170), which demonstrated lowered activity of NKA with increased non-insulin dependent diabetic state. This effect on intracellular sodium was not able to be demonstrated in diabetic patients (143, 152). Chen et al used a digoxin-based radioimmunoassay and discovered elevated levels in the type 2 diabetic rat model, similar to observations in non-insulin dependent diabetic patients using a similar methodology(143, 152). In this thesis, the detection of endogenous CTS is based on an ouabain sensitive primary antibody. Although not significant the patients from RATE-AF with type 2 diabetes show slight increased levels of ouabain. This is opposite to results from diabetic rats, where marinobufagenin increased while no change was observed in ouabain levels (170). This could potentially explain why the increase in the patients from the RATE-AF was not significant, as the methodology used in this thesis display limited cross-reactivity with marinobufagenin. Despite these few studies, more work is needed to explore the relation of these steroids further and to what degree they are involved in patients with type 2 diabetes.

All the patients recruited for this trial have been diagnosed with HF and were further assigned into the NYHA classification I-IV depending on severity of HF (Figure 5.8). Most studies looking at the intracellular sodium and HF using tissues or cells in rats, guinea pigs, mice and humans all observed increased intracellular sodium levels in left ventricular HF models when compared to controls(216-218, 258). One study utilising a right ventricular HF model detected no change in intracellular sodium(259). In this thesis,

endogenous ouabain increases with HF severity, with highest ouabain levels observed in NYHA class IV patients (Figure 7C). These results confirm some of the previous studies in HF patients demonstrating increased ouabain or digoxin-like levels in severe congestive HF patients compared to controls (121, 260). A single study found ouabain to increase with NYHA severity class(177, 195). Two studies found marinobufagenin rather than ouabain to be increased in congestive HF, with marinobufagenin even increasing with HF severity(50, 194). Studies in rats showed a more complicated picture with ouabain increasing as left ventricular hypertrophy worsens ultimately leading to high congestive HF, while marinobufagenin didn't increase in congestive HF but only in left ventricular hypertrophy(168). It seems evident that CTS are somehow involved in HF and potentially in the disease progression, but different reports attribute different CTS for the involvement which calls for more research to clarify the roles of endogenous CTS in left ventricular hypertrophy and HF.

A few studies have previously investigated the potential role of endogenous ouabain in myocardial infarctions. They discovered an increase in digoxin-like molecules in the plasma of patients with MI compared to controls, though these patients also demonstrated increased incidence of ventricular fibrillation events (113, 129). The results presented in this thesis did not reveal similar results as no change was observed in endogenous ouabain, although a small decrease was observed in intracellular sodium. The data is slightly underpowered which could potentially explain why no significant changes were observed in endogenous ouabain.

In this thesis the severity of atrial fibrillation assessed by the EHRA score correlated well with increase in endogenous ouabain, with significant increase in ouabain obeserved between patients in class 2b and 4. There are currently no publications investigating the involvement of endogenous CTS in atrial fibrillation. Thus the data presented here is the first data demonstrating the potential of endogenous ouabain to play a role in atrial fibrillation and its potential utlity as a biomarker for disease progression in these patients.

Unexpected hospitalisations are common for HF and AF patients when the diseases progress or due to complications like stroke. The RATE-AF patients showed a marked reduction in intracellular sodium which was supported by a marked increase in endogenous ouabain levels in this cohort of patients. The data together suggest a role for utitlity of endogenous ouabain as a biomarker for patients with unexpected hospital admission. These findings are limited by a small patient cohort and more work with higher patient numbers is warranted.

5.4.3 Baseline differences and future work

One of the key aims of this research project was to examine whether the levels of endogenous CTS affect digoxin treatment response in patients with AF. For this purpose, patient clinical characteristics and blood samples were collected at baseline, prior to randomisation to one of two treatment arms (digoxin or beta blockade), and 6 months after the treatment. Analysis of endogenous ouabain levels and the effects of serum extract from the RATE-AF patients on intracellular levels were not altered between the two treatment arms (Figure 5.13) at baseline. Whilst all the data has been collected for the 6-month post-treatment timepoint, we are not allowed to analyse the data and unblind

before the RATE-AF trial is closed. Thus the final aim of this project, whether the endogenous CTS levels affect digoxin treatment response, is not described in this thesis.

CHAPTER 6 FINAL CONSIDERATIONS AND FUTURE STUDIES

6.1. Outcomes

The primary aims of this thesis was to develop two assays, one for determination of changes in intracellular Na^+ and the other to quantify ouabain. These investigations were performed using HEK293t cells and an ELISA, both methodologies were optimised towards the use in a patient cohort available from the RATE-AF. Further aims were to test how the endogenous CTS correlate with AH and HF incidence and disease progression, with the aim of informing future biomarker development studies.

The main outcomes of this thesis are summarised below:

- Assay for determination of changes in intracellular Na^+ was successfully developed using both ANG-2 and SBFI fluorescent dyes. ANG-2 dye whilst displaying seemingly enhanced sensitivity was more variable compared to the ratiometric SBFI. Furthermore, the ability of using two different dyes with the optimised conditions in this methodology validates its ability and usefulness for investigations of CTS effects on intracellular Na^+. Lastly, the changes in intracellular Na^+ could be calibrated using the SBFI dye from fluorescent relative units to intracellular Na^+ concentration.

- Bufadienolides showed greater effects on intracellular Na^+ concentration compared to the cardenolides (except ouabain), in HEK293t cells. The difference

in IC50 could potentially be explained by differences in structure among the different CTS. Ouabain demonstrated bimodal effects on the intracellular Na^+, at 0.1-1 nM range ouabain lowered intracellular Na^+ levels whereas it increased the intracellular Na^+ concentration at higher concentrations. This bimodal effect was not observed with ouabagenin (no sugar group), indicating the structure of these steroids directly affect the affinity and effects.

- Competitive ELISA methodology for detection of ouabain was developed. ELISA demonstrated limited cross-reactivity to marinobufagenin and testosterone, while significant cross-reactivity was observed with digoxin.

- CTS were extracted from the serum of RATE-AF patients. 1) Extracts were tested for the effects on intracellular Na^+ concentration in HEK293t cells. 2) Endogenous ouabain was quantified in serum extract suing the ELISA.

- Reductions in intracellular Na^+ measured in HEK293t cells correlated with type 2 diabetes, heart failure, myocardial infarction and with a number of unexpected hospitalisations due to AF or HF.

- Significantly increased endogenous ouabain levels were detected in more severe HF (NYHA IV vs NYHA II) and also in unexpected hospitalisations due to AF or HF. Furthermore, endogenous ouabain concentrations correlated with AF (mEHRA) and HF (NYHA class) disease severity.

6.2. Study limitations

The limitations for all the experiments and methodologies carried out in this thesis are considered below.

6.2.1 HEK293t cell limitations

During working with the cell line used in this thesis some limitations have become clear and should be mentioned. Cell lines do not mimic the physiological conditions *in vivo.* Neither do they mimic the *ex vivo* conditions in tissue. Specifically, the HEK293t cells do not recapitulate cardiomyocytes (CMs) as they have their origin in the kidney and were transformed to a cancer cell line changing many properties of the cells. First of all, HEK293t cells have a resting membrane potential around -20 to -40mV(261), which is very different from the -80 to -90 mV in CMs(262). This is reflected in Hek293T not expressing the same ion channels and transporters related to AP generation as CMs and have low levels of expression of proteins involved in regulation of ion transport (263). Key proteins involved in the generation and conduction of AP, such as $K_{ir2.1}$, $Na_{v1.5}$, NHE and Cx_{43} have not been found to be present in Hek293T cells. NCX may be expressed at low levels in the HEK293t cells(264). Nevertheless, HEK293t cells have been shown to express $Na_v1.7$(265) as well as the Ca^{2+} channels that enable Ca^{2+} influx pathways mediated by receptors and internal stores (266, 267). Important to note is that HEK293T have been shown to express ouabain sensitive NKA(268), which is essential for the work performed here.

Therefore, whilst HEK293t share some similarities with CMs, they lack most Na^+ and several other key proteins related to excitability. Lastly, the cellular assay developed here can only provide information relevant to the effects of CTS on the intracellular Na^+ concentration in HEK293t cells but not inform on the cellular signaling pathways potentially activated by the CTS. Thus, other models such as human pluripotent stem cell-derived CMs or primary isolated CMs from mice should be used to validate the signaling effects of CTS.

6.2.2 ELISA limitations

The ELISA is based on a primary antibody and are measured by absorbent signal created from the oxidation of the HRP linked to the secondary antibody. The use of this sort of detection methodology is limited by the colorimetric sensitivity. Thus, basing the methodology on radioactivity could potentially have increased the sensitivity as seen by other studies in the past, but this was not an option due to regulatory protocol complexities at the University of Birmingham. Another way to address the limitation in detection and specificity of endogenous ouabain could be to use a liquid chromatography tandem mass spectrometry (LC-MS/MS) method, as was utilised previously for telocinobufagin(173) and other CTS. LC-MS/MS work is carried out in our lab by the MS specialists employed on the grant.

6.3. Future work

The future work utilising the two methodologies developed in this thesis are discussed below. Likewise, further validation using mice and human induced pluripotent stem cell CMs are discussed.

6.3.1 HEK293t experiments

In this thesis some evidence of antagonism between ouabain and digoxin were demonstrated in HEK293t. The interaction between ouabain and digoxin, but also other CTS suggested to exist in circulation should also be investigated in primary adult cardiomyocytes. For this purpose, in the Pavlovic group, a knock-in mouse with a humanised alpha-1 NKA isoform has been developed (see section below). This would provide more in depth understanding of the potential role of these endogenous steroids in patients and how they interact with digoxin therapy. It is possible that the endogenous CTS levels, through their interaction with digoxin, contribute to the response to digoxin therapy. This will be investigated utilising the samples and patient outcomes from the 6-month time point of the RATE-AF trial, see section 6.3.6 below.

It would also be interesting to utilise the assay for other patient groups where CTS are known to be involved, for example chronic kidney disease patients. This would need to include healthy controls for direct comparison.

6.3.2 Animal studies

As HEK293t are not CMs and are in many ways different. Investigations in CMs or cardiac tissue would be key to obtain in depth understanding on how the different CTS interact and their effects on cardiac function, and cellular electrophysiology.

The NKA in WT (α1 R/R α2 S/S) mice and rats are known to be CTS resistant. SWAP mice (α1 S/S α2 R/R), have been developed with a swap in the resistance from α1 to α2 making it possible to investigate effects mediated through α1. WT (α1 R/R α2 S/S) and SWAP (α1 S/S α2 R/R) mice have been bred in Pavlovic group to produce a "humanised", CTS sensitive mice (α1 S/S α2 S/S) on both α1 and α2, which increases the similarity to the sensitivity towards CTS in the human heart. Investigations on the effect of CTS on electrical function, calcium and sodium handling and the potential interactions between the CTS are of interest and currently ongoing in the Pavlovic group. This would be of interest as CTS has previously been shown to increase contractility and arrhythmogenesis in isolated guinea pig hearts(269), rise in intracellular Ca^{2+} in canine purkinje fibers(270) and having effects on both the AP characteristics and the contractility of ventricular myocytes from cats(271). Isolated primary CMs from the humanised mouse hearts will be used to specifically examine the effects of individual CTS and in combination with digoxin on calcium/sodium and contractility using the Ionoptix system. CTS has previously been shown to exert a increase of atrial conduction velocity in both dogs(272) and in humans (273). Studies in guinea pigs have also shown an increase of the propagation time from the atria to the ventricles with a reduction in the rate of the sinus node(274). Thus, it would be interesting to take these studies into whole atrial tissue to observe potential effects of CTS and also potential antagonism on conduction using an optical mapping setup. These experiments in the "humanised" CTS sensitive mice (α1

S/S α2 S/S) are also ongoing and should provide insight into the role of CTS in modulating electrical function and conduction in whole hearts and isolated atria.

6.3.4 IPS-CMs

The human induced pluripotent stem cell (iPSC) technology has become an important in vitro experimental platform for studying cardiac biology and electrophysiology. In order to further build on the work presented in this thesis, optimisation of the experimental protocols utilising iPS-derived CMs for measurement of intracellular Na^+ in a high-throughput screening system are required. These methodologies can then be used to investigate the effects and interactions of different CTS. This would be a better cardiac model, although still not fully comparable to primary CMs. It would also allow use of fewer animals for initial screenings, so more targeted approach could be used in fewer animals.

6.3.5 ELISA experiments

To further validate the ELISA methodology for measurement on ouabain, it would be of key interest to perform further cross-reactivity experiments on digitoxin (similar to digoxin and used in Germany), telocinobufagin but also the sugar free versions of ouabain (ouabagenin), digoxin (digoxigenin) and digitoxin (digitoxigenin), in order to get a better understanding of the detection limitations of the assay. Also, of interest could be a mix of different CTS, which is also likely to be the case in patients, to see how the assay performs under more patient relevant conditions.

6.3.6 RATE-AF patient Cohort

In this thesis the RATE-AF patient data from baseline only was included. Even though the 6-month ELISA and intracellular Na^+ experiments were completed, the data were not analysed nor included into the thesis. This is due to the fact that at the point of the submission of this thesis, the RATE-AF trial was not closed yet, therefore, the treatment groups with the results after 6 months treatment were not able to be included in the results. After the RATE-AF trial closes, analysis of 6-month data will be finalised. This will include analysis of differences between the two treatment arms after 6 months and analysis of whether the levels of endogenous ouabain correlate with the outcome in the digoxin arm. Ultimately, this set of studies is looking to examine whether endogenous CTS can be used as biomarkers to enable patient stratification in terms of whether to give digoxin or not.

REFERENCES

1. Boron WF, Boulpaep EL. Medical physiology. 2012(2nd edition).
2. Levick JR. An introduction to cardiovascular physiology. 2010(5th edition).
3. Holt JP. The normal pericardium. Am J Cardiol. 1970;26(5):455-65.
4. Hill RW, Wyse GA, Anderson M. Animal Physiology. 2008(2nd edition).
5. Bergmann O, Zdunek S, Felker A, Salehpour M, Alkass K, Bernard S, et al. Dynamics of Cell Generation and Turnover in the Human Heart. Cell. 2015;161(7):1566-75.
6. Doll S, Dressen M, Geyer PE, Itzhak DN, Braun C, Doppler SA, et al. Region and cell-type resolved quantitative proteomic map of the human heart. Nat Commun. 2017;8(1):1469.
7. Fawcett DW, McNutt NS. The ultrastructure of the cat myocardium. I. Ventricular papillary muscle. J Cell Biol. 1969;42(1):1-45.
8. Huxley AF, Niedergerke R. Structural changes in muscle during contraction; interference microscopy of living muscle fibres. Nature. 1954;173(4412):971-3.
9. Huxley H, Hanson J. Changes in the cross-striations of muscle during contraction and stretch and their structural interpretation. Nature. 1954;173(4412):973-6.
10. Bers DM. Cardiac excitation-contraction coupling. Nature. 2002;415(6868):198-205.
11. Wright SH. Generation of resting membrane potential. Adv Physiol Educ. 2004;28(1-4):139-42.
12. Vassalle M. Contribution of the Na+/K+-pump to the membrane potential. Experientia. 1987;43(11-12):1135-40.
13. Gelband H, Bush HL, Rosen MR, Myerburg RJ, Hoffman BF. Electrophysiologic properties of isolated preparations of human atrial myocardium. Circ Res. 1972;30(3):293-300.
14. Hoover DB, Ganote CE, Ferguson SM, Blakely RD, Parsons RL. Localization of cholinergic innervation in guinea pig heart by immunohistochemistry for high-affinity choline transporters. Cardiovascular research. 2004;62(1):112-21.
15. Habecker BA, Anderson ME, Birren SJ, Fukuda K, Herring N, Hoover DB, et al. Molecular and cellular neurocardiology: development, and cellular and molecular adaptations to heart disease. J Physiol. 2016;594(14):3853-75.
16. Huang WA, Boyle NG, Vaseghi M. Cardiac Innervation and the Autonomic Nervous System in Sudden Cardiac Death. Card Electrophysiol Clin. 2017;9(4):665-79.

17. Degeest H, Levy MN, Zieske H, Lipman RI. Depression of Ventricular Contractility by Stimulation of the Vagus Nerves. Circ Res. 1965;17:222-35.
18. Xenopoulos NP, Applegate RJ. The effect of vagal stimulation on left ventricular systolic and diastolic performance. The American journal of physiology. 1994;266(6 Pt 2):H2167-73.
19. Lewis ME, Al-Khalidi AH, Bonser RS, Clutton-Brock T, Morton D, Paterson D, et al. Vagus nerve stimulation decreases left ventricular contractility in vivo in the human and pig heart. J Physiol. 2001;534(Pt. 2):547-52.
20. Coote JH. Myths and realities of the cardiac vagus. J Physiol. 2013;591(17):4073-85.
21. Szentivanyi M, Pace JB, Wechsler JS, Randall WC. Localized myocardial responses to stimulation of cardiac sympathetic nerves. Circ Res. 1967;21(5):691-702.
22. Antzelevitch C, Sicouri S, Litovsky SH, Lukas A, Krishnan SC, Di Diego JM, et al. Heterogeneity within the ventricular wall. Electrophysiology and pharmacology of epicardial, endocardial, and M cells. Circ Res. 1991;69(6):1427-49.
23. Nabauer M, Beuckelmann DJ, Uberfuhr P, Steinbeck G. Regional differences in current density and rate-dependent properties of the transient outward current in subepicardial and subendocardial myocytes of human left ventricle. Circulation. 1996;93(1):168-77.
24. Thomas D, Kiehn J, Katus HA, Karle CA. Adrenergic regulation of the rapid component of the cardiac delayed rectifier potassium current, I(Kr), and the underlying hERG ion channel. Basic research in cardiology. 2004;99(4):279-87.
25. Cutler MJ, Jeyaraj D, Rosenbaum DS. Cardiac electrical remodeling in health and disease. Trends Pharmacol Sci. 2011;32(3):174-80.
26. Valdivia HH, Kaplan JH, Ellis-Davies GC, Lederer WJ. Rapid adaptation of cardiac ryanodine receptors: modulation by Mg2+ and phosphorylation. Science (New York, NY). 1995;267(5206):1997-2000.
27. Marx SO, Reiken S, Hisamatsu Y, Jayaraman T, Burkhoff D, Rosemblit N, et al. PKA phosphorylation dissociates FKBP12.6 from the calcium release channel (ryanodine receptor): defective regulation in failing hearts. Cell. 2000;101(4):365-76.
28. Shannon TR, Ginsburg KS, Bers DM. Reverse mode of the sarcoplasmic reticulum calcium pump and load-dependent cytosolic calcium decline in voltage-clamped cardiac ventricular myocytes. Biophysical journal. 2000;78(1):322-33.
29. Li YG, Benditt DG, Klingenheben T, Hu K, Feng D. Cardiac Arrhythmias: Update on Mechanisms and Clinical Managements. Cardiol Res Pract. 2016;2016:8023723.
30. Tse G. Mechanisms of cardiac arrhythmias. J Arrhythm. 2016;32(2):75-81.

31. Chugh SS, Havmoeller R, Narayanan K, Singh D, Rienstra M, Benjamin EJ, et al. Worldwide epidemiology of atrial fibrillation: a Global Burden of Disease 2010 Study. Circulation. 2014;129(8):837-47.
32. Zoni-Berisso M, Lercari F, Carazza T, Domenicucci S. Epidemiology of atrial fibrillation: European perspective. Clin Epidemiol. 2014;6:213-20.
33. Murin J, Naditch-Brule L, Brette S, Chiang CE, O'Neill J, Steg PG. Clinical characteristics, management, and control of permanent vs. nonpermanent atrial fibrillation: insights from the RealiseAF survey. PLoS One. 2014;9(1):e86443.
34. January CT, Wann LS, Alpert JS, Calkins H, Cigarroa JE, Cleveland JC, Jr., et al. 2014 AHA/ACC/HRS guideline for the management of patients with atrial fibrillation: a report of the American College of Cardiology/American Heart Association Task Force on practice guidelines and the Heart Rhythm Society. Circulation. 2014;130(23):e199-267.
35. Kirchhof P, Benussi S, Kotecha D, Ahlsson A, Atar D, Casadei B, et al. 2016 ESC Guidelines for the management of atrial fibrillation developed in collaboration with EACTS. Europace. 2016;18(11):1609-78.
36. Andrade J, Khairy P, Dobrev D, Nattel S. The clinical profile and pathophysiology of atrial fibrillation: relationships among clinical features, epidemiology, and mechanisms. Circ Res. 2014;114(9):1453-68.
37. Nattel S. New ideas about atrial fibrillation 50 years on. Nature. 2002;415(6868):219-26.
38. Wakili R, Voigt N, Kaab S, Dobrev D, Nattel S. Recent advances in the molecular pathophysiology of atrial fibrillation. J Clin Invest. 2011;121(8):2955-68.
39. Haissaguerre M, Jais P, Shah DC, Takahashi A, Hocini M, Quiniou G, et al. Spontaneous initiation of atrial fibrillation by ectopic beats originating in the pulmonary veins. N Engl J Med. 1998;339(10):659-66.
40. Iwasaki YK, Nishida K, Kato T, Nattel S. Atrial fibrillation pathophysiology: implications for management. Circulation. 2011;124(20):2264-74.
41. Verkerk AO, Wilders R, van Borren MM, Peters RJ, Broekhuis E, Lam K, et al. Pacemaker current (I(f)) in the human sinoatrial node. Eur Heart J. 2007;28(20):2472-8.
42. Allessie MA, Boyden PA, Camm AJ, Kleber AG, Lab MJ, Legato MJ, et al. Pathophysiology and prevention of atrial fibrillation. Circulation. 2001;103(5):769-77.
43. Waldo AL, Wit AL. Mechanisms of cardiac arrhythmias. Lancet. 1993;341(8854):1189-93.
44. Burashnikov A, Antzelevitch C. Role of late sodium channel current block in the management of atrial fibrillation. Cardiovasc Drugs Ther. 2013;27(1):79-89.
45. Mason FE, Sossalla S. The Significance of the Late Na(+) Current for Arrhythmia Induction and the Therapeutic

Antiarrhythmic Potential of Ranolazine. J Cardiovasc Pharmacol Ther. 2017;22(1):40-50.
46. Comtois P, Kneller J, Nattel S. Of circles and spirals: bridging the gap between the leading circle and spiral wave concepts of cardiac reentry. Europace. 2005;7 Suppl 2:10-20.
47. Dobrev D, Nattel S. New antiarrhythmic drugs for treatment of atrial fibrillation. Lancet (London, England). 2010;375(9721):1212-23.
48. Groenveld HF, Tijssen JG, Crijns HJ, Van den Berg MP, Hillege HL, Alings M, et al. Rate control efficacy in permanent atrial fibrillation: successful and failed strict rate control against a background of lenient rate control: data from RACE II (Rate Control Efficacy in Permanent Atrial Fibrillation). J Am Coll Cardiol. 2013;61(7):741-8.
49. Ruff CT, Giugliano RP, Braunwald E, Hoffman EB, Deenadayalu N, Ezekowitz MD, et al. Comparison of the efficacy and safety of new oral anticoagulants with warfarin in patients with atrial fibrillation: a meta-analysis of randomised trials. Lancet (London, England). 2014;383(9921):955-62.
50. Fauchier L, Grimard C, Pierre B, Nonin E, Gorin L, Rauzy B, et al. Comparison of beta blocker and digoxin alone and in combination for management of patients with atrial fibrillation and heart failure. Am J Cardiol. 2009;103(2):248-54.
51. Scheuermeyer FX, Grafstein E, Stenstrom R, Christenson J, Heslop C, Heilbron B, et al. Safety and efficiency of calcium channel blockers versus beta-blockers for rate control in patients with atrial fibrillation and no acute underlying medical illness. Acad Emerg Med. 2013;20(3):222-30.
52. Ulimoen SR, Enger S, Carlson J, Platonov PG, Pripp AH, Abdelnoor M, et al. Comparison of four single-drug regimens on ventricular rate and arrhythmia-related symptoms in patients with permanent atrial fibrillation. Am J Cardiol. 2013;111(2):225-30.
53. Elkayam U. Calcium channel blockers in heart failure. Cardiology. 1998;89 Suppl 1:38-46.
54. Goldstein RE, Boccuzzi SJ, Cruess D, Nattel S. Diltiazem increases late-onset congestive heart failure in postinfarction patients with early reduction in ejection fraction. The Adverse Experience Committee; and the Multicenter Diltiazem Postinfarction Research Group. Circulation. 1991;83(1):52-60.
55. Bavishi C, Chatterjee S, Ather S, Patel D, Messerli FH. Beta-blockers in heart failure with preserved ejection fraction: a meta-analysis. Heart Fail Rev. 2015;20(2):193-201.
56. Rienstra M, Damman K, Mulder BA, Van Gelder IC, McMurray JJ, Van Veldhuisen DJ. Beta-blockers and outcome in heart failure and atrial fibrillation: a meta-analysis. JACC Heart Fail. 2013;1(1):21-8.
57. Kotecha D, Holmes J, Krum H, Altman DG, Manzano L, Cleland JGF, et al. Efficacy of β blockers in patients with

heart failure plus atrial fibrillation: an individual-patient data meta-analysis. The Lancet. 2014;384(9961):2235-43.
58. Kotecha D, Manzano L, Krum H, Rosano G, Holmes J, Altman DG, et al. Effect of age and sex on efficacy and tolerability of beta blockers in patients with heart failure with reduced ejection fraction: individual patient data meta-analysis. BMJ. 2016;353:i1855.
59. Goldberger ZD, Alexander GC. Digitalis use in contemporary clinical practice: refitting the foxglove. JAMA internal medicine. 2014;174(1):151-4.
60. Ziff OJ, Kotecha D. Digoxin: The good and the bad. Trends Cardiovasc Med. 2016;26(7):585-95.
61. Ziff OJ, Lane DA, Samra M, Griffith M, Kirchhof P, Lip GY, et al. Safety and efficacy of digoxin: systematic review and meta-analysis of observational and controlled trial data. Bmj. 2015;351:h4451.
62. Nesher M, Bai Y, Li D, Rosen H, Lichtstein D, Liu L. Interaction of atrial natriuretic peptide and ouabain in the myocardium. Can J Physiol Pharmacol. 2012;90(10):1386-93.
63. McMahon WS, Holzgrefe HH, Walker JD, Mukherjee R, Arthur SR, Cavallo MJ, et al. Cellular basis for improved left ventricular pump function after digoxin therapy in experimental left ventricular failure. J Am Coll Cardiol. 1996;28(2):495-505.
64. Ten Eick RE, Hoffman BF. Chronotropic effect of cardiac glycosides in cats, dogs, and rabbits. Circ Res. 1969;25(4):365-78.
65. Group DI. The effect of digoxin on mortality and morbidity in patients with heart failure. The New England journal of medicine. 1997;336(8):525-33.
66. Hallberg P, Lindback J, Lindahl B, Stenestrand U, Melhus H, group R-H. Digoxin and mortality in atrial fibrillation: a prospective cohort study. Eur J Clin Pharmacol. 2007;63(10):959-71.
67. Turakhia MP, Santangeli P, Winkelmayer WC, Xu X, Ullal AJ, Than CT, et al. Increased mortality associated with digoxin in contemporary patients with atrial fibrillation: findings from the TREAT-AF study. J Am Coll Cardiol. 2014;64(7):660-8.
68. Kotecha D CM, Deeks JJ, Griffith M, Kirchhof P, Lip GYH, Mehta S, Slinn G, Stanbury M, Steeds RP, Townend JN. A review of rate control in atrial fibrillation, and the rationale and protocol for the RATE-AF trial. BMJ Open. 2017;In press.
69. Skou JC. The influence of some cations on an adenosine triphosphatase from peripheral nerves. Biochimica et biophysica acta. 1957;23(2):394-401.
70. Lingrel JB. The physiological significance of the cardiotonic steroid/ouabain-binding site of the Na,K-ATPase. Annual review of physiology. 2010;72:395-412.
71. Skou JC. Nobel Lecture. The identification of the sodium pump. Biosci Rep. 1998;18(4):155-69.

72. Kaplan JH. Biochemistry of Na,K-ATPase. Annu Rev Biochem. 2002;71:511-35.
73. Bagrov AY, Shapiro JI, Fedorova OV. Endogenous cardiotonic steroids: physiology, pharmacology, and novel therapeutic targets. Pharmacol Rev. 2009;61(1):9-38.
74. Morth JP, Pedersen BP, Toustrup-Jensen MS, Sorensen TL, Petersen J, Andersen JP, et al. Crystal structure of the sodium-potassium pump. Nature. 2007;450(7172):1043-9.
75. Sweadner KJ. Isozymes of the Na+/K+-ATPase. Biochimica et biophysica acta. 1989;988(2):185-220.
76. Pavlovic D. The role of cardiotonic steroids in the pathogenesis of cardiomyopathy in chronic kidney disease. Nephron Clin Pract. 2014;128(1-2):11-21.
77. Paczula A, Wiecek A, Piecha G. The role of endogenous cardiotonic steroids in pathogenesis of cardiovascular and renal complications of arterial hypertension. Postepy higieny i medycyny doswiadczalnej (Online). 2016;70:243-50.
78. Therien AG, Blostein R. Mechanisms of sodium pump regulation. American journal of physiology Cell physiology. 2000;279(3):C541-66.
79. Crambert G, Fuzesi M, Garty H, Karlish S, Geering K. Phospholemman (FXYD1) associates with Na,K-ATPase and regulates its transport properties. Proc Natl Acad Sci U S A. 2002;99(17):11476-81.
80. El-Armouche A, Wittkopper K, Fuller W, Howie J, Shattock MJ, Pavlovic D. Phospholemman-dependent regulation of the cardiac Na/K-ATPase activity is modulated by inhibitor-1 sensitive type-1 phosphatase. FASEB J. 2011;25(12):4467-75.
81. Pavlovic D, Fuller W, Shattock MJ. Novel regulation of cardiac Na pump via phospholemman. J Mol Cell Cardiol. 2013;61:83-93.
82. Huang BS, Van Vliet BN, Leenen FH. Increases in CSF [Na+] precede the increases in blood pressure in Dahl S rats and SHR on a high-salt diet. American journal of physiology Heart and circulatory physiology. 2004;287(3):H1160-6.
83. Simchon S, Manger W, Golanov E, Kamen J, Sommer G, Marshall CH. Handling 22NaCl by the blood-brain barrier and kidney: its relevance to salt-induced hypertension in dahl rats. Hypertension (Dallas, Tex : 1979). 1999;33(1 Pt 2):517-23.
84. Schoner W, Scheiner-Bobis G. Role of endogenous cardiotonic steroids in sodium homeostasis. Nephrol Dial Transplant. 2008;23(9):2723-9.
85. Akera T, Larsen FS, Brody TM. The effect of ouabain on sodium- and potassium-activated adenosine triphosphatase from the hearts of several mammalian species. J Pharmacol Exp Ther. 1969;170(1):17-26.
86. Berry RG, Despa S, Fuller W, Bers DM, Shattock MJ. Differential distribution and regulation of mouse cardiac

Na+/K+-ATPase alpha1 and alpha2 subunits in T-tubule and surface sarcolemmal membranes. Cardiovascular research. 2007;73(1):92-100.
87. Pavlovic D. Endogenous cardiotonic steroids and cardiovascular disease, where to next? Cell Calcium. 2020;86:102156.
88. Li Z, Xie Z. The Na/K-ATPase/Src complex and cardiotonic steroid-activated protein kinase cascades. Pflugers Arch. 2009;457(3):635-44.
89. Gruber KA, Rudel LL, Bullock BC. Increased circulating levels of an endogenous digoxin-like factor in hypertensive monkeys. Hypertension (Dallas, Tex : 1979). 1982;4(3):348-54.
90. Hamlyn JM, Ringel R, Schaeffer J, Levinson PD, Hamilton BP, Kowarski AA, et al. A circulating inhibitor of (Na+ + K+)ATPase associated with essential hypertension. Nature. 1982;300(5893):650-2.
91. Cloix JF, Devynck MA, Elghozi JL, Kamal LA, Lacerda-Jacomini LC, Meyer P, et al. Plasma endogenous sodium pump inhibitor in essential hypertension. Journal of hypertension Supplement : official journal of the International Society of Hypertension. 1983;1(2):11-4.
92. Kelly RA, O'Hara DS, Mitch WE, Steinman TI, Goldszer RC, Solomon HS, et al. Endogenous digitalis-like factors in hypertension and chronic renal insufficiency. Kidney international. 1986;30(5):723-9.
93. Odendaal HJ, Beyers AD, van Heyningen CF, Spruyt LL, Kotze TJ, van Jaarsveld PP. Immunoreactive digitalis-like substance in pre-eclampsia. South African medical journal = Suid-Afrikaanse tydskrif vir geneeskunde. 1986;70(9):535-7.
94. Sagnella GA, Jones JC, Shore AC, Markandu ND, MacGregor GA. Evidence for increased levels of a circulating ouabainlike factor in essential hypertension. Hypertension (Dallas, Tex : 1979). 1986;8(5):433-7.
95. Cloix JF, Crabos M, Grichois ML, Guicheney P, Meyer P. Endogenous Na+ transport inhibitor in human hypertension: further biochemical and chemical studies. Klinische Wochenschrift. 1987;65 Suppl 8:146-53.
96. Devynck MA, Pernollet MG, Meyer P. Endogenous digitalis-like compounds in essential and experimental hypertension. International journal of radiation applications and instrumentation Part B, Nuclear medicine and biology. 1987;14(4):341-52.
97. Kuske R, Moreth K, Renner D, Wizemann V, Schoner W. Sodium pump inhibitor in the serum of patients with essential hypertension and its partial purification from hemofiltrate. Klinische Wochenschrift. 1987;65 Suppl 8:53-9.
98. Vasdev S, Johnson E, Longerich L, Prabhakaran VM, Gault MH. Plasma endogenous digitalis-like factors in healthy individuals and in dialysis-dependent and kidney transplant patients. Clinical nephrology. 1987;27(4):169-74.

99. Clerico A, Balzan S, Del Chicca MG, Paci A, Cocci F, Bertelli A. Endogenous cardiac glycoside-like substances in newborns, adults, pregnant women and patients with hypertension or renal insufficiency. Drugs under experimental and clinical research. 1988;14(9):603-7.
100. Koren G, Farine D, Grundmann H, Heyes J, Soldin S, Taylor J, et al. Endogenous digoxin-like substance(s) associated with uneventful and high-risk pregnancies. Developmental pharmacology and therapeutics. 1988;11(2):82-7.
101. Takahashi H, Matsusawa M, Okabayashi H, Suga K, Ikegaki I, Nishimura M, et al. Endogenous digitalislike substance in an adult population in Japan. American journal of hypertension. 1988;1(3 Pt 3):168s-72s.
102. Valdes R, Jr., Hagberg JM, Vaughan TE, Lau BW, Seals DR, Ehsani AA. Endogenous digoxin-like immunoreactivity in blood is increased during prolonged strenuous exercise. Life sciences. 1988;42(1):103-10.
103. Graves SW, Eder JP, Schryber SM, Sharma K, Brena A, Antman KH, et al. Endogenous digoxin-like immunoreactive factor and digitalis-like factor associated with the hypertension of patients receiving multiple alkylating agents as part of autologous bone marrow transplantation. Clinical science (London, England : 1979). 1989;77(5):501-7.
104. Shilo L, Pomeranz A, Rathaus M, Bernheim J, Shenkman L. Endogenous digoxin-like factor raises blood pressure and protects against digitalis toxicity. Life sciences. 1989;44(24):1867-70.
105. Trachtman H, Delpizzo R, Chasalow FI. Endogenous digoxin-like material in normotensive and hypertensive strains of rats. Life sciences. 1989;44(24):1881-5.
106. Asbert M, Jimenez W, La Villa G, Claria J, Lopez C, Gines P, et al. Urinary excretion of endogenous digitalis-like natriuretic substances in healthy subjects. Effect of sodium load. Revista espanola de fisiologia. 1990;46(3):261-7.
107. Delva P, Barbieri E, Devynck MA, Capra C, Pernollet MA, Meyer P, et al. Increase in plasma digitalis-like activity during percutaneous transluminal coronary angioplasty in patients with coronary stenosis. Life sciences. 1990;47(5):385-9.
108. Devynck MA, David-Dufilho M, Astarie C, Mazeaud M, Pernollet MG, Le Quan Sang KH. Endogenous inhibitors of the Na+, K(+)-pump and platelet Ca2+ handling in hypertension. Physiologia Bohemoslovaca. 1990;39(1):71-8.
109. Imafuku T, Ogawa Z, Itoh H, Suzuki H, Saruta T. Na+, K(+)-ATPase inhibitory activity of fractionated urine during changes in dietary sodium intake in man. Endocrinologia japonica. 1990;37(1):39-46.
110. Le Quan Sang KH, Pernollet MG, Meyer P, Devynck MA. Plasma digitalis-like activity and cytosolic Ca2+ in essential hypertension. American journal of hypertension. 1990;3(3):171-5.
111. Liu ZQ, Yao RG, Yang DY. Endogenous digoxin-like substance as an important factor in the development of hypertension in children. Int J Cardiol. 1990;29(3):343-8.

112. Soszynski P, Slowinska-Srzednicka J, Zgliczynski S. Increased activity of digoxin-like substance in low-renin hypertension in acromegaly. Clinical and experimental hypertension Part A, Theory and practice. 1990;12(4):533-49.
113. Bagrov A, Fedorova OV, Maslova MN, Roukoyatkina NI, Ukhanova MV, Zhabko EP. Endogenous plasma Na,K-ATPase inhibitory activity and digoxin like immunoreactivity after acute myocardial infarction. Cardiovascular research. 1991;25(5):371-7.
114. Delva P, Devynck MA, Degan M, Pernollet MG, Carraroli M, Capra C, et al. Plasma levels of an endogenous Na(+)-K+ pump inhibitor in relation to haemodynamic data in cardiopathic patients. Clinical science (London, England : 1979). 1991;81(1):23-9.
115. Goto A, Yamada K, Ishii M, Sugimoto T, Yoshioka M. Immunoreactivity of endogenous digitalis-like factors. Biochemical pharmacology. 1991;41(8):1261-3.
116. Hamlyn JM, Blaustein MP, Bova S, DuCharme DW, Harris DW, Mandel F, et al. Identification and characterization of a ouabain-like compound from human plasma. Proc Natl Acad Sci U S A. 1991;88(14):6259-63.
117. Khatter JC, Agbanyo M, Navaratnam S. Endogenous inotropic substance from heart tissue has digitalis-like properties. Life sciences. 1991;48(5):387-96.
118. Okamoto S, Ikeda M, Morise T, Miyamori I, Takeda R. Elevated endogenous Na-K-ATPase inhibitor activity in hypertensive diabetic patients with a family history of hypertension. The Journal of diabetic complications. 1991;5(2-3):146-7.
119. Okamoto S, Ikeda M, Morise T, Miyamori I, Takeda R. Elevated endogenous digitalis-like substance in hypertensive diabetic patients with a family history of hypertension. Journal of endocrinological investigation. 1991;14(5):357-60.
120. Andronico G, Mule G, Mangano MT, Piazza G, Donatelli M, Cerasola G, et al. Insulin resistance and endogenous digoxin-like factor in obese hypertensive patients with glucose intolerance. Acta diabetologica. 1992;28(3-4):203-5.
121. Gottlieb SS, Rogowski AC, Weinberg M, Krichten CM, Hamilton BP, Hamlyn JM. Elevated concentrations of endogenous ouabain in patients with congestive heart failure. Circulation. 1992;86(2):420-5.
122. Koga M, Ideishi M, Matsusaki M, Tashiro E, Kinoshita A, Ikeda M, et al. Mild exercise decreases plasma endogenous digitalislike substance in hypertensive individuals. Hypertension (Dallas, Tex : 1979). 1992;19(2 Suppl):Ii231-6.
123. Kohn R, Lichardus B, Rusnak M. Endogenous digitalis-like factor in patients with acute myocardial infarction. Cor et vasa. 1992;34(3):227-37.
124. Lloyd MA, Sandberg SM, Edwards BS. Role of renal Na+,K(+)-ATPase in the regulation of sodium excretion under normal conditions and in acute congestive heart failure. Circulation. 1992;85(5):1912-7.

125. Bagrov AY, Fedorova OV, Roukoyatkina NI, Zhabko EP. Effect of endogenous digoxin-like factor and digoxin antibody on myocardial Na+, K(+)-pump activity and ventricular arrhythmias in acute myocardial ischaemia in rats. Cardiovascular research. 1993;27(6):1045-50.
126. Chen S, Yuan C, Clough D, Haddy FJ, Pamnani MB. Role of digitalis-like substance in experimental insulin-dependent diabetes mellitus hypertension. Journal of cardiovascular pharmacology. 1993;22 Suppl 2:S20-1.
127. Takahashi H, Matsusawa M, Nishimura M, Nakanishi T, Yoshimura M. Digoxin-like immunoreactivity may contribute to hyperinsulinemia-associated hypertension in patients with glucose intolerance. Journal of cardiovascular pharmacology. 1993;22 Suppl 2:S22-4.
128. Yuan C, Manunta P, Chen S, Hamlyn JM, Haddy FJ, Pamnani MB. Role of ouabain-like factors in hypertension: effects of ouabain and certain endogenous ouabain-like factors in hypertension. Journal of cardiovascular pharmacology. 1993;22 Suppl 2:S10-2.
129. Bagrov AY, Kuznetsova EA, Fedorova OV. Endogenous digoxin-like factor in acute myocardial infarction. J Intern Med. 1994;235(1):63-7.
130. Doris PA. Ouabain in plasma from spontaneously hypertensive rats. The American journal of physiology. 1994;266(1 Pt 2):H360-4.
131. Bagrov AY, Fedorova OV, Austin-Lane JL, Dmitrieva RI, Anderson DE. Endogenous marinobufagenin-like immunoreactive factor and Na+, K+ ATPase inhibition during voluntary hypoventilation. Hypertension (Dallas, Tex : 1979). 1995;26(5):781-8.
132. Graves SW, Lincoln K, Cook SL, Seely EW. Digitalis-like factor and digoxin-like immunoreactive factor in diabetic women with preeclampsia, transient hypertension of pregnancy, and normotensive pregnancy. American journal of hypertension. 1995;8(1):5-11.
133. Komiyama Y, Mori T, Murakami T, Masuda M, Takahashi H. Production of ouabain-like factors of hypothalamo-pituitary origin, determined by a sensitive ELISA for ouabain, is increased in DOCA-salt hypertensive rats. Pathophysiology : the official journal of the International Society for Pathophysiology. 1995;2(1):35-40.
134. Kramer HJ, Krampitz G, Backer A, Michel H, Krampitz G, Meyer-Lehnert H. Endogenous sodium pump inhibitors in human urine. Further identification of inhibitors of Na-K-ATPase. American journal of hypertension. 1995;8(7):753-60.
135. Rossi G, Manunta P, Hamlyn JM, Pavan E, De Toni R, Semplicini A, et al. Immunoreactive endogenous ouabain in primary aldosteronism and essential hypertension: relationship with plasma renin, aldosterone and blood pressure levels. J Hypertens. 1995;13(10):1181-91.
136. Bagrov AY, Dmitrieva RI, Fedorova OV, Kazakov GP, Roukoyatkina NI, Shpen VM. Endogenous marinobufagenin-like immunoreactive substance. A possible endogenous Na, K-ATPase inhibitor with vasoconstrictor activity. American journal of hypertension. 1996;9(10 Pt 1):982-90.

137. Bagrov AY, Fedorova OV, Dmitrieva RI, French AW, Anderson DE. Plasma marinobufagenin-like and ouabain-like immunoreactivity during saline volume expansion in anesthetized dogs. Cardiovascular research. 1996;31(2):296-305.
138. Nguyen AT, Doris PA. Role of endogenous cardiac glycosides in the spontaneously hypertensive rat--antagonism by active immunization. American journal of hypertension. 1996;9(1):81-5.
139. Semra YK, Butt AN, Swaminathan R. Effect of salt intake on excretion of endogenous ouabain-like substance, measured by RIA. Clinical chemistry. 1996;42(12):1949-54.
140. Yamada K, Goto A, Hui C, Omata M. Role of ouabain-like compound in the regulation of plasma aldosterone concentration in rats. Life sciences. 1996;58(21):1833-7.
141. Butt AN, Semra YK, Ho CS, Swaminathan R. Effect of high salt intake on plasma and tissue concentration of endogenous ouabain-like substance in the rat. Life sciences. 1997;61(24):2367-73.
142. Ferrandi M, Manunta P, Balzan S, Hamlyn JM, Bianchi G, Ferrari P. Ouabain-like factor quantification in mammalian tissues and plasma: comparison of two independent assays. Hypertension (Dallas, Tex : 1979). 1997;30(4):886-96.
143. Martinka E, Galajada P, Ochodnicky M, Lichardus B, Straka S, Mokan M. Endogenous digoxin-like immunoactivity and diabetes mellitus: facts and hypotheses. Medical hypotheses. 1997;49(3):271-5.
144. Worgall S, Rascher W, Gyodi G, Nyul Z, Baranyai Z, Sulyok E. Urinary excretion of endogenous ouabain-like substance is reduced in NaCl supplemented premature infants. Biology of the neonate. 1997;72(6):337-44.
145. Bagrov AY, Fedorova OV, Dmitrieva RI, Howald WN, Hunter AP, Kuznetsova EA, et al. Characterization of a urinary bufodienolide Na+,K+-ATPase inhibitor in patients after acute myocardial infarction. Hypertension (Dallas, Tex : 1979). 1998;31(5):1097-103.
146. Bernini G, Paci A, Sgro M, Moretti A, Salvetti A. Endogenous digitalis-like factor and ouabain immunoreactivity in adrenalectomized patients and normal subjects after acute and prolonged salt loading. American journal of hypertension. 1998;11(1 Pt 1):1-7.
147. Crambert G, Balzan S, Paci A, Decollogne S, Montali U, Ghione S, et al. Inhibition of rat Na+/K+-ATPase isoforms by endogenous digitalis extracts from neonatal human plasma. Clinical and experimental hypertension (New York, NY : 1993). 1998;20(5-6):669-74.
148. Fedorova OV, Anderson DE, Bagrov AY. Plasma marinobufagenin-like and ouabain-like immunoreactivity in adrenocorticotropin-treated rats. American journal of hypertension. 1998;11(7):796-802.
149. Fedorova OV, Doris PA, Bagrov AY. Endogenous marinobufagenin-like factor in acute plasma volume expansion. Clinical and experimental hypertension (New York, NY : 1993). 1998;20(5-6):581-91.

150. Garbagnati E. Serum digoxin-like immunoreactive factor in children and its relation to sodium metabolism. Acta paediatrica (Oslo, Norway : 1992). 1998;87(5):500-4.
151. Kramer HJ, Krampitz G, Backer A, Meyer-Lehnert H. Ouabain-like factors in human urine: identification of a Na-K-ATPase inhibitor as vanadium-diascorbate adduct. Clinical and experimental hypertension (New York, NY : 1993). 1998;20(5-6):557-71.
152. Martinka E, Ocenasova A, Kamenistiakova L, Dobrota D, Kerny J, Mokan M. Endogenous digoxin-like immunoactivity in subjects with diabetes mellitus and hypertension. American journal of hypertension. 1998;11(6 Pt 1):667-76.
153. Takada T, Nakagawa M, Ura N, Kaide J, Yoshida H, Shimamoto K. Endogenous immunoreactive ouabain-like and digoxin-like factors in reduced renal mass hypertensive rats. Hypertension research : official journal of the Japanese Society of Hypertension. 1998;21(3):193-9.
154. Bentur Y, Tsipiniuk A, Taitelman U. Postmortem digoxin-like immunoreactive substances (DLIS) in patients not treated with digoxin. Human & experimental toxicology. 1999;18(2):67-70.
155. Lopatin DA, Ailamazian EK, Dmitrieva RI, Shpen VM, Fedorova OV, Doris PA, et al. Circulating bufodienolide and cardenolide sodium pump inhibitors in preeclampsia. J Hypertens. 1999;17(8):1179-87.
156. Manunta P, Stella P, Rivera R, Ciurlino D, Cusi D, Ferrandi M, et al. Left ventricular mass, stroke volume, and ouabain-like factor in essential hypertension. Hypertension (Dallas, Tex : 1979). 1999;34(3):450-6.
157. Bagrov AY, Dmitrieva RI, Dorofeeva NA, Fedorova OV, Lopatin DA, Lakatta EG, et al. Cicletanine reverses vasoconstriction induced by the endogenous sodium pump ligand, marinobufagenin, via a protein kinase C dependent mechanism. J Hypertens. 2000;18(2):209-15.
158. Fedorova OV, Lakatta EG, Bagrov AY. Endogenous Na,K pump ligands are differentially regulated during acute NaCl loading of Dahl rats. Circulation. 2000;102(24):3009-14.
159. Yuan WQ, Lu ZR, Wang H, Yuan YK, Ren HX. Effects of endogenous ouabain on the development of hypertension in 1k1c hypertensive rats. Hypertension research : official journal of the Japanese Society of Hypertension. 2000;23 Suppl:S61-5.
160. Fedorova OV, Kolodkin NI, Agalakova NI, Lakatta EG, Bagrov AY. Marinobufagenin, an endogenous alpha-1 sodium pump ligand, in hypertensive Dahl salt-sensitive rats. Hypertension (Dallas, Tex : 1979). 2001;37(2 Pt 2):462-6.
161. Harwood S, Mullen AM, McMahon AC, Dawnay A. Plasma OLC is elevated in mild experimental uremia but is not associated with hypertension. American journal of hypertension. 2001;14(11 Pt 1):1112-5.
162. Oda M, Kurosawa M, Numazawa S, Tanaka S, Akizawa T, Ito K, et al. Determination of bufalin-like

immunoreactivity in serum of humans and rats by time-resolved fluoroimmunoassay for using a monoclonal antibody. Life sciences. 2001;68(10):1107-17.
163. Pierdomenico SD, Bucci A, Manunta P, Rivera R, Ferrandi M, Hamlyn JM, et al. Endogenous ouabain and hemodynamic and left ventricular geometric patterns in essential hypertension. American journal of hypertension. 2001;14(1):44-50.
164. Fedorova OV, Talan MI, Agalakova NI, Lakatta EG, Bagrov AY. Endogenous ligand of alpha(1) sodium pump, marinobufagenin, is a novel mediator of sodium chloride--dependent hypertension. Circulation. 2002;105(9):1122-7.
165. Fridman AI, Matveev SA, Agalakova NI, Fedorova OV, Lakatta EG, Bagrov AY. Marinobufagenin, an endogenous ligand of alpha-1 sodium pump, is a marker of congestive heart failure severity. J Hypertens. 2002;20(6):1189-94.
166. Berendes E, Cullen P, Van Aken H, Zidek W, Erren M, Hubschen M, et al. Endogenous glycosides in critically ill patients. Critical care medicine. 2003;31(5):1331-7.
167. Wang JG, Staessen JA, Messaggio E, Nawrot T, Fagard R, Hamlyn JM, et al. Salt, endogenous ouabain and blood pressure interactions in the general population. J Hypertens. 2003;21(8):1475-81.
168. Fedorova OV, Talan MI, Agalakova NI, Lakatta EG, Bagrov AY. Coordinated shifts in Na/K-ATPase isoforms and their endogenous ligands during cardiac hypertrophy and failure in NaCl-sensitive hypertension. J Hypertens. 2004;22(2):389-97.
169. Bagrov YY, Manusova NB, Egorova IA, Fedorova OV, Bagrov AY. Endogenous digitalis-like ligands and Na/K-ATPase inhibition in experimental diabetes mellitus. Frontiers in bioscience : a journal and virtual library. 2005;10:2257-62.
170. Bagrov YY, Manusova NB, Egorova IA, Frolova EV, Fedorova OV, Bagrov AY. Marinobufagenin, an endogenous inhibitor of alpha-1 Na/K-ATPase, is a novel factor in pathogenesis of diabetes mellitus. Doklady biological sciences : proceedings of the Academy of Sciences of the USSR, Biological sciences sections. 2005;404:333-7.
171. Bauer N, Muller-Ehmsen J, Kramer U, Hambarchian N, Zobel C, Schwinger RH, et al. Ouabain-like compound changes rapidly on physical exercise in humans and dogs: effects of beta-blockade and angiotensin-converting enzyme inhibition. Hypertension (Dallas, Tex : 1979). 2005;45(5):1024-8.
172. Fedorova OV, Kolodkin NI, Agalakova NI, Namikas AR, Bzhelyansky A, St-Louis J, et al. Antibody to marinobufagenin lowers blood pressure in pregnant rats on a high NaCl intake. J Hypertens. 2005;23(4):835-42.
173. Komiyama Y, Dong XH, Nishimura N, Masaki H, Yoshika M, Masuda M, et al. A novel endogenous digitalis, telocinobufagin, exhibits elevated plasma levels in patients with terminal renal failure. Clinical biochemistry. 2005;38(1):36-45.
174. Manunta P, Iacoviello M, Forleo C, Messaggio E, Hamlyn JM, Lucarelli K, et al. High circulating levels of

endogenous ouabain in the offspring of hypertensive and normotensive individuals. J Hypertens. 2005;23(9):1677-81.
175. Kennedy DJ, Vetteth S, Periyasamy SM, Kanj M, Fedorova L, Khouri S, et al. Central role for the cardiotonic steroid marinobufagenin in the pathogenesis of experimental uremic cardiomyopathy. Hypertension (Dallas, Tex : 1979). 2006;47(3):488-95.
176. Manunta P, Hamilton BP, Hamlyn JM. Salt intake and depletion increase circulating levels of endogenous ouabain in normal men. American journal of physiology Regulatory, integrative and comparative physiology. 2006;290(3):R553-9.
177. Pitzalis MV, Hamlyn JM, Messaggio E, Iacoviello M, Forleo C, Romito R, et al. Independent and incremental prognostic value of endogenous ouabain in idiopathic dilated cardiomyopathy. European journal of heart failure. 2006;8(2):179-86.
178. Zvartau NE, Conrady AO, Sviryaev YV, Rotari OP, Merkulova NK, Kalinkin AL, et al. Marinobufagenin in hypertensive patients with obstructive sleep apnea. Cellular and molecular biology (Noisy-le-Grand, France). 2006;52(8):24-7.
179. Bagrov YY, Manusova NB, Frolova EV, Egorova IA, Kashkin VA, Tapilskaya NI, et al. Endogenous sodium pump inhibitors, diabetes mellitus and preeclampsia Preliminary observations and a hypothesis. Pathophysiology : the official journal of the International Society for Pathophysiology. 2007;14(3-4):147-51.
180. Skoumal R, Szokodi I, Aro J, Foldes G, Gooz M, Seres L, et al. Involvement of endogenous ouabain-like compound in the cardiac hypertrophic process in vivo. Life sciences. 2007;80(14):1303-10.
181. Wu L, Xiong C, Su P. Endogenous ouabain in hypertensive disorder complicating pregnancy. Journal of Huazhong University of Science and Technology Medical sciences = Hua zhong ke ji da xue xue bao Yi xue Ying De wen ban = Huazhong keji daxue xuebao Yixue Yingdewen ban. 2007;27(6):717-20.
182. Anderson DE, Fedorova OV, Morrell CH, Longo DL, Kashkin VA, Metzler JD, et al. Endogenous sodium pump inhibitors and age-associated increases in salt sensitivity of blood pressure in normotensives. American journal of physiology Regulatory, integrative and comparative physiology. 2008;294(4):R1248-54.
183. Fedorova OV, Simbirtsev AS, Kolodkin NI, Kotov AY, Agalakova NI, Kashkin VA, et al. Monoclonal antibody to an endogenous bufadienolide, marinobufagenin, reverses preeclampsia-induced Na/K-ATPase inhibition and lowers blood pressure in NaCl-sensitive hypertension. J Hypertens. 2008;26(12):2414-25.
184. Manunta P, Maillard M, Tantardini C, Simonini M, Lanzani C, Citterio L, et al. Relationships among endogenous ouabain, alpha-adducin polymorphisms and renal sodium handling in primary hypertension. J Hypertens. 2008;26(5):914-20.
185. Stella P, Manunta P, Mallamaci F, Melandri M, Spotti D, Tripepi G, et al. Endogenous ouabain and cardiomyopathy in dialysis patients. J Intern Med. 2008;263(3):274-80.

186. Bagrov AY, Agalakova NI, Kashkin VA, Fedorova OV. Endogenous cardiotonic steroids and differential patterns of sodium pump inhibition in NaCl-loaded salt-sensitive and normotensive rats. American journal of hypertension. 2009;22(5):559-63.
187. Tripodi G, Citterio L, Kouznetsova T, Lanzani C, Florio M, Modica R, et al. Steroid biosynthesis and renal excretion in human essential hypertension: association with blood pressure and endogenous ouabain. American journal of hypertension. 2009;22(4):357-63.
188. Kolmakova EV, Haller ST, Kennedy DJ, Isachkina AN, Budny GV, Frolova EV, et al. Endogenous cardiotonic steroids in chronic renal failure. Nephrol Dial Transplant. 2011;26(9):2912-9.
189. Nagy G, Gaszner B, Lanyi E, Marko L, Feher E, Cseh J, et al. Selective association of endogenous ouabain with subclinical organ damage in treated hypertensive patients. Journal of human hypertension. 2011;25(2):122-9.
190. Nikitina ER, Mikhailov AV, Nikandrova ES, Frolova EV, Fadeev AV, Shman VV, et al. In preeclampsia endogenous cardiotonic steroids induce vascular fibrosis and impair relaxation of umbilical arteries. J Hypertens. 2011;29(4):769-76.
191. Bignami E, Casamassima N, Frati E, Lanzani C, Corno L, Alfieri O, et al. Preoperative endogenous ouabain predicts acute kidney injury in cardiac surgery patients. Critical care medicine. 2013;41(3):744-55.
192. Jablonski KL, Fedorova OV, Racine ML, Geolfos CJ, Gates PE, Chonchol M, et al. Dietary sodium restriction and association with urinary marinobufagenin, blood pressure, and aortic stiffness. Clinical journal of the American Society of Nephrology : CJASN. 2013;8(11):1952-9.
193. Haller ST, Drummond CA, Yan Y, Liu J, Tian J, Malhotra D, et al. Passive immunization against marinobufagenin attenuates renal fibrosis and improves renal function in experimental renal disease. American journal of hypertension. 2014;27(4):603-9.
194. Kennedy DJ, Shrestha K, Sheehey B, Li XS, Guggilam A, Wu Y, et al. Elevated Plasma Marinobufagenin, An Endogenous Cardiotonic Steroid, Is Associated With Right Ventricular Dysfunction and Nitrative Stress in Heart Failure. Circulation Heart failure. 2015;8(6):1068-76.
195. Simonini M, Pozzoli S, Bignami E, Casamassima N, Messaggio E, Lanzani C, et al. Endogenous Ouabain: An Old Cardiotonic Steroid as a New Biomarker of Heart Failure and a Predictor of Mortality after Cardiac Surgery. Biomed Res Int. 2015;2015:714793.
196. Tomaschitz A, Piecha G, Ritz E, Meinitzer A, Haas J, Pieske B, et al. Marinobufagenin in essential hypertension and primary aldosteronism: a cardiotonic steroid with clinical and diagnostic implications. Clinical and experimental hypertension (New York, NY : 1993). 2015;37(2):108-15.
197. Haller ST, Yan Y, Drummond CA, Xie J, Tian J, Kennedy DJ, et al. Rapamycin Attenuates Cardiac Fibrosis in Experimental Uremic Cardiomyopathy by Reducing Marinobufagenin Levels and Inhibiting Downstream Pro-Fibrotic Signaling. J Am Heart Assoc. 2016;5(10).

198. Kantaria N, Pantsulaia I, Andronikashvili I, Simonia G. Assosiation Of Endogenous Cardiotonic Steroids With Salt-Sensitivity Of Blood Pressure In Georgian Population. Georgian medical news. 2016(258):33-7.
199. Fedorova LV, Raju V, El-Okdi N, Shidyak A, Kennedy DJ, Vetteth S, et al. The cardiotonic steroid hormone marinobufagenin induces renal fibrosis: implication of epithelial-to-mesenchymal transition. American journal of physiology Renal physiology. 2009;296(4):F922-34.
200. Hamlyn JM, Manunta P. Endogenous cardiotonic steroids in kidney failure: a review and an hypothesis. Adv Chronic Kidney Dis. 2015;22(3):232-44.
201. Ludens JH, Clark MA, DuCharme DW, Harris DW, Lutzke BS, Mandel F, et al. Purification of an endogenous digitalislike factor from human plasma for structural analysis. Hypertension (Dallas, Tex : 1979). 1991;17(6 Pt 2):923-9.
202. Delva P, Capra C, Degan M, Minuz P, Covi G, Milan L, et al. High plasma levels of a ouabain-like factor in normal pregnancy and in pre-eclampsia. European journal of clinical investigation. 1989;19(1):95-100.
203. Feldmann T, Glukmann V, Medvenev E, Shpolansky U, Galili D, Lichtstein D, et al. Role of endosomal Na+-K+-ATPase and cardiac steroids in the regulation of endocytosis. Am J Physiol Cell Physiol. 2007;293(3):C885-96.
204. Nesher M, Shpolansky U, Viola N, Dvela M, Buzaglo N, Cohen Ben-Ami H, et al. Ouabain attenuates cardiotoxicity induced by other cardiac steroids. Br J Pharmacol. 2010;160(2):346-54.
205. Song H, Karashima E, Hamlyn JM, Blaustein MP. Ouabain-digoxin antagonism in rat arteries and neurones. J Physiol. 2014;592(5):941-69.
206. Kotecha D, Chudasama R, Lane DA, Kirchhof P, Lip GY. Atrial fibrillation and heart failure due to reduced versus preserved ejection fraction: A systematic review and meta-analysis of death and adverse outcomes. Int J Cardiol. 2016;203:660-6.
207. Harris DW, Clark MA, Fisher JF, Hamlyn JM, Kolbasa KP, Ludens JH, et al. Development of an immunoassay for endogenous digitalislike factor. Hypertension (Dallas, Tex : 1979). 1991;17(6 Pt 2):936-43.
208. Minta A, Tsien RY. Fluorescent indicators for cytosolic sodium. J Biol Chem. 1989;264(32):19449-57.
209. Slack C, Warner AE, Warren RL. The distribution of sodium and potassium in amphibian embryos during early development. J Physiol. 1973;232(2):297-312.
210. Horowitz SB, Paine PL. Reference phase analysis of free and bound intracellular solutes. II. Isothermal and isotopic studies of cytoplasmic sodium, potassium, and water. Biophysical journal. 1979;25(1):45-62.
211. Liebling MS, Gupta RK. A comparison of intracellular sodium ion concentrations in neoplastic and nonneoplastic

human tissue using 23Na NMR spectroscopy. Annals of the New York Academy of Sciences. 1987;508:149-63.
212. Springer CS, Jr. Transmembrane ion pumping: high resolution cation NMR spectroscopy. Annals of the New York Academy of Sciences. 1987;508:130-48.
213. Wilde AA, Kleber AG. The combined effects of hypoxia, high K+, and acidosis on the intracellular sodium activity and resting potential in guinea pig papillary muscle. Circ Res. 1986;58(2):249-56.
214. Schmied R, Wang GX, Korth M. Intracellular Na+ activity and positive inotropic effect of sulmazole in guinea pig ventricular myocardium. Comparison with a cardioactive steroid. Circ Res. 1991;68(2):597-604.
215. Wang GX, Schmied R, Ebner F, Korth M. Intracellular sodium activity and its regulation in guinea-pig atrial myocardium. J Physiol. 1993;465:73-84.
216. Despa S, Islam MA, Weber CR, Pogwizd SM, Bers DM. Intracellular Na(+) concentration is elevated in heart failure but Na/K pump function is unchanged. Circulation. 2002;105(21):2543-8.
217. Pieske B, Maier LS, Piacentino V, 3rd, Weisser J, Hasenfuss G, Houser S. Rate dependence of [Na+]i and contractility in nonfailing and failing human myocardium. Circulation. 2002;106(4):447-53.
218. Boguslavskyi A, Pavlovic D, Aughton K, Clark JE, Howie J, Fuller W, et al. Cardiac hypertrophy in mice expressing unphosphorylatable phospholemman. Cardiovascular research. 2014;104(1):72-82.
219. Roder P, Hille C. ANG-2 for quantitative Na(+) determination in living cells by time-resolved fluorescence microscopy. Photochemical & photobiological sciences : Official journal of the European Photochemistry Association and the European Society for Photobiology. 2014;13(12):1699-710.
220. Antolović R. Low nanomolar concentrations of ouabain may induce higher. VETERINARSKI ARHIV 2006;76(6):489-95.
221. Despa S, Islam MA, Pogwizd SM, Bers DM. Intracellular [Na+] and Na+ pump rate in rat and rabbit ventricular myocytes. J Physiol. 2002;539(Pt 1):133-43.
222. Mahmmoud YA, Shattock M, Cornelius F, Pavlovic D. Inhibition of K+ transport through Na+, K+-ATPase by capsazepine: role of membrane span 10 of the alpha-subunit in the modulation of ion gating. PLoS One. 2014;9(5):e96909.
223. Gal D, MacDonald PC, Porter JC, Smith JW, Simpson ER. Effect of cell density and confluency on cholesterol metabolism in cancer cells in monolayer culture. Cancer research. 1981;41(2):473-7.
224. Cornelius F, Mahmmoud YA. Interaction between cardiotonic steroids and Na,K-ATPase. Effects of pH and ouabain-induced changes in enzyme conformation. Biochemistry. 2009;48(42):10056-65.

225. Ozaki H, Nagase H, Urakawa N. Interaction of palytoxin and cardiac glycosides on erythrocyte membrane and (Na+ + K+) ATPase. European journal of biochemistry. 1985;152(2):475-80.
226. Pullen MA, Brooks DP, Edwards RM. Characterization of the neutralizing activity of digoxin-specific Fab toward ouabain-like steroids. J Pharmacol Exp Ther. 2004;310(1):319-25.
227. Pavlovic D. The Role of Cardiotonic Steroids in the Pathogenesis of Cardiomyopathy in Chronic Kidney Disease. Nephron Clin Pract. 2014(128):11-21.
228. Liu J, Tian J, Haas M, Shapiro JI, Askari A, Xie Z. Ouabain interaction with cardiac Na+/K+-ATPase initiates signal cascades independent of changes in intracellular Na+ and Ca2+ concentrations. J Biol Chem. 2000;275(36):27838-44.
229. Eisner DA, O'Neill SC, Donoso P. Properties of the fluorescent sodium indicator SBFI in rat and rabbit cardiac myocytes. J Cardiovasc Electrophysiol. 1994;5(7):637-9.
230. Levi AJ, Lee CO, Brooksby P. Properties of the fluorescent sodium indicator "SBFI" in rat and rabbit cardiac myocytes. J Cardiovasc Electrophysiol. 1994;5(3):241-57.
231. Tian J, Haller S, Periyasamy S, Brewster P, Zhang H, Adlakha S, et al. Renal ischemia regulates marinobufagenin release in humans. Hypertension (Dallas, Tex : 1979) [Internet]. 2010; 56(5):[914-9 pp.]. Available from: http://onlinelibrary.wiley.com/o/cochrane/clcentral/articles/574/CN-00760574/frame.html

http://hyper.ahajournals.org/content/hypertensionaha/56/5/914.full.pdf.
232. Manunta P, Hamlyn JM, Simonini M, Messaggio E, Lanzani C, Bracale M, et al. Endogenous ouabain and the renin-angiotensin-aldosterone system: distinct effects on Na handling and blood pressure in human hypertension. J Hypertens. 2011;29(2):349-56.
233. Fedorova OV, Lakatta EG, Bagrov AY, Melander O. Plasma level of the endogenous sodium pump ligand marinobufagenin is related to the salt-sensitivity in men. J Hypertens. 2015;33(3):534-41; discussion 41.
234. Shimoni Y, Gotsman M, Deutsch J, Kachalsky S, Lichtstein D. Endogenous ouabain-like compound increases heart muscle contractility. Nature. 1984;307(5949):369-71.
235. Fagoo M, Godfraind T. Further characterization of cardiodigin, Na+, K+-ATPase inhibitor extracted from mammalian tissues. FEBS letters. 1985;184(1):150-4.
236. Khatter JC, Agbanyo M, Hoeschen RJ. Endogenous digitalis-like substance in pig left ventricle. Life sciences. 1986;39(25):2483-92.
237. Delva P, Devynck MA, Degan M, Pernollet MG, Capra C, Meyer P, et al. Correlations between plasma levels of an endogenous digitalis-like substance and haemodynamic parameters measured during cardiac catheterization. Journal of hypertension Supplement : official journal of the International Society of Hypertension. 1988;6(4):S348-50.

238. Wauquier I, Devynck MA. Body fluid variations and endogenous digitalis-like compounds during chronic NaCl loading in Wistar rats. Clinical and experimental hypertension Part A, Theory and practice. 1989;11(7):1217-34.
239. Gomez-Sanchez EP, Foecking MF, Sellers D, Blankenship MS, Gomez-Sanchez CE. Is the circulating ouabain-like compound ouabain? American journal of hypertension. 1994;7(7 Pt 1):647-50.
240. Lewis LK, Yandle TG, Lewis JG, Richards AM, Pidgeon GB, Kaaja RJ, et al. Ouabain is not detectable in human plasma. Hypertension (Dallas, Tex : 1979). 1994;24(5):549-55.
241. Naruse K, Naruse M, Tanabe A, Yoshimoto T, Watanabe Y, Kurimoto F, et al. Does plasma immunoreactive ouabain originate from the adrenal gland? Hypertension (Dallas, Tex : 1979). 1994;23(1 Suppl):I102-5.
242. Harwood S, Little JA, Gallacher G, Perrett D, Edwards R, Dawnay A. Development of enzyme immunoassay for endogenous ouabain-like compound in human plasma. Clinical chemistry. 1997;43(5):715-22.
243. Bagrov AY, Fedorova OV. Effects of two putative endogenous digitalis-like factors, marinobufagenin and ouabain, on the Na+, K+-pump in human mesenteric arteries. J Hypertens. 1998;16(12 Pt 2):1953-8.
244. Shimada T, Nagasaka Y, Ishibashi Y, Tsukihashi H, Murakami Y, Sano K, et al. A probable relationship between an endogenous digitalis-like substance and concentric cardiac hypertrophy in primary aldosteronism. Internal medicine (Tokyo, Japan). 1999;38(8):655-9.
245. Meyer-Lehnert H, Backer A, Kramer HJ. Inhibitors of Na-K-ATPase in human urine: effects of ouabain-like factors and of vanadium-diascorbate on calcium mobilization in rat vascular smooth muscle cells: comparison with the effects of ouabain, angiotensin II, and arginine-vasopressin. American journal of hypertension. 2000;13(4 Pt 1):364-9.
246. Nesher M, Dvela M, Igbokwe VU, Rosen H, Lichtstein D. Physiological roles of endogenous ouabain in normal rats. American journal of physiology Heart and circulatory physiology. 2009;297(6):H2026-34.
247. Berson SA, Yalow RS. General principles of radioimmunoassay. Clinica chimica acta; international journal of clinical chemistry. 1968;22(1):51-69.
248. Elkareh J, Kennedy DJ, Yashaswi B, Vetteth S, Shidyak A, Kim EG, et al. Marinobufagenin stimulates fibroblast collagen production and causes fibrosis in experimental uremic cardiomyopathy. Hypertension (Dallas, Tex : 1979). 2007;49(1):215-24.
249. Haller ST, Kennedy DJ, Shidyak A, Budny GV, Malhotra D, Fedorova OV, et al. Monoclonal antibody against marinobufagenin reverses cardiac fibrosis in rats with chronic renal failure. American journal of hypertension. 2012;25(6):690-6.

250. Liu C, Bai Y, Chen Y, Wang Y, Sottejeau Y, Liu L, et al. Reduction of Na/K-ATPase potentiates marinobufagenin-induced cardiac dysfunction and myocyte apoptosis. J Biol Chem. 2012;287(20):16390-8.
251. European Medicines Agency.Guideline for good clinical practice E6(R2). 2016. https://www.ema.europa.eu/en/documents/scientific-guideline/ich-e-6-r2-guideline-good-clinical-practice-step-5_en.pdf. Opened August 2020.
252. Kotecha D, Calvert M, Deeks JJ, Griffith M, Kirchhof P, Lip GY, et al. A review of rate control in atrial fibrillation, and the rationale and protocol for the RATE-AF trial. BMJ open. 2017;7(7):e015099.
253. Dudink EA, Weijs B, Tull S, Luermans JG, Fabritz L, Chua W, et al. The Biomarkers NT-proBNP and CA-125 are Elevated in Patients with Idiopathic Atrial Fibrillation. J Atr Fibrillation. 2018;11(4):2058.
254. Gasparovic H, Burcar I, Kopjar T, Vojkovic J, Gabelica R, Biocina B, et al. NT-pro-BNP, but not C-reactive protein, is predictive of atrial fibrillation in patients undergoing coronary artery bypass surgery. Eur J Cardiothorac Surg. 2010;37(1):100-5.
255. Shin DI, Jaekel K, Schley P, Sause A, Muller M, Fueth R, et al. Plasma levels of NT-pro-BNP in patients with atrial fibrillation before and after electrical cardioversion. Z Kardiol. 2005;94(12):795-800.
256. Richards AM. Variability of NT-proBNP levels in heart failure: implications for clinical application. Heart. 2007;93(8):899-900.
257. Shattock MJ, Ottolia M, Bers DM, Blaustein MP, Boguslavskyi A, Bossuyt J, et al. Na+/Ca2+ exchange and Na+/K+-ATPase in the heart. J Physiol. 2015;593(6):1361-82.
258. Jelicks LA, Siri FM. Effects of hypertrophy and heart failure on [Na+]i in pressure-overloaded guinea pig heart. American journal of hypertension. 1995;8(9):934-43.
259. Baudet S, Noireaud J, Leoty C. Intracellular Na activity measurements in the control and hypertrophied heart of the ferret: an ion-sensitive micro-electrode study. Pflugers Arch. 1991;418(4):313-8.
260. Liu ZQ, Ma AQ, Zhang L, Yang DY. Intra-cellular electrolyte changes and levels of endogenous digoxin-like substance within the plasma in patients with congestive heart failure. Int J Cardiol. 1990;27(1):47-53.
261. Thomas P, Smart TG. HEK293 cell line: a vehicle for the expression of recombinant proteins. J Pharmacol Toxicol Methods. 2005;51(3):187-200.
262. Denning C, Borgdorff V, Crutchley J, Firth KS, George V, Kalra S, et al. Cardiomyocytes from human pluripotent stem cells: From laboratory curiosity to industrial biomedical platform. Biochimica et biophysica acta. 2016;1863(7 Pt B):1728-48.

263. Kirkton RD, Bursac N. Engineering biosynthetic excitable tissues from unexcitable cells for electrophysiological and cell therapy studies. Nat Commun. 2011;2:300.
264. Hafver TL, Hodne K, Wanichawan P, Aronsen JM, Dalhus B, Lunde PK, et al. Protein Phosphatase 1c Associated with the Cardiac Sodium Calcium Exchanger 1 Regulates Its Activity by Dephosphorylating Serine 68-phosphorylated Phospholemman. J Biol Chem. 2016;291(9):4561-79.
265. He B, Soderlund DM. Human embryonic kidney (HEK293) cells express endogenous voltage-gated sodium currents and Na v 1.7 sodium channels. Neurosci Lett. 2010;469(2):268-72.
266. Berjukow S, Doring F, Froschmayr M, Grabner M, Glossmann H, Hering S. Endogenous calcium channels in human embryonic kidney (HEK293) cells. Br J Pharmacol. 1996;118(3):748-54.
267. Bugaj V, Alexeenko V, Zubov A, Glushankova L, Nikolaev A, Wang Z, et al. Functional properties of endogenous receptor- and store-operated calcium influx channels in HEK293 cells. J Biol Chem. 2005;280(17):16790-7.
268. Kockskamper J, Gisselmann G, Glitsch HG. Comparison of ouabain-sensitive and -insensitive Na/K pumps in HEK293 cells. Biochimica et biophysica acta. 1997;1325(2):197-208.
269. Guo L, Qian JY, Abrams R, Tang HM, Weiser T, Sanders MJ, et al. The electrophysiological effects of cardiac glycosides in human iPSC-derived cardiomyocytes and in guinea pig isolated hearts. Cellular physiology and biochemistry : international journal of experimental cellular physiology, biochemistry, and pharmacology. 2011;27(5):453-62.
270. Wier WG, Hess P. Excitation-contraction coupling in cardiac Purkinje fibers. Effects of cardiotonic steroids on the intracellular [Ca2+] transient, membrane potential, and contraction. The Journal of general physiology. 1984;83(3):395-415.
271. Ruch SR, Nishio M, Wasserstrom JA. Effect of cardiac glycosides on action potential characteristics and contractility in cat ventricular myocytes: role of calcium overload. J Pharmacol Exp Ther. 2003;307(1):419-28.
272. Hashimoto K, Motomura S, Iijima T, Taira N. Effects of Ouabain on atrioventricular conduction: simultaneous observation in the isolated AV node preparation and the in situ heart of the dog. The Tohoku journal of experimental medicine. 1980;132(3):245-9.
273. Dhingra RC, Amat YLF, Wyndham C, Wu D, Denes P, Rosen KM. The electrophysiological effects of ouabain on sinus node and atrium in man. J Clin Invest. 1975;56(3):555-62.
274. Stark G, Schulze-Bauer C, Stark U, Kasper K, Decrinis M, Tritthart HA. Comparison of the frequency-dependent effects on the atrioventricular node of verapamil, amiodarone, digoxin, and diltiazem in isolated guinea pig hearts. Journal of cardiovascular pharmacology. 1995;25(2):330-5.